DESIGN OF REPROGRAMMED NEURONAL TRANSPLANTATION AND NANOBIOMATERIAL-BASED MICROGLIAL THERAPEUTIC TECHNOLOGIES FOR MANAGEMENT OF PARKINSON'S DISEASE

By

NEAL KELSEY BENNETT

A dissertation submitted to the

Graduate School – New Brunswick

Rutgers, The State University of New Jersey

And

The Graduate School of Biomedical Sciences

In partial fulfillment of the requirements

For the degree of

Doctor of Philosophy

Graduate Program in Biomedical Engineering

Written under the direction of

Prabhas V. Moghe

and approved by

_____

_____

_____

_____

New Brunswick, New Jersey

OCTOBER 2016

ABSTRACT OF THE DISSERTATION

DESIGN OF REPROGRAMMED NEURONAL TRANSPLANTATION AND NANOBIOMATERIAL-BASED MICROGLIAL THERAPEUTIC TECHNOLOGIES FOR MANAGEMENT OF PARKINSON'S DISEASE

By NEAL KELSEY BENNETT

Dissertation Director:

Prabhas V. Moghe

Parkinson's disease (PD) is a progressive neurodegenerative disorder marked by motor dysfunction, eventual cognitive impairment and dementia in advanced stages. These symptoms arise as a result of decreased activity or death of dopaminergic (DA) neurons in the *substantia nigra* region of the brain, leading to dopamine depletion in the striatum disruption of neuronal circuitry in the basal ganglia. The current most common treatment for PD is levodopa, which can be converted into dopamine by surviving DA neurons, offering temporary relief of the motor dysfunction symptoms of PD. However, a key disadvantage of levodopa as a therapeutic strategy is that it does little to address the progression of PD and symptoms typically worsen as DA neurons continue to degenerate or die. Based on the a critical need for more comprehensive therapeutic approaches to PD that do more than relieve dopamine deficiency, but also disrupt the factors causing disease progression, the work in this dissertation focus on our efforts to address key aspects of Parkinson's disease pathology: neuronal degeneration, neuroinflammation, and

synucleinopathy. To address neuronal degeneration, we investigated the potential for 3D fibrous synthetic substrates to support and transplant populations of human reprogrammed neurons into the brain. We found that fibrous substrate geometries could be tuned to shift reprogrammed cell populations towards either neuronal differentiation or maintenance of pluripotency. Microscale scaffolds generated from these fibrous substrates improved transplanted neuronal survival by at least an order of magnitude over traditional cell transplantation techniques. These proof-of-concept studies could be used to inform the future design of transplantable scaffolds supporting neurons reprogrammed to best address DA deficiency in PD. To address neuroinflammation and synucleinopathy, we examined the potential of microglia-targeting nanotherapeutics. We first identified scavenger receptors as a microglial receptor for α-synuclein (ASYN), a protein that forms characteristic protein aggregates and activates microglia in PD. We then designed nanoparticles targeting this interaction using synthetic amphiphilic scavenger receptor ligands. These amphiphilic molecules could reduce ASYN internalization and intracellular aggregation by microglia. We used nanoparticle constructs made using these synthetic ligands to target delivery of antioxidants to microglia, decreasing microglial activation in response to aggregated ASYN *in vitro* and *in vivo*. In summary, the studies described in this dissertation establish a valuable foundation for future therapeutic strategies addressing key features of PD pathophysiology and progression.

Table of Contents

List of Figures

List of Tables

CHAPTER 1 - AN INTRODUCTION TO CURRENT STRATEGIES FOR ADDRESSING KEY ASPECTS OF PARKINSON'S DISEASE: NEURONAL DEGENERATION, NEUROINFLAMMATION, AND SYNUCLEINOPATHY

Parkinson's disease (PD) is a progressive neurodegenerative disorder, characterized by movement-related dysfunction, which eventually leads to cognitive impairment and dementia in advanced stages [1, 2]. The total number of PD patients is expected to rise to 1.34 million people by 2050, with skyrocketing medical expenses exceeding $14.4 billion in 2010 [3]. The dysfunctions associated with PD, beginning with movement-related dysfunction and progressing to cognitive impairment and dementia in late stages [1, 2] are caused by the death of dopaminergic neurons in the *substantia nigra* region of the brain. This dopaminergic neuronal death results in dopamine (DA) depletion in the striatum and subsequent disruption of neuronal circuitry in the basal ganglia [2, 4], although the exact causes the disease progression and early cell death are unknown and are continuing subjects of study. In spite of the pressing need to develop treatments for neurodegenerative diseases like PD, key obstacles persist, including limited survival and function of neurons transplanted to relieve deficits, and the antagonistic environment created by patient immune cells. The following thesis is concerned with two key branches of therapeutic technologies for PD with the aims of 1) ameliorating **inflammatory condition and neurotoxic conditions** leading to the continuing loss of dopamine neurons and 2) addressing **DA neuron deficiency and dysfunction** (**Figure 1.1**). The major foci of this thesis then are to develop novel **immunomodulatory molecular approaches** and **three-dimensional (3D) microscale neuronal cultures** for the management of neurodegenerative disease, particularly focusing on the management of PD.

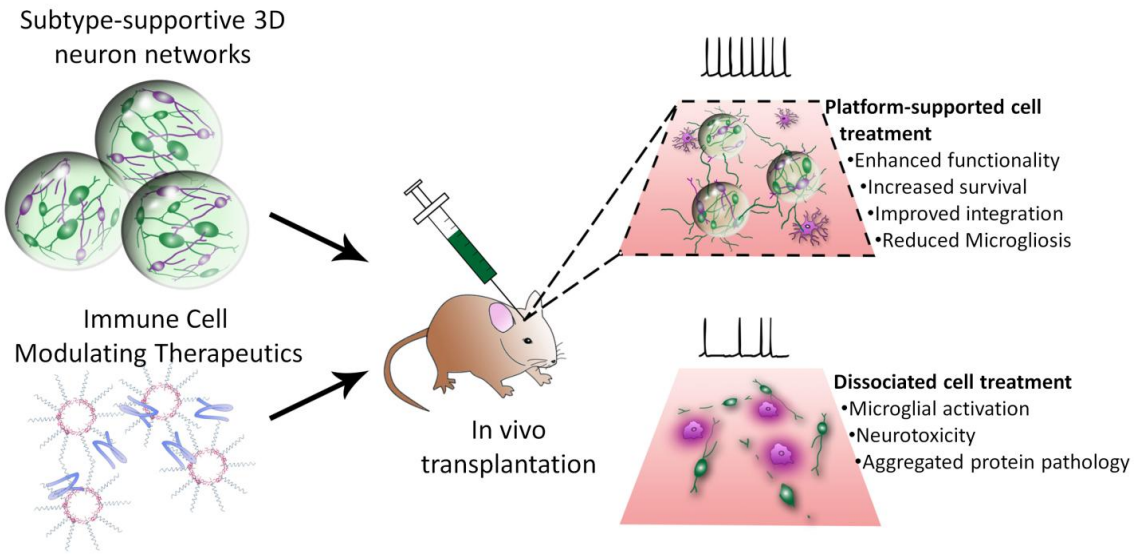

Figure 1.1 - Schematic of the two objectives of this dissertation.

The work described herein attempts to address key aspects of Parkinson's disease (PD), dopaminergic (DA) neuronal deficits neuroinflammation, and synucleinopathy, using scaffolds that support 3D networks of neurons and via modulation of immune cells.

1.1 Neuronal Degeneration

A key motor symptom of PD is hypokinesia, or slowness of movement and difficulty in initiating movement. To understand how this symptom arises, it is important to understand the brain parts and circuits involved in initiating movement. Under physiological conditions, movement is controlled by the motor cortex, which is regulated by the thalamus, which in turn is regulated by two antagonistic pathways between components of the basal ganglia, a collection of brain structures at the base of the forebrain and includes the striatum, the internal and external globus pallidus, the subthalamic nucleus, the substantia nigra pars compacta and the substantia nigra pars reticulata. The organization of these pathways, known as the "direct" and "indirect" pathways, are depicted in **Figure 1.2**.

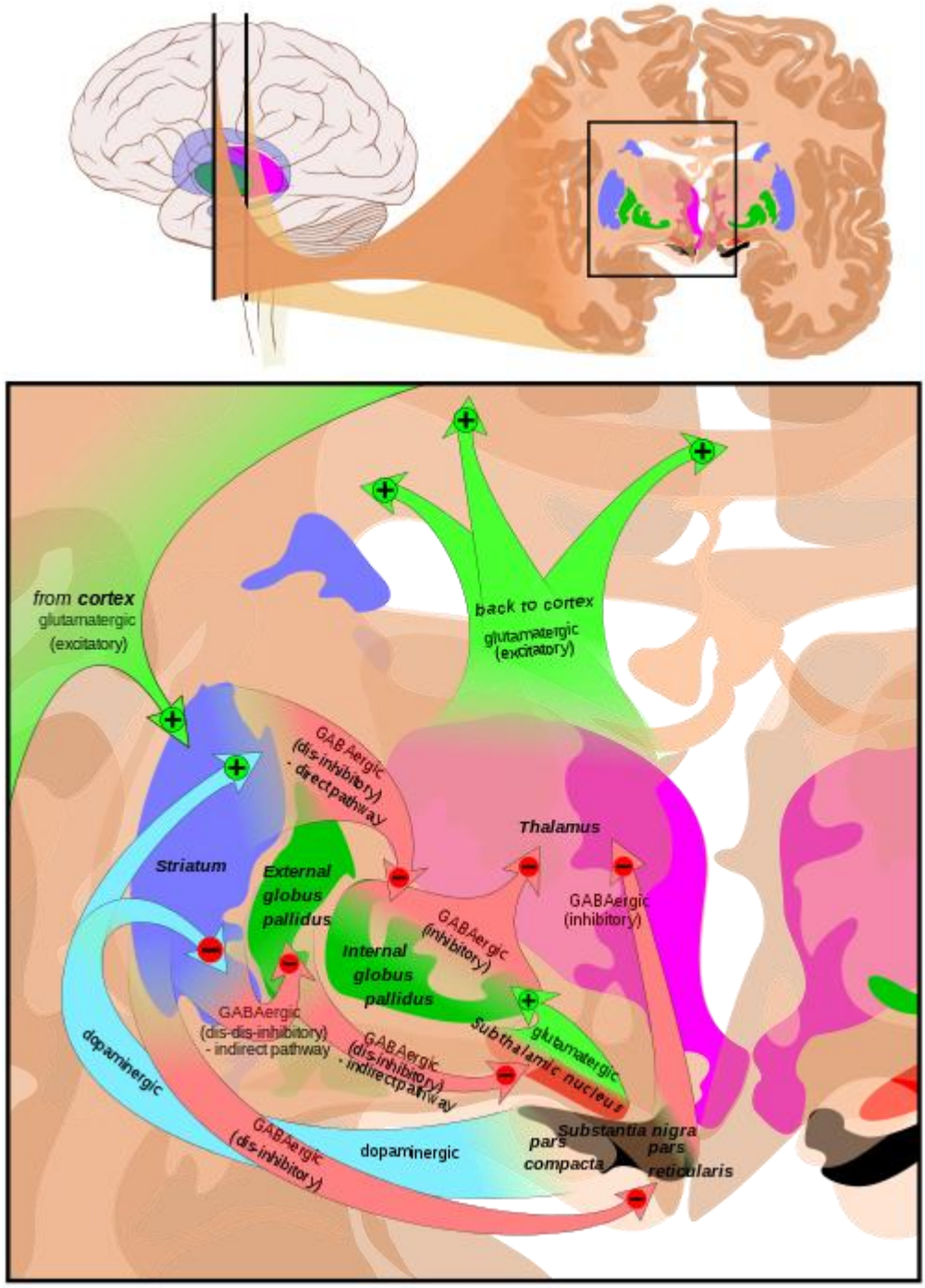

Figure 1.2 - Schematic of motor control pathways in the basal ganglia under physiological conditions.

Figure reproduced without changes and with permission from [5].

In the "direct" pathway, cortical excitatory inputs project to the striatum, which then projects inhibitory inputs to the globus pallidus interna, which then directly projects inhibitory neurons onto the thalamus. The thalamus then projects excitatory inputs directly to the motor cortex. The cumulative effect then of excitation of the direct pathway is excitation of the motor cortex and initiation of movement. Conversely, the indirect pathway acts to suppress movement. In the indirect pathway, inhibitory neurons from the striatum extend to the globus pallidus externa, which in turn inhibits the subthalamic nucleus. The subthalamic nucleus projects excitatory inputs to the globus pallidus interna, which inhibits the thalamus. Thus, activation of the indirect pathway has the net effect of inhibiting signaling to the thalamus, inhibiting signalling to the motor cortex and increasing resistance to movement. Control of motion requires careful regulation between activating these antagonistic pathways, which is conducted by DA inputs from the substantia nigra pars compacta, which serve to excite the direct pathway and inhibit the indirect pathway. Therefore, increased DA neuronal activity in the substantia nigra pars compacta serve to promote the initiation of movement. [6]

The seminal work of Hornykiewicz et. al. first determined that a fundamental element of the neuropathology observed in PD patients was the loss of DA neurons in the substantia nigra, a structure in the mesencephalon or midbrain [7]. This results in increased activity of the indirect pathway and reduced activity in the direct pathway (**Figure 1.3**), causing the common PD symptom of hypokinesia.

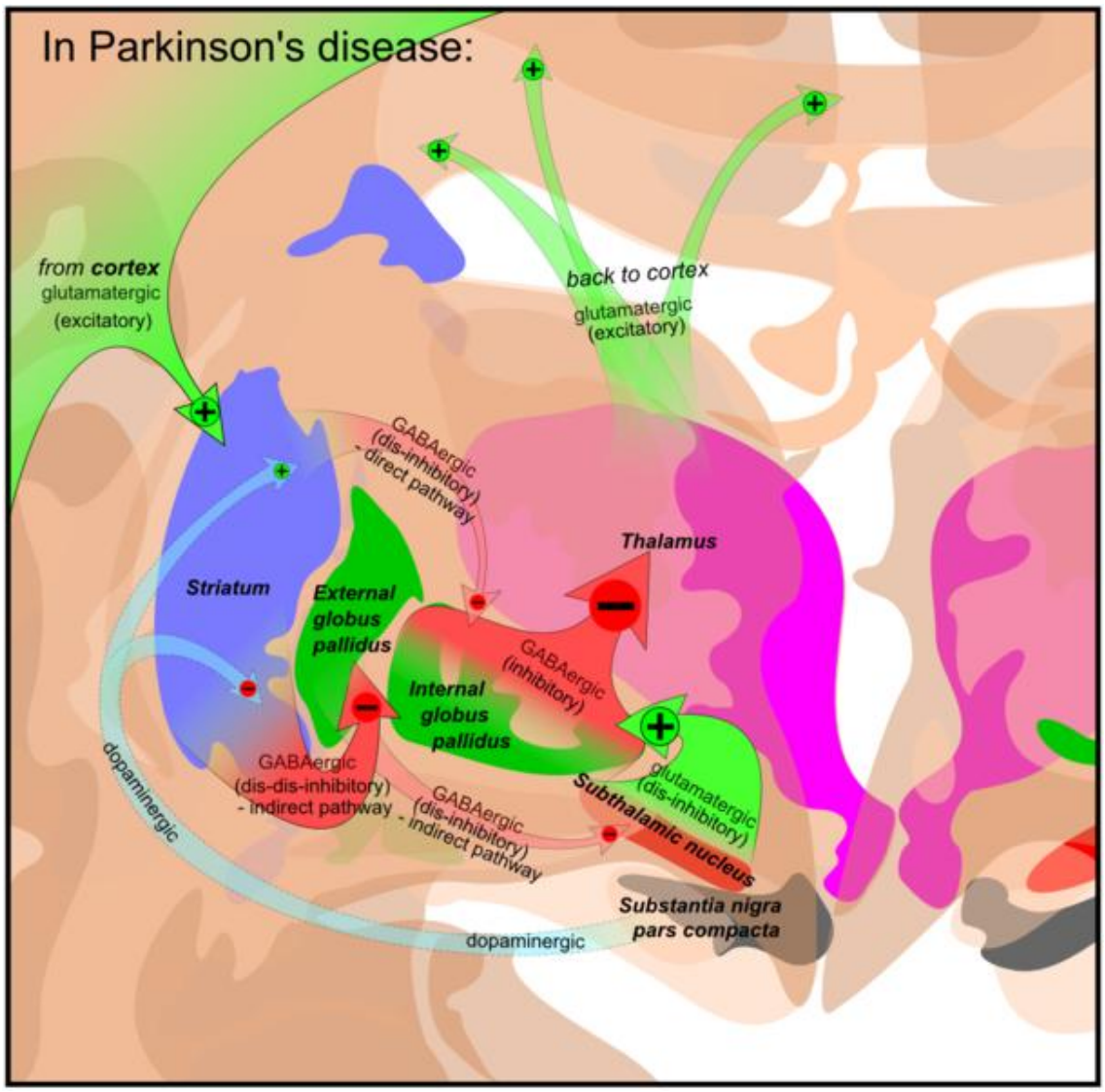

Figure 1.3 – Schematic of motor control pathways in the basal ganglia under conditions of Parkinson's disease.

Figure reproduced without changes and with permission from [8].

In part due to this discovery, the connectivity and organization of mammalian midbrain neurons have been extensively studied and reviewed [9]. It has since been determined that the pathogenesis of PD affects many brain regions prior to reaching dopaminergic regions of the mesencephalon, including dorsal motor nuclei of the glossopharyngeal and vagus nerves as well as the anterior olfactory nucleus, followed by an ascending course in the brain stem, reaching dopaminergic regions of the mesencephalon and sensory association areas in later phases [10].

While the degeneration of DA neurons alone does not wholly recapitulate the early lesions that occur in PD, it has been well established that the key motor symptoms of PD are the consequence of DA degeneration.

1.1.1. Pharmaceutical and Molecular Interventions

Currently, the most commonly used treatment for PD is levodopa (L-DOPA), which surviving DA neurons can convert into dopamine. This replenishment of dopamine provides temporary relief for the motor dysfunctions characteristic of PD [11-13]. However, L-DOPA suffers from a key disadvantage since it loses its efficacy over time, and long-term administration does not counteract the progressive nature of PD, with symptoms worsening as DA neurons continue to die and degenerate [13].

Other molecular interventions seek to prolong the presence or effect of dopamine on denervated targets. Dopamine receptor agonists, such as bromocriptine, ropinrole, and pramipexole, bind to post-synaptic receptors, with similar therapeutic effects as levodopa, and do not require enzymatic conversion or depend on functional capacity of nigrostriatal neurons [14]. However, these have been noted to be less efficacious in treating motor symptoms compared to levodopa, and result in undesirable side effects including nausea, hallucinations, dizziness, and insomnia, as well as addiction and other behavioral changes [14, 15]. Due to the shortcomings of existing molecular interventions, there is a need for more comprehensive therapeutic approaches to PD that go beyond relieving dopamine deficiency, by offering a longer-term solution and by restoring neuronal feedback circuits for improved motor function recovery.

1.1.2. Deep Brain Stimulation

Surgical interventions have been developed for PD patients whose motor symptoms are not adequately controlled by medication or cannot use medication. The most commonly used surgical treatment implemented for PD is deep brain stimulation, where a neurostimulator is implanted into specific parts of the brain including the subthalamic nucleus or the globus pallidus interna [16, 17] (**Figure 1.4**).

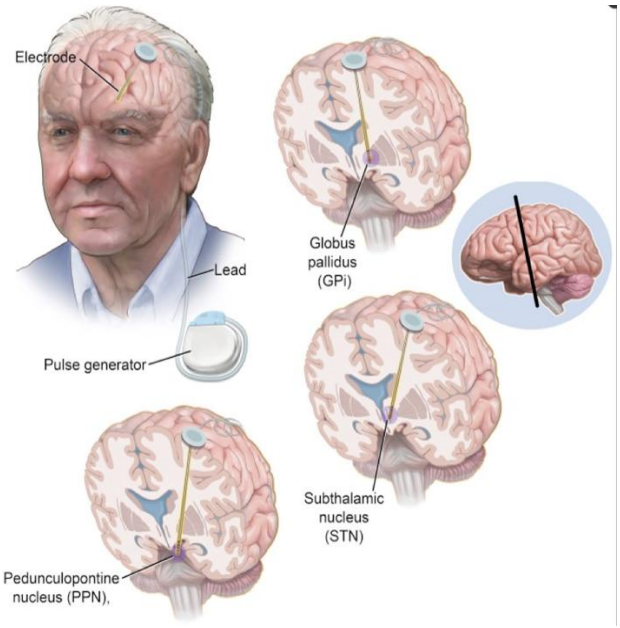

Figure 1.4 - Schematic depicting common targets of deep brain stimulation for PD treatment.

Figure reproduced with permission from [18].

It is understood that deep brain stimulation has comparable efficacy to surgical ablation of the stimulated regions of the brain, the globus pallidus interna or subthalamic nucleus, through pallidotomy or thalamotomy respectively [19], however, the exact mechanism of action for this inhibition is not well understood. Deep brain stimulation however is more desirable than these surgical interventions and is suitable for use with more aged patients, as the stimulation parameters can be adjusted as symptoms change. While deep brain stimulation reflects a more circuit-based and long-term approach towards addressing motor symptoms of PD, patients receiving deep brain stimulation have been reported to experience behavioral changes and impulse control disorders including weight gain [15, 20, 21]. Additionally, as an implanted medical device, deep brain stimulators are subject to hardware complications, as they can cause foreign body responses or become displaced [22].

1.1.3. Cell Replacement Therapies

The temporary effectiveness and undesirable side effects of the most common current treatments for PD, levodopa and deep brain stimulation, indicate that DA neuronal deficits must be addressed comprehensively and directly. Cell replacement of DA neurons via transplantation presents a promising, circuit-based, and potentially longer-lasting therapeutic option to address motor symptoms of PD (**Figure 1.5**).

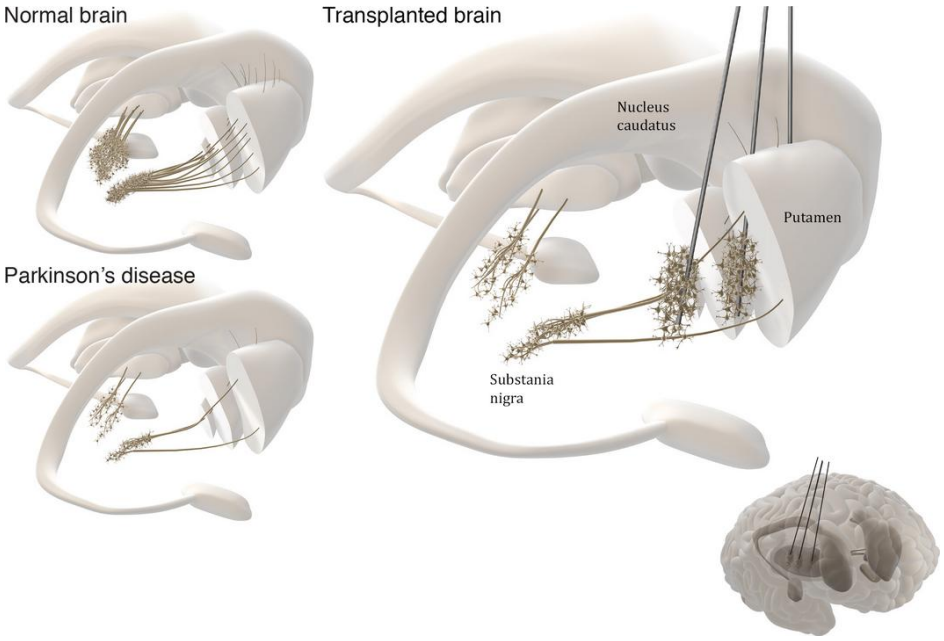

Figure 1.5- Schematic depiction of the principle of cell replacement therapy for addressing DA neuronal deficits in PD.

Compared to healthy brains, PD patients suffer from DA neuronal death in the substantia nigra and denervation of the striatum and putamen. By transplanting new DA neurons into the putamen motor impairment can be ameliorated. Figure reproduced with permission from [23].

Many previous lab and clinical studies have investigated the idea of transplanting DA producing cells to replenish DA deficits in the striatum. As early as 1979 it was reported that grafts of fetal mesencephalic tissue, rich in DA neurons, alleviated PD symptoms in PD model rats [24, 25]. The translation of these results faced practical and ethical issues over whether it were possible to isolate the ventral mesencephalon of fetal tissue, and whether the use of tissue from

aborted fetuses was morally justified. In response to these concerns, early clinical trials, pioneered by Backlund et. al., transplanted adrenal medulla cells, but observed limited beneficial effects [26, 27]. Promising results emerged from preclinical trials performing intrastriatal transplantation of human fetal mesencephalic tissue [28], demonstrating proof of the concept of cell replacement therapy to address motor symptoms of PD. However, some studies continued to not observe beneficial results with these techniques, with some observing the development of troubling dyskinesias in graft recipients [29]. Since then, some reviews of studies on graft-induced dyskinesia suggest that the cause of these graft-induced dyskinesias may be due to excessive innervation by serotonergic neurons within grafted tissue [30-32]. These results suggest that future cell transplantation efforts should seek to encourage the survival of DA neurons transplanted into diseased striatum and reduce the presence of other contaminating neuronal subtypes.

One especially attractive cell source for neural tissue engineering applications is human induced pluripotent stem cells (IPSCs), due to their ability to differentiate into many different neural cell types and their ability to expand in culture [33-40]. IPSCs can be converted into specific subtypes of neurons in a number of ways, however, one especially rapid method was developed by Wernig et al, in which adult somatic cells and pluripotent stem cells were directly converted to functional, mature neurons using lentivirus-based expression of several critical neuronal transcription factors, particularly *Brn2, Ascl1*, *Myt1l* and *NeuroD1* (also known as "BAMN" factors) [41, 42]. This neuronal reprogramming approach has been observed to yield functionally mature neurons much more rapidly and with high conversion efficiency, relative to traditional differentiation protocols [42-45]. With the ability to control the differentiation of IPSCs into specific subtypes, IPSCs have great potential as a therapeutic in PD (**Figure 1.6**).

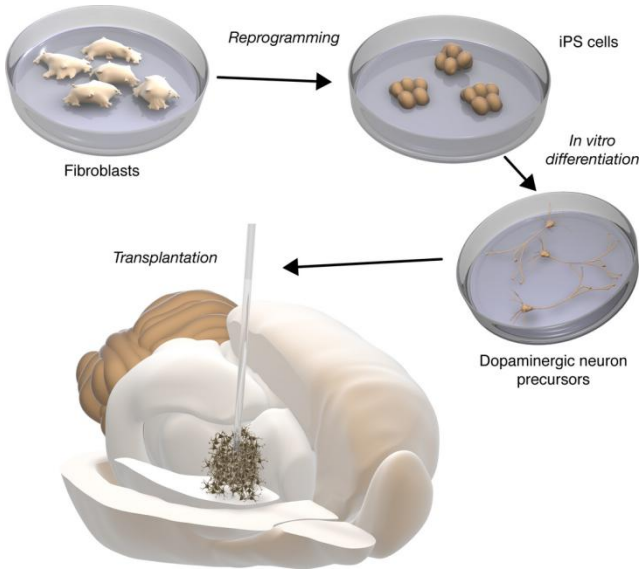

Figure 1.6 - Schematic depiction of the conversion of patient-derived somatic cells into pluripotent stem cells and finally transplantable DA neuron precursors or mature DA neurons.

Figure reproduced with permission from [23].

Mature DA neurons differentiated from IPSCs have been transplanted into a mouse PD models, with some functional motor recovery observed [43] (**Figure 1.7**). However, key remaining obstacles that limit functional recovery are the survival and functional integration of transplanted dissociated neurons, and the potential risk of transplanting undifferentiated and possibly tumorigenic cells. In this dissertation work, we address these limitations by advancing innovative cell transplantation platforms based on functionalized, multicellular spatially organized assemblies of human neurons.

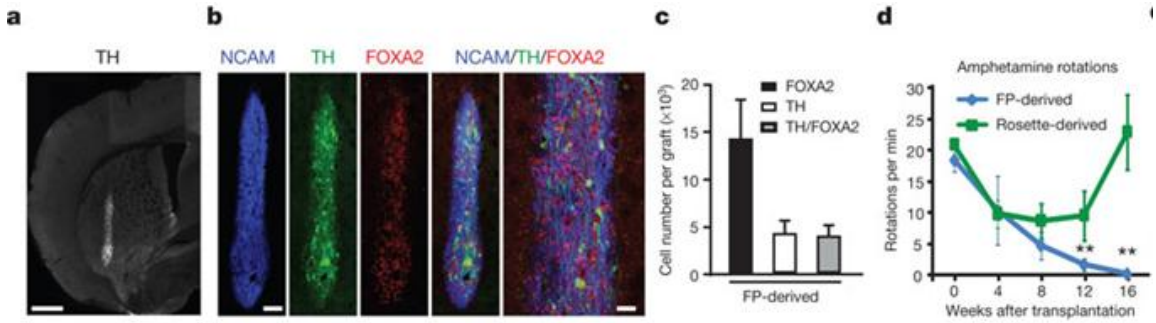

Figure 1.7 - Transplantation of pluripotent stem cell-derived DA neurons and alleviation of motor symptoms in PD model mice.

a-c, Transplanted human pluripotent stem cell-derived DA neurons survive months after transplantation into immunocompromised mouse striatum and continue to express mature midbrain DA markers. **d**, Different differentiation procedures yield DA populations of different efficacies at reducing motor symptoms in PD model mice. Figure adapted with permission from [43].

1.2 Neuroinflammation & Synucleinopathy

Two additional key features of PD pathogenesis are chronic neuroinflammation and the abnormal intraneuronal accumulations of α-synuclein (ASYN) in Lewy bodies, both factors that believed to contribute to neuronal loss and dysfunction [46, 47].

The proposed mechanism of how neuroinflammation contributes to progressive DA neurodegeneration is based on observations of the physiology of DA neurons and microglia in the brain. Advancements in the understanding of toxins such as 6-hydroxydopamine (6-OHDA), rotenone, and 1-methyl-4-phenyl-1,2,3,6-tetrahydropyridine (MPTP) have revealed that oxidative stress is an important contributor towards DA neuronal death [48]. DA neurons have reduced antioxidant capacity, which renders them susceptible to oxidative stress to a greater degree relative to other cell types within the brain [49-51]. A prominent source of such oxidative stress in the CNS are immune cells such as microglia, which produce reactive oxidative species and other neuroinflammatory agents when activated. The substantia nigra, a key site of DA neurodegeneration, contains a 4.5-fold larger population of microglia compared to other regions of the brain [52], further corroborating the hypothesis that activation of microglia is an important contributor to neuroinflammation and DA neurodegeneration. Cell debris from dying DA neurons can further attract and activate microglia, resulting in a self-perpetuating cycle of inflammation and neurotoxicity (**Figure 1.8**).

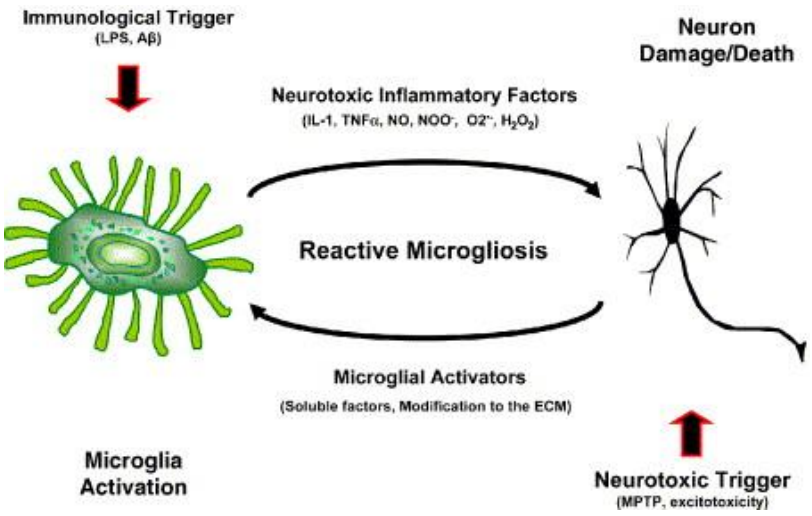

Figure 1.8 – Reactive microgliosis is a self-perpetuating cycle involving activated microglia and dying neurons.

Many possible intial toxic insults can cause microglial activation or neuronal toxicity. With sustained contributions of immunological triggers or neurotoxic triggers or decreased ability to eliminate these insults, reactive microgliosis can contribute to progressive neuronal damage and death. Figure reproduced with permission from [49].

While it is not well understood how abnormal protein inclusions propagate within the brains of PD patients, a possible mechanism has been advanced through studies that uncovered mutations associated with familial forms of PD. Familial PD affected proteins include ASYN (a protein found in synapses throughout the nervous system), parkin (a ligase which ubiquitinates proteins targeted for degradation), LRRK2 (Leucine-rich repeat kinase 2, which associates with parkin and is a key component of the lysosomal pathway), and UCH-L1 (ubiquitin carboxy-terminal hydrolase L1, another key element of neuronal ubiquitination pathways) [53, 54]. Disruptions to protein clearance pathways caused by the mutations mentioned above [55-57] or by overabundance of ASYN [58] have been observed to result in dramatic increases in extracellularly released ASYN [59]. Elevated levels of extracellular ASYN could in turn contribute to the interneuronal spreading of pathological ASYN species (**Figure 1.9**).

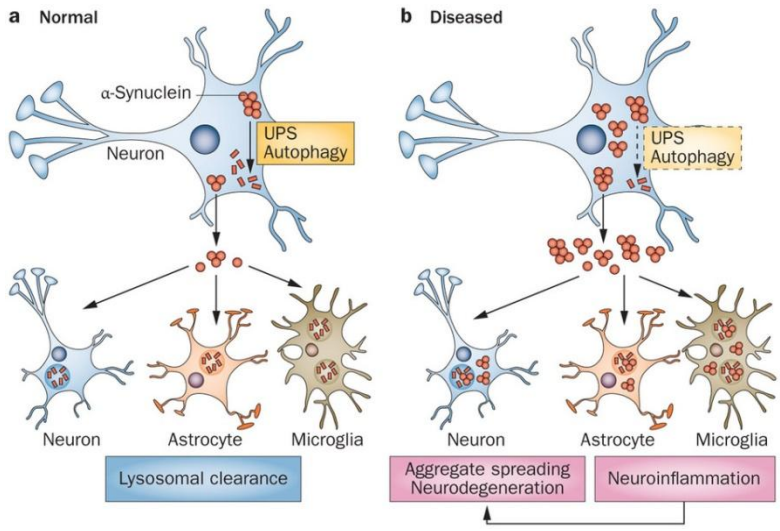

Figure 1.9 – Schematic depicting physiological and pathogenic dysregulated processing of α-synuclein (ASYN).

a, healthy neurons are capable of degrading ASYN through a set of pathways, with some small amount of ASYN released into the extracellular space, to be taken up by neighboring neurons and glia. **b**, however, in diseased neurons, ASYN degradation is impaired, resulting in increased ASYN and aggregated ASYN release into the extracellular space. Once in the extracellular space, aggregated ASYN can go on to potentially seed further aggregate formation and activate glia. Figure reproduced with permission from [60].

1.2.1. Interventions and Targets for Microglial Activation

Some previous research efforts have attempted to achieve a general decreased inflammatory response in microglia, for instance, using peroxisome proliferator-activated receptor gamma (PPAR-γ) agonists or nonsteroidal anti-inflammatory drugs (NSAIDS) [61-65]. However, clinical trials with these drugs have had generally disappointing results [65]. PPAR-γ agonists are noted to increase insulin sensitivity, which could be an undesirable side effect in PD treatment [66]. Additionally, multiple meta-analyses demonstrated an association between PPAR- γ agonists and increased risk of heart failure, peripheral edema, myocardial infarction, and death [66-68]. Therapies designed to decrease microglial activation should incorporate knowledge of specific interactions between microglial cells, toxins, and relevant receptors. In this

dissertation work, we advance a new therapeutic strategy specific to the mechanism of microglial activation in PD.

A number of toxins have been demonstrated to cause selective death of DA neurons both *in vitro* and *in vivo* [69-72]. While some of these agents act directly on DA neurons, some are capable damaging and killing DA neurons at concentrations where they no longer directly cause DA neuronal death, dependent on the presence of microglia (**Figure 1.10**). Identifying these "dual mode toxins" may be important to understanding the early pathogenesis of DA neurotoxicity in PD. One such specific contributor to microglial activation in the context of PD is believed to be ASYN, a key component of Lewy body pathology observed in PD neurons. A considerable body of work indicates that intercellularly transmitted ASYN from neuron-to-glia triggers microglial activation [70, 73-76], and chronic and excessive ASYN exposure has been observed to result in microglial secretion of neurotoxic substances including reactive oxygen species [77]. Based on these observations, in these studies we hypothesized that a synuclein binding competitor would aid in normalizing the dysregulated trafficking of synuclein by microglia and interfere with persistent microglial activation.

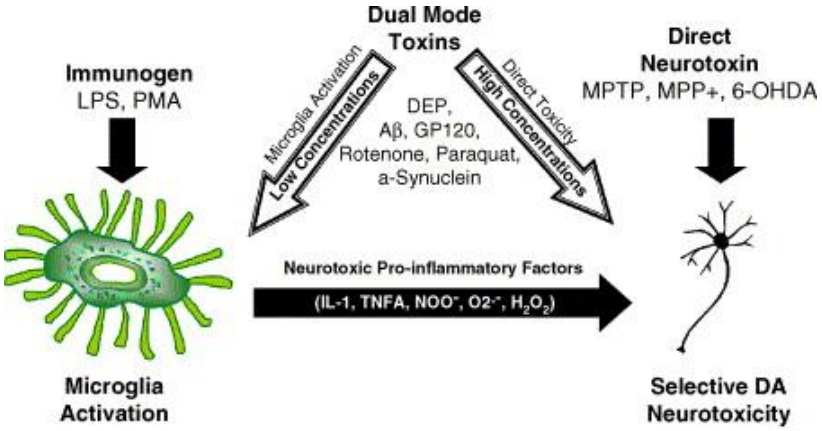

Figure 1.10 – Mechanism for selective microglia-induced DA neurotoxicity.

A number of toxins result in selective death of DA neurons by inducing the production of neurotoxic pro-inflammatory factors by microglia, while some toxins have direct effects on DA neurons. Alternatively, there are a number of toxins that are capable of direct DA neurotoxicity, but can continue to selectively harm DA neurons through their ability to activate microglia. Figure reproduced with permission from [49].

1.2.2. Synucleinopathy Interventions

Toxic oligomers of ASYN can cause a wide range of harm to neurons, resulting in decreased synaptic activity, neurite retraction and death (**Figure 1.11**). The deposition, further aggregation, and intercellular transmission of aggregated ASYN may play a major role in the progressive neuronal dysfunction observed in PD patients, therefore, a valuable therapeutic approach would target key steps in the ASYN aggregation process. A number of intracellular factors are known to contribute to ASYN aggregation, including low local pH [78], level of expression [79] high calcium concentrations [80], restricted space and high macromolecule

concentrations [81, 82], and phosphorylation [83].

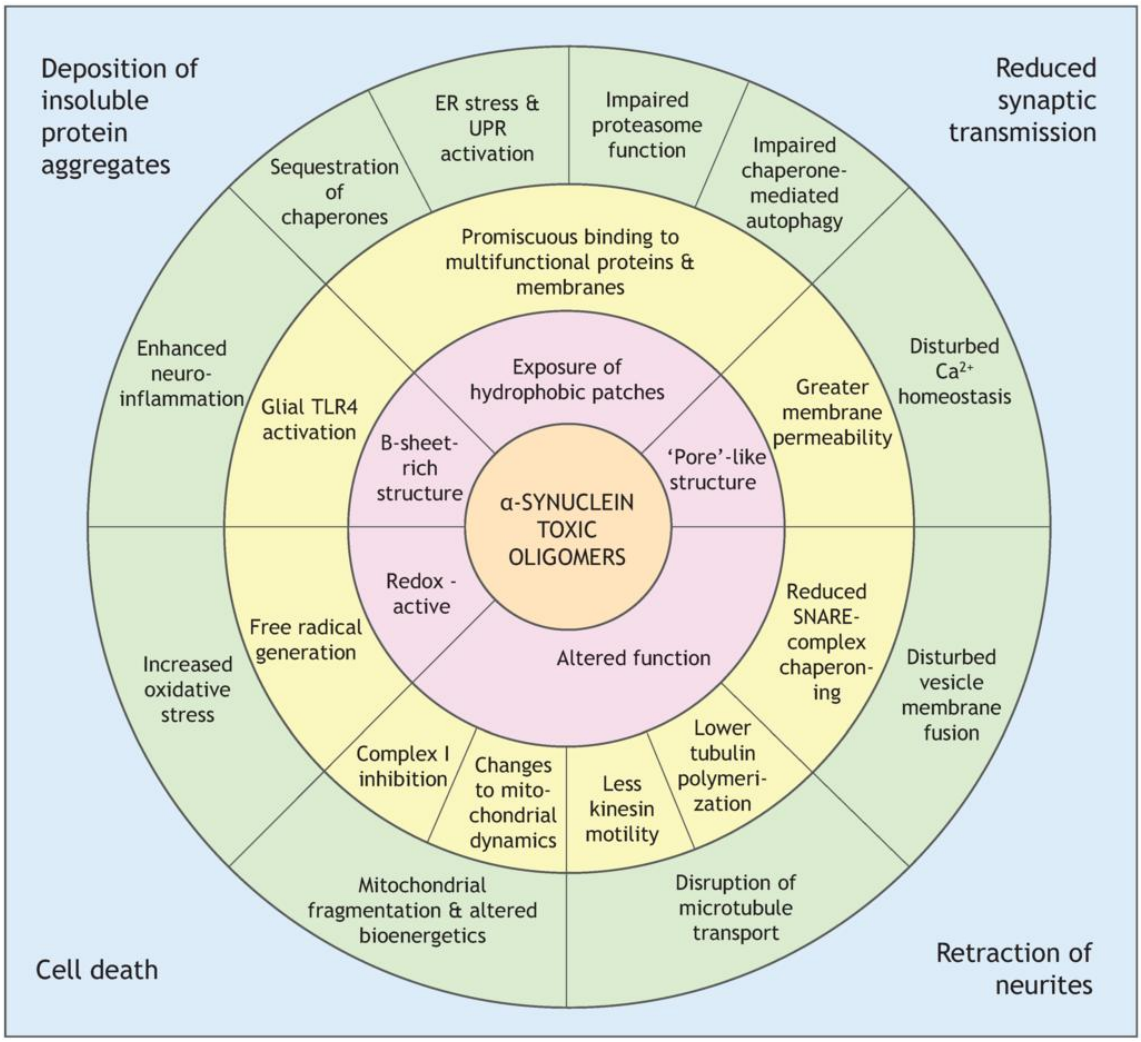

Figure 1.11 – Potential links between ASYN oligomers and pathological cellular outcomes.

The inner circle (pink) here depicts properties of ASYN oligomeric species that may contribute to their toxicity. The middle circle (yellow) cidepicts molecular effects that ASYN oligomers may cause due to these properties. The outer circle (green) depicts cellular systems that may be disrupted as a result of the described molecular events. The outer box (blue) depicts cellular outcomes of the described disrupted cellular systems. Figure reproduced with permission from [84].

Previous research efforts have been devoted to counteract some of these factors in order to decrease the risk of ASYN aggregation. For instance, RNA interference has been demonstrated to have much success in knocking down expression of target genes, and the level of ASYN appears to be a critical part of PD pathogenesis since multiplication of its gene locus has been observed to result in the autosomal dominant form of PD. Due to these observations, some believe that RNA-based therapies may have promise in reducing ASYN levels and as a result, ASYN aggregation. Kabaria et. al. found that microRNAs miR-34b and miR-34c inhibit the expression of ASYN in neuronal cells, and that inhibition of these microRNAs result in increased ASYN aggregate formation [79]. However, microRNA-based therapeutics face several challenges, including possible off-target effects, disrupting normal neuronal function, and delivery of the molecules to appropriate cells within the nervous system and across the blood-brain barrier. An alternative to regulating the post-transcriptional expression of ASYN with microRNAs would be to disrupt post-translational modifications to ASYN that result in aggregation, such as phosphorylation. Lee et. al. identified that ASYN phosphorylation and aggregation in mice brains could be reduced through a diet supplemented with eicosanoyl-5-hydroxytryptamide, an extract from coffee which enhanced phosphoprotein phosphatase 2A methylation and activity [85]. While approaches of this nature have shown promise, they have largely focused on intracellular aggregation within neuronal cells. On the other hand, microglia have been demonstrated as the primary cell type responsible for rapidly internalize and degrade ASYN, making them a natural target for regulating ASYN trafficking and associated neuroinflammation [86]. Under physiological conditions, microglia play a role in the clearing of ASYN. In this dissertation work, we advance microglia as a key target in the process of ASYN aggregation and transmission in PD, and hypothesize that a synuclein binding competitor will reduce intracellular aggregation of ASYN within microglia.

1.3 Thesis Overview and Hypothesis

The objective of this thesis is to examine therapeutic approaches in addressing major components of PD: neurodegeneration, neuroinflammation, and synucleinopathy. The central hypotheses of this work are that three-dimensional (3D) microenvironments with tuned properties can control cell-cell and cell-material contacts, improving transplanted cell performance when transplanted into the brain; and that regulating ASYN interactions with microglia will decrease ASYN-mediated activation and intracellular aggregation. To test these hypotheses we created the following three specific aims:

1) To elucidate 3D synthetic microenvironment properties that enhance neuronal population survival, maturation, and functionality *in vitro* and post-transplantation *in vivo*.
2) To develop a synthetic ASYN binding competitor and examine the effects on intracellular aggregation
3) To develop synthetic nanotherapeutic technologies to reduce ASYN-mediated microglial activation

In all studies investigating design of synthetic 3D microenvironments for the support of neuronal populations, reprogrammed IPSCs were used as a cell source due to their expandable nature, relatively fast maturation, and since in the future these could be recipient-derived. Chapter 2 describes studies culturing these reprogrammed neurons on polymeric microfibrous electrospun substrates. These substrate allowed us to investigate the effects of substrate geometry on neuronal populations prior to transplantation; we found that tuning cell-cell contacts by tuning the geometry of microfibrous substrates affected neuronal maturation. We also investigated the ability of these substrates to serve as cell transplantation scaffolds *in vivo*, comparing cell survival and immune cell recruitment for scaffold-supported neuronal populations versus dissociated cell transplantation. We found that these scaffolds improved survival of transplanted neuronal populations by at least an order of magnitude over dissociated cell transplantation. In Chapter 3, we first identify scavenger receptors as a receptor for ASYN, and design a nanotherapeutic targeting this interaction in order to reduce microglial activation and ASYN aggregation. We

found that synthetic sugar-based amphiphilic macromolecules targeting scavenger receptors could reduce ASYN internalization and intracellular aggregation by microglia. In Chapter 4, we find that that scavenger-based delivery of antioxidants could decrease microglial activation in response to aggregated ASYN *in vitro* and *in vivo*. In Chapter 5, we discuss continuing studies building on our findings in these three valuable therapeutic trajectories. Overall, these studies provide a valuable foundation for design of future therapies to counteract fundamental aspects of PD, namely neurodegeneration, synucleinopathy, and neuroinflammation, and may be applicable in broader central nervous system disease contexts as well.

CHAPTER 2 – CULTURE AND TRANSPLANTATION OF REPROGRAMMED HUMAN NEURONS INTO THE BRAIN WITH 3D MICROFIBROUS SCAFFOLDS

With permission from the publisher, figures and major sections presented in this chapter have been excerpted from the following work:

Carlson A.L.*, **Bennett N.K.***, Francis N.A., Halikere A., Clarke S., Moore J.C., Paradiso K., Pang Z.P., Hart R.P., Moghe P.V. Generation and transplantation of reprogrammed human neurons in the brain using 3D microtopographic scaffolds. *Nature Communications* 7:10862 (2016).
*Denotes equal first author contribution

Abstract

Cell replacement therapy with human pluripotent stem cell-derived neurons has the potential to ameliorate neurodegenerative dysfunction and central nervous system injuries, but reprogrammed neurons are dissociated and spatially disorganized during transplantation, rendering poor cell survival, functionality and engraftment *in vivo*. Here we present the design of 3D microtopographic scaffolds, using tunable electrospun microfibrous polymeric substrates that promote *in situ* stem cell neuronal reprogramming, neural network establishment, *and* support neuronal engraftment into the brain. Scaffold-supported, reprogrammed neuronal networks were successfully grafted into organotypic hippocampal brain slices, showing a ~3.5-fold improvement in neurite outgrowth and increased action potential firing relative to injected isolated cells. Transplantation of scaffold-supported neuronal networks into mouse brain striatum improved survival ~38-fold at the injection site relative to injected isolated cells, and allowed delivery of multiple neuronal subtypes. Thus, 3D microscale biomaterials represent a promising platform for the transplantation of therapeutic human neurons with broad neuro-regenerative relevance.

2.1 Introduction

With the exciting development of subject specific IPSCs, cell-replacement therapies could be poised to resolve the functional deficits of neurodegenerative diseases using functional, regional- and subtype-specific neurons [43]. However, four critical barriers remain: (a) lack of an effective cell source of human neurons; (b) poor survival of transplanted cells *in vivo*, which remains a bottle-neck, with reported survival rates of less than 10% [43], (c) lack of control over differentiation, maturation, or subtype outcome of transplanted cells and (d) limited or sporadic interactions of grafted neurons with the host neural network. In order to address these barriers, we believed that the design of a microenvironment that could support the culture and maturation of neuronal populations *in* vitro would be a first step in our efforts towards developing a scaffold that could support neuronal populations transplanted *in vivo*. We hypothesized that 3D fibrous microenvironment populated with IPSC-derived neurons will preserve and control cell-cell contacts, and as a result can manipulate the maturation of neuronal populations *in vitro*.

The recent discoveries of somatic cell reprogramming into IPSCs, and of IPSCs into mature neurons presents a promising simultaneous solution to the lack of cell sources of human neurons for transplantation and lack of control over differentiation [41, 42, 87, 88]. Among the findings by Zhang et. al. was that the single neuronal transcription factors NeuroD1 was sufficient to induce neuronal character in human IPSCs [88]. As a proof of concept, our studies focused on the culture and transplantation of neuronal populations generated via inducible expression of NeuroD1 in IPSCs, which we have observed to generate primarily glutamatergic excitatory neurons. In this chapter, we employ these techniques to rapidly generate neuronal populations to test multiple substrates' ability to culture reprogrammed human neurons.

Much previous work has demonstrated the importance of cell-cell contacts in the maintenance of pluripotent stem cells, differentiation processes, and neuronal population function. Embryonic and pluripotent stem cells initially were both necessarily co-cultured on a feeder layer of mitotically inactivated fibroblasts [89, 90]. Additionally, enzymatic detachment and dissociation of pluripotent stem cells for routine passaging was typically accompanied by

large amounts of cell death until the discovery and supplementation of rho-assisted kinase (ROCK) inhibitor Y-27633 [91]. This discovery not only led to the widespread use of ROCK inhibitor in pluripotent cell culture, but also elucidated the importance of E-cadherin mediated cell-cell contacts in pluripotent cell survival. Upon disruption of E-cadherin-based cell-cell contacts, the Rho-ROCK-myosin pathway becomes activated, culminating in myosin hypercontractility and ultimately cell death [92, 93], hence the effectiveness of ROCK inhibitors in preventing cell death upon dissociation. Similar effects have been observed in neuronal cultures, with cell-cell signaling via hemophilic binding proteins such as N-cadherin or L1 mediating a wide range of critical cell behaviors including differentiation [94], cell adhesion, synaptogenesis and synaptic plasticity, neurite outgrowth, dendritic arborization, , and survival [95, 96].

While cell-cell contacts have been demonstrated to be important to pluripotent cell maintenance, there is increasing evidence that some elements of the support provided by neighboring cells can be adequately replaced by appropriate media and matrix components. The earliest feeder-free pluripotent stem cell culture system used culture media conditioned by fibroblasts and tissue culture dishes treated with Matrigel, a basement membrane mixture derived from Engelbreth-Holm-Swarm mouse sarcoma cells [97]. While Matrigel has become widely used in the culture of pluripotent stem cells, it is animal in origin and generally undefined, with risk for immune response when transplanted in vivo [98]. Due to these obstacles, researchers have dedicated efforts to creating fully defined and humanized culture substrates based on receptors found to be expressed by pluripotent stem cells. Based on knowledge of the specific integrins expressed by pluripotent stem cells, it was found that pluripotent stem cell culture could be maintained on surfaces functionalized with single recombinant proteins vitronectin, laminin isoforms, or integrin-engaging peptides [99-101]. Previous work in our lab has found that pluripotent stem cells cultured in 3D microfibrous electrospun scaffolds are capable of secreting similar extracellular matrix proteins capable of maintaining their survival and undifferentiated state [102] (**Figure 2.1**).

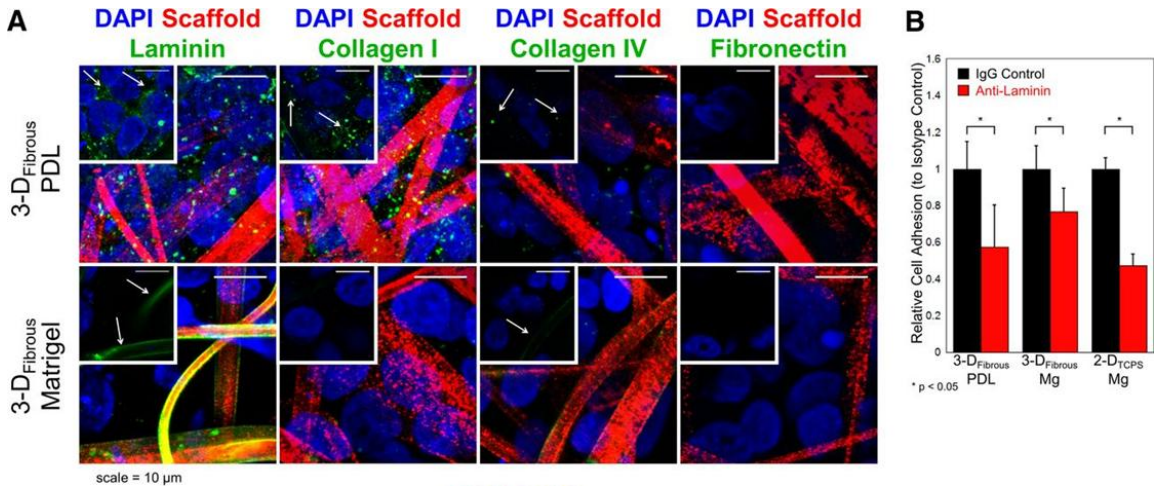

Figure 2.1 – Pluripotent stem cells are capable of surviving in and remodeling microfibrous substrates.

A) human embryonic stem cells produced laminin, collagen type I and collagen type IV in polycation-treated 3D microfibrous scaffolds, but not in Matrigel-treated 3D microfibrous scaffolds. B) Initial cell adhesion and survival was dependent on stem cell binding to secreted laminin. Figure adapted with permission from [102].

Additionally, it was found in our lab that controlled display of cell-cell signaling molecules N-cadherin and L1 on 3D fibrous scaffolds enhanced survival and neurite outgrowth and differentiation [103]. These findings combined suggest that 3D synthetic microenvironments may be able to support the culture of neuronal and pluripotent cell populations, as well as their transplantation if functionalized with appropriate extracellular matrix proteins.

A number of both natural and synthetic biomaterials have been studied for applications in CNS repair. Some natural polymers used include alginate [104], agarose [105], fibrin [106, 107], hyaluronic acid [108], and collagen [109], of which there are also a number of commercially available scaffolds for use in peripheral nerve injury, including NeuroMend [110] and NeuraGen

[111]. While natural materials seem like attractive candidates for scaffold design given that they have physiologically suitable mechanical properties and can be readily remodel led by host cells, they are also subject to high batch variability, are difficult to sterilize and can trigger host immune response. To overcome these challenges, a number of synthetic polymers have been investigated, including poly(lactic-co-glycolic acid) [112], poly(ethylene glycol) [113], and poly(ε-caprolactone) [114]. However, synthetic polymers often have undesirable degradation properties, either having difficulty degrading or forming toxic byproducts. Additionally, synthetic polymers often need to be functionalized with polycations or extracellular matrix proteins in order to permit cell-material adhesion and interaction. We have taken these obstacles into consideration in the selection and design of our biomaterial substrates and scaffolds. In this chapter, we investigated a promising class of 3D synthetic fibrous microenvironments, microfibrous electrospun scaffolds comprised of tyrosine-derived polymers with tunable properties, as possible culture systems for reprogrammed neurons.

The biomaterial we chose to investigate was first developed in the lab of Dr. Kohn last the NJ center for biomaterials as part of a combinatorial library of polymers [115]. The base polymer of this library of tyrosine-derived polycarbonates, poly(desaminotyrosyl tyrosine ethyl ester carbonate) (pDTEc) (**Figure 2.2A**) can be copolymerized with poly(ethylene glycol) (PEG) or desaminotyrosyl tyrosine (DT), which can confer hydrophilicity or negative charge, respectively. Varying the ratio of these three polymers, pDTEc, PEG, and DT, can influence a wide range of polymer properties, including hydrophilicity, mechanical stiffness, degradation rates, and adsorption of proteins [116-118]. Due to the high potential for future optimization of scaffold properties, we chose to focus on the base polymer pDTEc as a material for neuronal cell scaffolds. This polymer has demonstrated ability to support pluripotent stem cell populations when fabricated in an electrospun fibrous format [102], seen in **Figure 2.2B-C** and Figure 2.1. We intend to build on these studies by exploring the capability of microfibrous pDTEc substrates to support the culture of neurons reprogrammed from IPSCs.

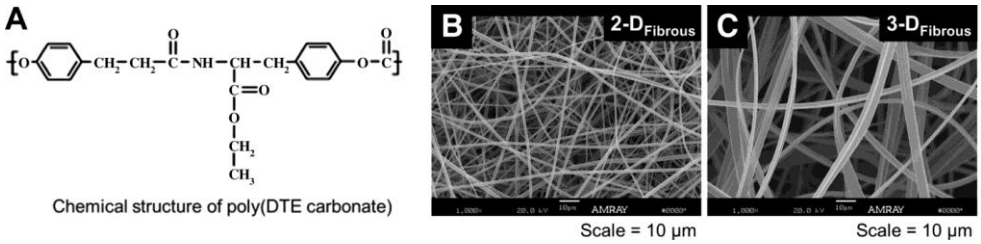

Figure 2.2 – Chemical structure and fabrication of microfibrous substrates from pDTEc.

A) The chemical structure of pDTEc is depicted. B-C) This polymer can be electrospun into substrates with varied microfibrous geometries, based on the electrospinning parameters used. Figure reproduced with permission from [102].

The overall process of cell transplantation into the brain consists of a number of steps, including 1) initial cell culture, 2) loading of cells into injection devices or syringes, 3) injection of cells, and 4) interaction with host tissue. Each step in this process presents unique challenges to cell survival and integration with host tissue. In the previous chapter we discussed the design of synthetic 3D fibrous scaffolds that supported the initial culture of neuronal populations, where cultured neuronal cells showed high viability as well as phenotypic and functional maturity. In this chapter, we hypothesize that 3D fibrous culture substrates can be prefabricated into injectable forms that enhance survival and integration of neuronal populations post-transplantation *in vivo*.

Conventional adherent cell culture is conducted on 2D tissue culture treated vessels, meaning the loading of cells cultured in this manner into injection devices or syringes necessitates detachment from these vessels. Transplantation efforts using 2D-cultured cells have typically used enzymatic means to detach cells, disrupting both cell-substrate as well as cell-cell interactions. This is undesirable, since as was mentioned previously, cell-cell interactions are known to play a role in cell survival via E-cadherin mediated pathways, and in neuronal function and maturation via hemophilic cell signaling molecules like N-cadherin or L1. One possible solution to this obstacle may be the culturing of neuronal cells in suspension as floating neurospheres, not attached to any tissue culture vessel, an approach that has been often applied

with neural stem cells [119-121]. Cells cultured in this manner would not require enzymatic detachment for loading into injection devices. However, neurospheres often form a heterogeneous mix of cell types *in vitro* and *in vivo* owing to spatial differences in cell contact, cell density, and nutrient availability [119, 121, 122]. We believe that prefabricated injectable scaffolds will obviate the need for dissociation of cell-cell contacts, resulting in improved transplant survival and functionality.

Several studies have used scaffolds to support cell transplantation into the CNS. Commonly studied forms of such a scaffold are gels of ECM protein that are either shear thinning [123, 124] or cross-linked post-transplantation [125, 126]. These forms of scaffold can provide cells with structural support [125, 126] or growth factors [127, 128] during initial culture and post-transplantation. However, for these gels to be injectable they must exist in a fluid-like state. Injected cells within these gels likely suffer from a disruption to cell-cell and cell-material interactions that were formed during initial culture, similar to detachment of cells from conventional 2D culture substrates. To address this challenge, we hypothesized that microscale prefabricated scaffolds could be used for the culture and intact injection of neuronal populations.

Previous research has found that survival and functionality of transplanted DA neurons in PD model mice improves with greater numbers of transplanted cells [129]. However, reported transplanted neuron survival rates are typically under 10%, with some on the order of 0.1% [43, 88], suggesting that many transplanted neurons may not survive initial transplantation or succumb to stresses in the host transplant site environment. Debris from dead or dying transplanted cells can create stress for other local cells, potentially translating into dysfunction, poor integration, and overall poor performance of surviving transplanted cells. While some functional improvements have been observed with DA neuron transplantation, the exceptionally low survival rate typically observed through dissociated neuron transplantation suggests that there may be much room for further improvement. We hypothesize that reducing cell death during transplantation by using microscale prefabricated and injectable scaffolds will improve transplanted cell survival, integration, and function post-transplantation.

2.2 Materials and Methods

2.2.1. Lentivirus production

The lentiviral constructs rtTA-FUW, Tet-O-FUW *NeuroD1*, Tet-O-FUW *EGFP,* Tet-O-FUW *Ascl1*, Tet-O-FUW *Nurr1*, Tet-O-FUW *Lmx1a*, Tet-O-FUW *Pitx3*, Tet-O-FUW *EN1*, Tet-O-FUW *Foxa2*, and the packaging plasmids pMDL.g/pRRE, pMD.2 (VSVg), and RSV-REV were constructed by the Marius Wernig laboratory at Stanford University. Lentivirus particles were generated by first transfecting 293FT cells by the calcium phosphate precipitation method with each of the three packaging plasmids and one of the lentiviral plasmids in standard 293FT medium, which consists of DMEM supplemented with 10% fetal bovine serum (FBS), 1% non-essential amino acids (NEAA) (all from Life Technologies, Carlsbad, CA) and 1% penicillin/streptomycin (Lonza, Walkersville, PA)[41]. Medium is replaced after 24 hours and medium containing viral particles is collected at 48 and 72 hours. Viral particles are concentrated 200x by ultracentrifugation at 25,000 RPM for 2 hours at 4°C, and stored at -80°C until use.

2.2.2. iPS cell culture and neuronal conversion

Human IPSCs were obtained from the Rutgers University RUCDR® Infinite Biologics. IPSCs were derived from human foreskin fibroblasts by retroviral infection with Oct4, Sox2, Klf4, and c-Myc [130]. Human IPSCs were cultured on Matrigel treated dishes in mTeSR-1[102]. IPSCs were passaged with dispase every 5-7 days with manual removal of spontaneously differentiated areas with fire-polished glass pipets. IPSCs from passage 15-35 were used in these studies. IPSCs were passaged as single cells with Accutase (Stem Cell Technologies) plated at high density ($8x10^4$ cells/cm^2) in mTeSR-1 supplemented with 5 μM Y-27632 (R&D Systems, Minneapolis, MN) [131]. The following day, medium was replaced with mTeSR-1 with 5 μM Y-27632 and 2 μM polybrene (Sigma-Aldrich, St. Louis, MO) and concentrated virus was added (rtTA-FUW, Tet-O-FUW *NeuroD1*, and in some experiments, Tet-O-FUW *EGFP*). The following day, medium was replaced with mTeSR-1 and cells were returned to normal culture for up to 8 additional passages. To induce neuronal conversion, infected IPSCs (termed IPSC-RNs) were passaged with accutase and Y-27632, and the following day switched to an N2-based conversion medium (N2M) consisting of DMEM/F12, 2 mM L-glutamine, 1x N2 Supplement, 1x NEAA, 1%

penicillin/streptomycin, and 2 μg mL^{-1} doxycycline, which induces expression of the *NeuroD1* and *EGFP* constructs. Medium was replaced daily, and cells were replated on day 3-5 onto 2D or 3D substrates. One day after replating, medium was switched to NBM, consisting of Neurobasal medium, 2 mM L-glutamine, 1x B27 supplement without Vitamin A (Life Technologies), 0.2 mM Ascorbic acid, 1 μM cAMP (Sigma-Aldrich), 2 μg mL^{-1} doxycycline and 10 ng mL^{-1} each of Brain derived neurotrophic factor (BDNF), Glial cell-line derived neurotrophic factor (GDNF), and Neurotrophin-3 (NT-3) (Peprotech). Medium was replaced every 2-3 days for the duration of the experiments.

To generate dopamine (DA) iNs for co-culture studies, $2.5x10^5$ cells per 6 well plate were plated, and the following day medium was replaced with mTeSR-1 with 5 μM Y-27632, 2 μM polybrene, and concentrated virus was added (rtTA-FUW, Ascl1, Nurr1, Lmx1a, and in some experiments, Tet-O-FUW *RFP*). After three days, medium was replaced with Neurobasal media (Life Technologies) and concentrated virus (Pitx3, EN1, Foxa2). Four days after initial infection, the DA iNs would be co-seeded onto microscale scaffolds.

2.2.3. Electrospun fibrous substrate fabrication

Fibrous substrates and 2D polymer film controls were fabricated from tyrosine-derived polycarbonate poly(desaminotyrosyl tyrosine ethyl ester carbonate) (pDTEc) via electrospinning and spin-coating, respectively[102]. These polymers come from a combinatorial library of polymers with tunable hydrophobicity and degradation properties. pDTEc was dissolved in 1,1,1,3,3,3-Hexafluoro-2-propanol (HFIP, Sigma-Aldrich) at 9%, or 18% weight by volume. For the 9% weight by volume solution, 5% N,N-dimethylformamide (DMF) was added to prevent beading of fibers. Polymer solutions were electrospun from a +18 kV spinneret to a -6 kV flat plate collector at 3 mL hr^{-1}over a distance of 30 cm, resulting in fiber mats 250-500 μm thick. Surface morphology was observed on an AMRAY 1830 I scanning electron microscope (SEM). and fiber diameter was quantified by measuring 100 individual fibers from each fibrous substrate using NIH-ImageJ software (http://rsb.info.nih.gov/ij/). Quantitative data are presented as mean ± 95% confidence interval. Control 2D polymer films were prepared using a 1% polymer solution dissolved in tetrahydrofuran (THF), which was then spin-coated onto glass coverslips at 4,000

rotations per minute for 30 seconds [132]. For *in vitro* studies, electrospun fibers were sterilized by UV treatment, oxygen plasma treated for hydration, and adsorbed with 10 μg mL^{-1} poly-D-lysine (PDL) in HEPES buffer (pH 8.4) and 4 μg mL^{-1} laminin in PBS prior to seeding dissociated iNs 4 days after initiating neuronal conversion with N2M+dox.

2.2.6. Electrophysiology

Electrophysiolocial recordings were performed at prescribed time intervals from iN cells in 2D or 3D configurations in whole-cell mode using a Multiclamp 700B amplifier [41, 42]. The bath solution contained 140 mM NaCl, 5 mM KCl, 2 mM $MgCl_1$, 2 mM $CaCl_2$, 10 mM HEPES, and 10 mM glucose, at pH 7.4. The pipette solution for whole-cell voltage-dependent current recordings and for current-clamp experiments contained 10 mM KCl, 123 mM K-gluconate, 1 mM $MgCl_2$, 10 mM HEPES, 4 mM glucose, 1 mM EGTA, 0.1 mM $CaCl_2$, 1 mM K_2ATP, 0.2 mM Na_4GTP, pH 7.2. Membrane resting potentials were kept in the range of -65 to -70 mV, with step currents injected to elicit action potentials.

2.2.7. Immunocytochemistry

Neuronal phenotypes were characterized by immunocytochemistry (ICC) for 2D and 3D substrates. Cells were fixed with 4% paraformaldehyde for 30 minutes at room temperature, followed by three washes with PBS. Cells were simultaneously blocked and permeabilized in blocking buffer consisting of PBS supplemented with 5% normal goat serum (MP Biomedicals), 1% bovine serum albumin (BSA, Sigma-Aldrich), and 0.1% Triton X-100 (Sigma-Aldrich) for 1 hour at room temperature. Primary antibodies were incubated in blocking buffer at 4°C overnight, followed by three 15-minute PBS washes. Fluorophore-conjugated secondary antibodies (Alexa Fluor 488, 594, or 647, Life Technologies) were incubated in blocking buffer for 1 hour at room temperature, followed by three 15 minute washes and at least one wash of 1-2 hours. Samples were counter-stained with 4′,6-Diamidino-2-phenylindole dihydrochloride (DAPI, Sigma-Aldrich) to visualize nuclei and mounted with Prolong Gold Anti-Fade reagent (Life Technologies) prior to imaging. Samples were imaged on a Leica SP2 laser scanning confocal microscope using 10x dry or 63x immersion objectives. Images of cells on 3-D electrospun fibers are presented as maximum intensity projections of z-stacks, unless otherwise stated. Image

quantification was performed via custom ImageJ macros and manual counting. A complete listing of the primary antibodies used in this study can be found in Supplementary Table S2.1.

2.2.8. Calcium Imaging

iPS-iN cells were labeled with 3 μM Fluo-4 AM calcium indicator dye for 30 minutes at room temperature in extracellular bath solution (147 μM NaCl, 5 μM KCl, 2 mM $CaCl_2$, 2 mM $MgCl_2$, 10 mM HEPES, and 10 uM Glucose, pH 7.4 and osmolarity 290-300 mOsm) containing 0.02% pluronic F-127. After incubation, cells were rinsed twice with bath solution and incubated for an additional 30 minutes at room temperature to allow complete de-esterification of the Fluo-4 AM dye prior to imaging. Time-lapse imaging was performed on a Leica SP2 confocal microscope at a resolution of 512x512 pixels and a time resolution of 1 Hz. Image analysis was performed using custom ImageJ macros and MATLAB routines for semi-automated ROI selection and peak detection to quantify the fraction of cells that were electrically active. Cells were considered to be electrically active if they showed a spike in fluorescence following application of an electrical stimulus. The electrical stimulus was applied using a function generator (Global Specialties) and consisted of a 5 second stimulus at 7.5 V $cm^{-1}$with 5 ms square pulses at 40 Hz.

2.2.9. Quantitative Real Time Polymerase Chain Reaction

Total RNA was extracted from IPSCs cultured in 2D or 3D using the RNEasy kit (Qiagen, Valencia, CA) according to the manufacturer's instructions, including treatment with RNase-free DNase to remove genomic DNA. A high capacity cDNA reverse transcription kit (Applied Biosystems, Foster City, CA) containing random primers was used to reverse transcribe 200 ng total RNA from each sample to cDNA. Taqman gene 194 expression master mix and Taqman gene expression assays (Applied Biosystems) were used for template amplification of 10 ng cDNA per reaction. Quantitative real-time polymerase chain reaction (qRT-PCR) was carried out on a 7500 Fast Real-Time PCR instrument (Applied Biosystems). Relative gene expression was calculated using the ΔΔCT method, normalizing to GAPDH as the endogenous control and undifferentiated IPSCs in standard 2D culture (on Matrigel-coated dishes in mTeSR media) after 7 days as the reference sample. Taqman gene expression assays were used in these studies, listed in Supplementary Table S2.2.

2.2.10. Microscale electrospun scaffold preparation and neuronal seeding

Microscale electrospun fibrous scaffolds (MEFS) were prepared by cutting oxygen plasma treated and hydrated electrospun fiber mats into 100 μm squares with a McIlwain tissue chopper (Vibratome), and sterilized and coated with PDL and laminin as described above. On day 4 of neuronal conversion, iN cells were dissociated with Accutase and resuspended in N2M with dox at 5 million cells per mL. The scaffolds and iN cell suspension were mixed in a 48-well non-TCPS plate for 1 hour with occasional gentle agitation, followed by 3 washes to remove unattached cells. Scaffolds containing iN cells were cultured for 1 day in N2M, then cultured in NBM until used for *ex vivo* or *in vivo* experiments. For experiments examining co-cultures of DA iNs and NeuroD1 iNs, dissociated DA and NeuroD1 iNs were dissociated, resuspended and combined 1:1 ratios to a concentration of 5 million total cells per mL.

2.2.11. *Ex vivo* slice preparation and scaffold transplantation

Organotypic mouse brain slice cultures were prepared by isolating the cortico-striatal area of 6-day-old C57BL/6 mouse brains and cutting into 300 μm slices using a vibratome (Leica Microsystems) in ice cold sucrose solution (204 mM sucrose, 26.2 mM $NaHCO_3$, 11 mM glucose, 2.5 mM KCl, 2 mM $MgSO_4$, 1 mM NaH_2PO_4, 0.5 mM $CaCl_2$ saturated with 95% O_2 and 5% CO_2)[133]. Slices were transferred onto Millicell organotypic cell culture inserts (Millipore) in a 6 well tissue culture plate and cultured in Neurobasal A medium (Life Technologies) supplemented with 1 μg mL^{-1} insulin, 0.5 mM ascorbic acid, 25% horse serum, and 1% penicillin/streptomycin. Mouse brain slices were cultured for 2 days prior to iN cell transplantation. Two days after preparing brain slices, dissociated and scaffold-seeded GFP+ iN cells (day 6 post-conversion) were transplanted onto the surface of the cortico-striatal slices using a pipette. Medium was changed every 2-3 days and slices were fixed in 4% paraformaldehyde after 7 days for immunohistochemistry to quantify neurite outgrowth, or cultured 14 days prior to electrophysiology studies.

2.2.12. *In vivo* cell injection and scaffold transplantation

All animal experiments were carried out according to the Rutgers University Policy on Animal Welfare and were approved by the Institutional Animal Care and Use Committee (IACUC)

at Rutgers University Robert Wood Johnson Medical School. Male, 5-week old *NOD-SCID IL2Rγc* null mice (20-35 g; Jackson Laboratory) were anesthetized with isoflurane (induction at 4% and maintained at 0.5-1% inhalation) and for electrospun microscaffold experiments, injected with a total volume of 10 μL, containing either $1x10^3$, $1x10^5$ dissociated GFP+ iN cells or ~10 scaffolds seeded with GFP+ iN cells (~85 cells per scaffold) at days 6-8 after initiating neuronal conversion, resuspended in ice cold MEM (Life Technologies). Cells or cells on scaffolds were injected stereotactically into the striatum using a 100 μL gastight Hamilton syringe and 21G Hamilton needle. Bilateral injections were made at the following coordinates (in mm): AP, 0.5 (from bregma); ML, −2.0; DV, −3.0 (from dura).

2.2.13. Statistical Analysis

All data are presented as mean ± standard deviation. Statistical significance is evaluated by single factor ANOVA and a Tukey post-hoc test, with $p < 0.05$ considered statistically significant.

2.3 Results

2.3.1 Induction of neurons via single defined transcription factor

We initially identified that of the four transcription factors (TFs), i.e. *Brn2, Ascl1, Myt1L* and *NeuroD1,* used by Pang et al. to reprogram human fibroblasts to neurons, only *Ascl1* and *NeuroD1* could individually induce neuronal conversion of IPSCs, as also reported elsewhere [42, 88]. Early neurons induced by *NeuroD1* expression exhibited complex neuronal morphologies and express mature neuronal markers, so all subsequent studies were done using *NeuroD1* as the single TF for generating iN cells. We transduced human IPSCs with lentiviruses encoding tetracycline-inducible, tetOn-*NeuroD1*, rtTA, and in selected cases, tetOn-*EGFP,* and maintained them as undifferentiated IPSCs in mTeSR medium for multiple passages in the absence of doxycycline (*dox*) (**Supplementary Figure S2.1a**). We refer to these cells as "RN-iPS" cells, since these cells were transduced with rtTA and NeuroD1. RN-iPS cells maintain expression of pluripotency markers SSEA-4 and Oct-4 over multiple passages in the absence of dox, indicating that they remain undifferentiated after transduction (**Supplementary Figure S2.1a**).

To assess neuronal induction from RN-iPS cells, dense cultures of RN-iPS cells were seeded and *dox* was added 24 hours after plating (**Supplementary Figure S2.1b**). Early stage iN cells expressed neuronal marker βIII-tubulin and residual undifferentiated IPSCs expressed Oct-4 (**Supplementary Figure S2.1c**). *Dox* addition rapidly induces the loss of undifferentiated morphology and the acquisition of bipolar, early neuronal morphologies in a subset of cells within 48 hours (**Supplementary Figure S2.1c-e**). *Dox* also rapidly induces *EGFP* expression in control cells transduced with tetOn-*EGFP*. By contrast, cells transduced with only tetOn-*EGFP* and rtTA (lacking tetOn-*NeuroD1*) show strong GFP fluorescence but maintain undifferentiated hPSC morphology upon *dox* addition (**Supplementary Figure S2.1e**).

Despite the rapid, *dox*-induced neuronal conversion of a subset of RN-iPS cells, the remaining undifferentiated cells proliferated and rapidly overtook iN cultures. To address this, cells were replated 4 days post *dox* treatment, which established more uniform human neuronal cultures and eliminated many undifferentiated cells (**Figure 2.3a**). The replating process may

disrupt the cell-cell contacts necessary for undifferentiated iPS cell survival. After replating, enriched iN cells could be maintained for 4 weeks or longer prior to characterization.

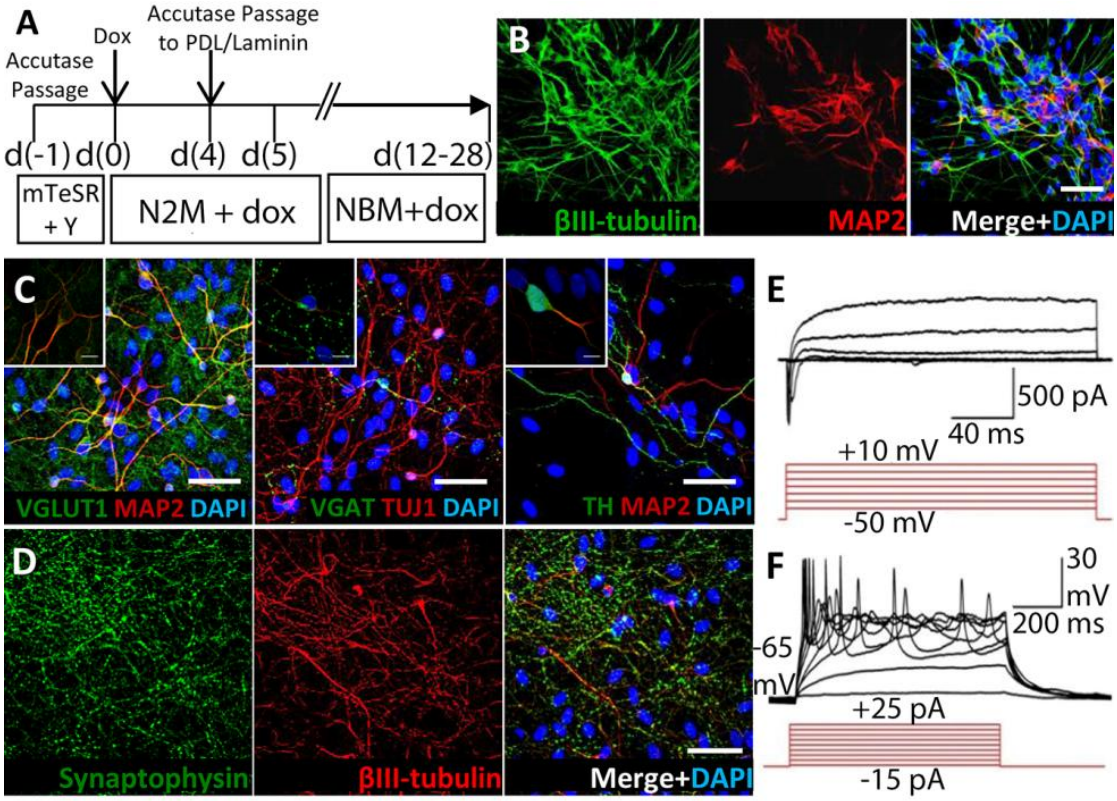

Figure 2.3 - Characterization of neuronal conversion and maturation in iPS-RN cells.

(A) Schematic of long term iPS-iN reprogramming to functional neurons. (B) After 12 days of conversion, iPS-iN cells express βIII-tubulin and MAP2. (C) Further differentiation on glial cells for 28 days allows specification of several neuronal subtypes, including vGAT-expressions GABAergic neurons and TH-expressing dopaminergic neurons, in addition to the predominantly vGLUT-expressing glutamatergic neurons. (D) Day 28 iPS-iN cells also extensively express mature neuronal makers such as the synaptic vesicle protein synaptophysin. (E) Whole cell current recordings demonstrate that iPS-iN cells after 14 days culture in the absence of glia are predominantly electrically active with functional voltage dependent Na^+ channels as well as voltage-dependent K^+ channels, and (F) and fire repetitive induced action potentials (n=27/27). Scale bar = 50 μm, inset scale bar = 10 μm.

As expected, human iN cells robustly express βIII-tubulin and microtubule-associated protein 2 (MAP2) by day 12-14 after *dox* addition (**Figure 2.3b**). To identify the neuronal subtypes generated by this procedure, iN cells were replated 4 days after *dox* addition onto glial cell monolayers as reported elsewhere[134]. Immunocytochemistry (ICC) on 28 days iNs post replating revealed that most cells expressed glutamate vesicular transporter VGLUT1, indicating that these cells are predominantly excitatory glutamatergic neurons (**Figure 2.3c**). Occasional cells expressing markers of other neuronal subtypes were also observed, including inhibitory GABAergic neurons (expressing vesicular GABA transporter VGAT) and dopaminergic neurons (expressing tyrosine hydroxylase – TH) (**Figure 2.3c**). Most cells also robustly expressed the presynaptic protein synaptophysin (**Figure 2.3d**). Finally, patch-clamp electrophysiology demonstrated that iN cells are electrically active and express functional voltage dependent Na^+ channels as well as voltage dependent K^+ channels as revealed by whole cell current recordings (**Figure 2.3e**). Strikingly, these human iN cells were capable of firing repetitive action potentials (**Figure 2.3f**). Taken together, these data indicate the robust generation of functional neuronal cells via *NeuroD1* overexpression.

2.3.2. Generation of functional neurons on 3D electrospun microfibers

Next, we investigated whether *NeuroD1* expression would similarly induce neuronal conversion and maturation within model 3D electrospun substrates. We constructed fibrous substrates by electrospinning poly(desaminotyrosyl tyrosine ethyl ester carbonate) (pDTEc), into two architectures, which will be referred to as “thin” and “thick” fiber substrates with average fiber diameters of 1.25 ± .05 μm and 3.23 ± 0.06 μm respectively (**Figure 2.4a-d**) [102]. pDTEc is the lead candidate polymer from a combinatorial library of tyrosine-derived polycarbonates [135], as it effectively supports pluripotent stem cell culture when fabricated into microscale fibrous substrates [102], and is biocompatible [136]. Similarly, our results with 3D polymeric substrates compared to 2D polymeric substrates suggest that the fibrous architecture governs the longer term cellular behaviors observed in contrast to the polymer composition that plays a role on early interfacial phenomena. The thick fiber substrates are volumetrically permeable to cellular infiltration whereas the thin fiber substrates are relatively impermeable, due to decreased

void space between fibers. Without additional material modifications, it is difficult to produce equal fiber sizes with variable porosity, as both properties are simultaneously modulated when altering electrospinning parameters. We hypothesize that cell permeable, thick fiber substrates will support improved iN maturation and functionality by promoting enhanced 3D organization and cell-cell contacts relative to less permeable, thin fiber substrates and 2D controls.

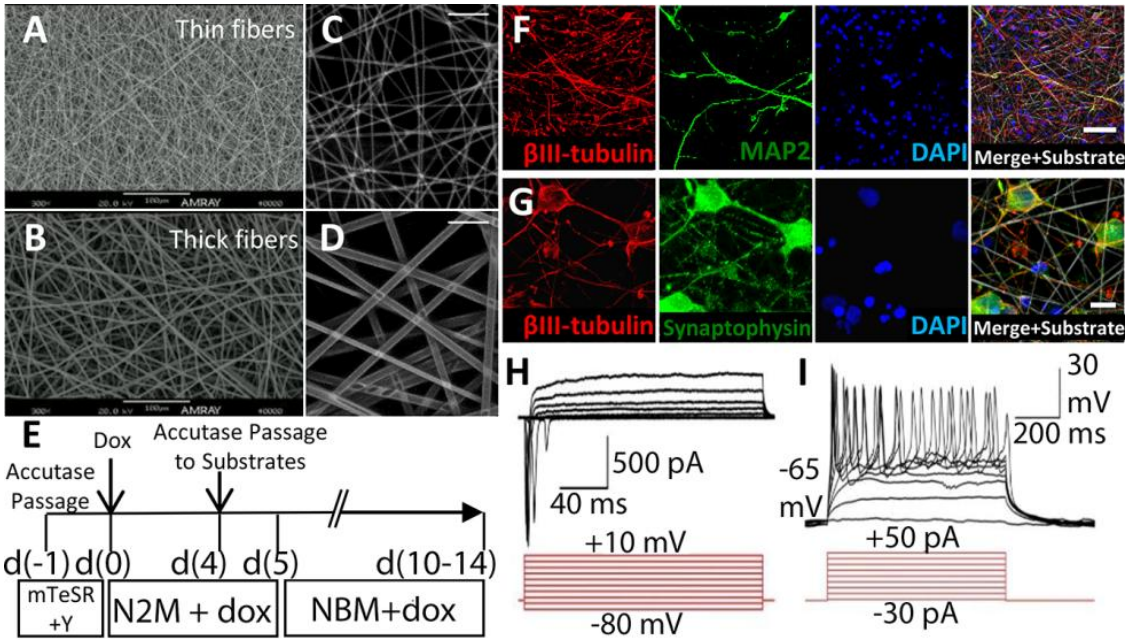

Figure 2.4 - Characterization of electrospun pDTEc fibers and validation for support of iN differentiation.

(A-B) SEM and (C-D) reflectance images of 2-D fibrous and 3-D electrospun fibers, with substantially variable fiber architectures and porosities that respectively do not allow and allow cellular infiltration. (E) Schematic of iPS-RN reprogramming on 3-D electrospun fibers. (F-G) iPS-RN reprogramming was carried out on 3-D electrospun fibers, demonstrating that generation of βIII-tubulin and MAP2 positive iN cells on 3-D electrospun fibers after 12 days proceeds similarly to 2-D controls shown in Figure 2. (H) Whole cell current recordings demonstrate that iPS-iN cells cultured for 10 days on 3-D electrospun fibers, 14 days total were predominantly electrically active with functional voltage dependent sodium channels as well as voltage-dependent potassium channels, and (I) and fire repetitive induced action potentials (n=18/20). Scale bar (C-D, F) = 50 μm; G = 10 μm.

Human iN cells were generated within 3D construct by treating RN-iPS cells, cultured on 2D tissue culture plates, with *dox* for 4 days, followed by replating onto 3D electrospun substrates or 2D controls, according to the timecourse schematic shown in **Figure 2.4e**. Human iN cells on 3D electrospun fibers showed complex morphology with extensive neurite outgrowth and expressed βIII-tubulin, MAP2, and synaptophysin after 12 days of reprogramming, similarly to 2D cultures (**Figure 2.4f-g**). In addition, electrophysiological recordings revealed iN cells in electrospun substrates fired action potentials, demonstrating the derivation of functional iN cells (**Figure 2.4h-i**).

2.3.3. Effect of 3D microfibrous substrate architecture on human iN conversion

Next, we examined whether the fiber architecture could be tuned to enhance human iN maturation, as we and others have shown that geometric cues can influence both human iPS cell and neural cell behaviors [102, 137]. RN-iPS cells were treated with *dox* for 4 days, then replated onto 3D fibrous substrates or 2D controls, including 2D polymer coated controls, for an additional 8 days of culture. ICC for proliferation marker Ki-67 and Oct-4 revealed that significantly more proliferative and pluripotent cells were retained when iN cells were replated onto 2D substrates compared to 3D fibrous substrates ($p < 0.05$, 1-way ANOVA) (**Figures 2.5a, 2.5c, Supplementary Figures S2.2, S2.3**). This suggests that the fibrous architectures may be able to selectively reduce the presence of residual proliferative and pluripotent IPSCs.

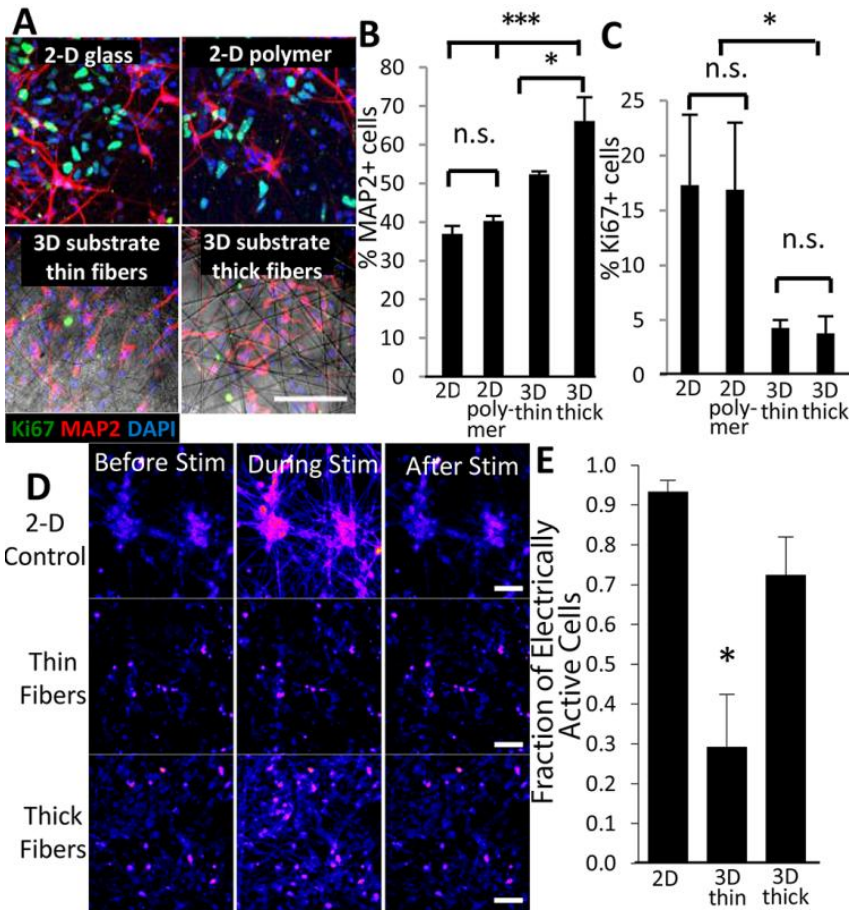

Figure 2.5 - Comparison of neuronal selection and maturation in 2D and 3D substrates.

(a) Human iN populations robustly express MAP2 in 2D and 3D conditions, while populations of unconverted, proliferative Ki67-expressing iPS cells persist in iN populations plated in 2D conditions. Scale bar = 100 μm(b) Quantification reveals an enhancement of maturation as assessed by MAP2 expression in 3D electrospun 18% pDTEc fibers relative (thick fibers) to 9% pDTEc fibers (thin fibers), as well as in both 3D fibrous conditions relative to 2D conditions. n=3 *P<0.05, ***P<0.001 by 1-way ANOVA. (c) Quantification reveals an enhancement of neuronal selection, as assessed by Ki67 expression, fewer residual proliferative cells remained in iNs replated into 3D fibrous conditions relative to 2D conditions. 100 um scale bar, n=3 *P<0.05, by 1-way ANOVA. (d) Heat map images from calcium recordings of human iN cells before (left), during (middle) and after field electrical stimulation). Scale bar = 75 μm. (e) Quantification of the fraction of cells that respond to electrical stimulation with a substantial increase in fluorescence

intensity reveals highly active cell populations in 2D and 3D electrospun 18% pDTEc fibrous conditions (thick fibers) relative to cells in the 9% pDTEc fibrous condition (thin fibers). n=3*$p < 0.05$ by 1-way ANOVA, all error bars presented as mean ± 1 standard deviation.

Human iN cells in all conditions expressed extensive βIII-tubulin-positive processes, along with robust MAP2 expression **(Figures 2.5a, Supplementary Figure S2.2)**. Significantly greater numbers of human iN cells expressed MAP2 in thick fiber substrates relative to 2D controls ($p < 0.0001$, 1-way ANOVA) and thin fiber substrates ($p < 0.05$, 1-way ANOVA), indicating accelerated maturation (**Figure 2.5b**). qRT-PCR also revealed increasing trends in expression of several neuronal genes in 3D substrates relative to 2D controls, including βIII-tubulin, MAP2, synapsin 1, and VGLUT1, though not statistically significant (**Supplementary Figure S2.4**). Most importantly, calcium imaging to identify the fraction of cells that respond to a field electrical stimulation indicated that thick fiber substrates yielded a high degree of activity, namely, > 70% electrically active cells by day 12 of culture (**Figure 2.5d-e**), which was significantly greater than those on the thin fiber substrates ($p < 0.05$, 1-way ANOVA). Inhibition of E-cadherin dependent cell-cell contacts markedly reduced neuronal outgrowth in 2D, and decreased activity measured by calcium imaging for iNs on 2D and 3D thick fiber substrates but not thin fiber substrates (**Supplementary Figure S2.5**). This indicates that three-dimensional microfibrous architectures establish neuronal networks with enhanced cell-cell contacts and influence both functional and phenotypic maturity of iN cellular networks.

2.3.4. Microscale electrospun scaffolds support outgrowth and survival in brain

Based on the promising fibrous substrates described in the last chapter, transplantable constructs were designed to deliver human iN cells into the brain for regenerative therapies. The large mats of electrospun fibers (0.3 to 2 cm diameter discs) conventionally fabricated for *in vitro* studies cannot be easily transplanted into the CNS. To allow for injection *in vivo*, 100 μm square microscale electrospun fibrous scaffolds (MEFS) that could be injected through a 21 gauge needle were created by down-scaling thick fiber electrospun substrates with a Vibratome. Human iN cells were seeded in suspension onto MEFS analogous to our previous studies, which resulted in efficient population of microscale scaffolds with iN cells. Cells in microscale scaffolds matured

into βIII-tubulin and MAP2 expressing neuronal cells, similarly to cells on macroscale fibrous substrates (**Supplementary Figure S2.6**). The average number of live human iN cells in each scaffold was 83±13 (n=19) (**Supplementary Figure S2.7**).

The ability of MEFS to promote human iN cell survival and engraftment was first assessed using an *ex vivo* model consisting of organotypic hippocampal slice cultures from *NOD-SCID IL2Rγc* null mice **(Figure 2.6a).** Human iN cells on 4-5 MEFS were injected into hippocampal slices, alongside equivalent numbers of dissociated cells on paired slices, and engraftment and functionality was assessed. ICC revealed that 3 days after transplantation, injected MEFS-supported iN cells had average neurite lengths of 831 ± 169 μm, which was significantly greater ($p<0.0001$, 1-way ANOVA) than those of injected dissociated iNs, which had neurite lengths of 241 ± 42 μm (**Figure 2.6b-e**).

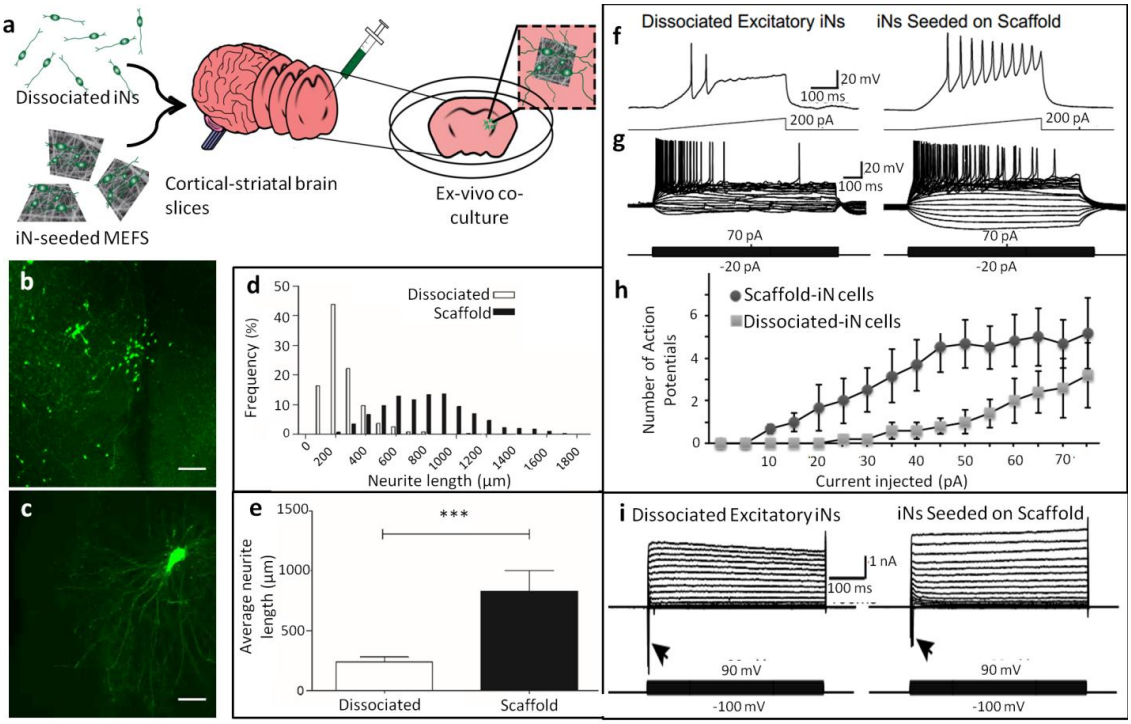

Figure 2.6 - iNs supported by scaffolds support outgrowth and survival ex-vivo.

(a) 100 micrometer edge scaffolds were cut from electrospun fibers prior to seeding with iNs, followed by injection onto ex-vivo cultured mouse pup brain slices. (b-e) Neurite length was found to be significantly enhanced in transplanted scaffold-supported iNs when comparing

dissociated GFP labeled iNs (b) with iNs seeded on scaffolds (c) injected onto mouse ex-vivo brain slices (n=8 brain slices for each transplantation mode). (f-h) Both scaffold-supported iNs (n=6) and dissociated iNs (n=5) fire action potentials in response to current injection 14 days after transplantation onto mouse ex-vivo brain slices, however scaffold-supported iNs displayed enhanced excitability relative to dissociated iNs. Both modes of transplanted iNs were observed to have mature sodium channel expression (i). ***P<0.0001 by 1-way ANOVA. Scale bar 20 μm, all error bars presented as mean ± 1 standard deviation.

Electrophysiological recordings from human iN cells after 3 weeks indicated that both dissociated and MEFS-supported iN cells fire action potentials in response to current injection (**Figure 2.6f-g**), with MEFS-seeded iN cells displaying enhanced excitability in response to injected currents (**Figure 2.6h**). Additionally, both modes of transplanted cells had mature Na^+ channel expression **(Figure 2.6i)**. This suggests that MEFS enhance engraftment and functionality of transplanted iN cells.

Next, human iN cell survival was assessed after transplantation of MEFS-supported or dissociated cells into the mouse striatum *in vivo*. Three weeks after transplantation (**Figure 2.7a**), IHC imaging of a 1.8 mm x 1.8 mm field including the injection site **(Figure 2.7b-e)** revealed an average survival rate of 5.74 ± 3.16% based on injected MEFS-seeded iN cells, a 38-fold improvement ($p < 0.05$, 1-way ANOVA) compared to an average survival rate of 0.15 ± 0.15% of 100,000 injected dissociated iN cells **(Figure 2.7g)**. The survival rate of dissociated iN cell controls was comparable to that reported by Zhang et al. [88]. When magnitude of injected cells were matched at ~1000 cells, quantification of surviving cells yielded an average of 7.58 ± 4.60% of injected MEFS-seeded iN cells compared to 0 ± 0% out of 1,000 injected dissociated iN cells. The MEFS-seeded iNs maintained neurite length (35 ± 8μm) comparable to those of viable, dissociated iNs (39 ± 15 μm) in the experiment when number of injected cells was unmatched. No overt difference in inflammatory response was detected between injection modes, and some ingrowth of host tissue into MEFS was observed (**Supplementary Figure S2.8**).

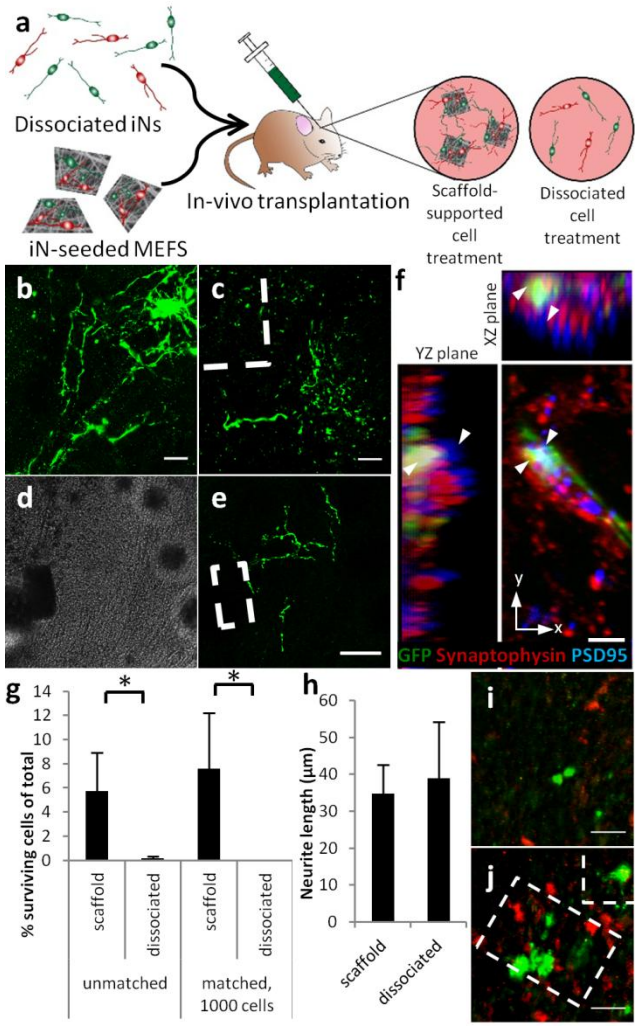

Figure 2.7 - iNs supported by scaffolds support outgrowth and survival in-vivo.

(a) iN-seeded scaffolds were injected into mouse striatum and compared to injected dissociated cells. GFP-expressing surviving iNs were found three weeks post transplantation in mouse striatum, both for dissociated iNs (b) and with iN-seeded microscaffolds (c-e), located in the vicinity of microscaffolds (indicated with dashed line). Scale bar B,C: 25 µm, D,E: 100 µm. (f) Post synaptic density protein 95 (PSD-95) (blue, indicated using downward pointing arrows) was detected adjacent to transplanted GFP-labeled iN neurite terminals, which co-localized with synaptophysin (red, with red+green or yellow regions indicated with upward pointing arrows), suggestive of synaptic integration with host tissue. Scale bar = 5 µm. (g) Quantification of surviving cells yielded an average survival rate of 5.74 ± 3.16% out of an average 802 ± 95.8

injected scaffold-seeded iN cells (n=3), compared to an average survival rate of 0.15 ± 0.15% out of 100,000 injected dissociated iN cells, or 7.58 ± 4.60% of injected scaffold-seeded iN cells compared to 0 ± 0% out of 1,000 injected dissociated iN cells, for a similar-magnitude number of injected cell comparison (n=3). *P < 0.05 by 1-way ANOVA , all error bars presented as mean ± 1 standard deviation. There was no significant difference in neurite length between the two modes of transplanted cells (h). GFP-expressing NeuroD1 iNs and RFP-expressing DA neurons were preserved in close proximity when co-transplanted on microscaffolds (indicated with dashed line)(j), while only some sparse dissociated and transplanted iNs survived (i) one week post transplantation into mouse striatum. Scale bar 25μm.

Surviving transplanted iNs expressed neuronal cell adhesion molecule CD56, beta III tubulin, and synaptophysin (**Figure 2.7f, Supplementary Figure S2.9**). Post synaptic density protein 95 (PSD-95) (depicted in blue, with downward pointing arrows) was detected adjacent or co-localized to transplanted GFP-labeled and synaptophysin-expressing iN neurite terminals, suggestive of synaptic integration with host tissue (**Figure 2.7f**). Notably, when MEFS were used to transplant multiple subtypes of neurons, we observed retention of neurons of distinct specificity in close apposition *in vivo* **(Figure 2.7i-j).** Similar differences in survival were also seen when glutamatergic and dopamine iNs (**Supplementary Figure S2.10**) were co-transplanted either dissociated or on microscaffolds. In all in vivo experiments, some human iNs were observed to migrate off scaffolds, and minimal scaffold degradation was observed in the 1-3 weeks post-transplantation.

2.4 Discussion

Cell therapies for treatment of CNS brain injury and disease are challenged by poor cell survival, engraftment, and retention after transplantation both into the brain and spinal cord, with cell survival of < 1% routinely reported [138]. The objective of this study was to advance a new integrated biomaterials-based paradigm to both rapidly reprogram pluripotent stem cells to neurons and efficiently deliver enriched, organized neuronal networks to the brain. To achieve this, we engineered human IPSCs with the neuronal transcription factor, *NeuroD1*, and demonstrated efficient and rapid neuronal conversion in 3D substrates of tunable microfibrous geometry to accelerate neuronal maturation and network establishment. In the previous chapter, we report that functionalized 3D microfibrous substrates can guide many important characteristics of human iN cells derived from IPSCs that are relevant for *in vivo* applications, including (1) *in vitro* maturation, electrical activity, and purification; (2) neurite outgrowth, survival, and electrical activity after transplantation into *ex vivo* brain tissue, and (3) survival and engraftment after transplantation *in vivo* into the striatum. These results highlight the promise of biomaterials-based delivery as a platform for reprogramming and regenerative cell sourcing in the CNS and as a potential model that can be further adapted and evaluated for therapeutic efficacy.

Our primary hypothesis was that microfibrous substrates with thick fibers and interfiber spacing would provide a 3D microniche for rapid, high-purity conversion and accelerated maturation of IPSC-derived induced neurons, and that such 3D substrate-supported neuronal networks would exhibit improved levels of retention and engraftment following transplantation into the brain. *In vitro*, thick fiber substrates enhanced human iNs maturation and excitability, while selectively excluding residual undifferentiated IPSCs. Both of these phenomena arise from controlled cell confinement and 3D juxtacrine signaling organization. While the enhanced MAP2 expression in iN cells in thick fiber substrates is consistent with previously reported results [103, 139-141], the concurrent increase in excitability indicates active both phenotypic and functional maturation. We propose that the thick fiber substrates drive iN confinement [102], leading to accelerated maturation due to increased engagement of neural cell adhesion molecules such as L1

or N-cadherin, which have known roles in neural development [142-144] and neuritogenesis [103, 140]. In contrast, the thin fiber substrates fail to support neuronal infiltration and aggregation, resulting in the diminished excitability relative to more 3D, thick fiber substrates.

For effective scaffolds that can form reprogrammed neuronal networks, a key feature is that the proliferation of undifferentiated IPSCs should be suppressed. The geometry we have identified for electrospun substrates limits the proportion of undifferentiated IPSCs. Undifferentiated human ES and IPSCs require media supplementation with the rho-associated kinase (ROCK) inhibitor Y-27632 to survive dissociation to single cells [131]. In the absence of Y-27632, the degree to which dissociated IPSCs can re-establish E-cadherin-mediated cell-cell contacts that have been demonstrated to be required for survival and proliferation [145] is severely diminished when seeded onto electrospun fibrous substrates. Isolated pluripotent stem cells have been observed to form viable colonies largely based on motility-induced aggregation rather than single cell clonal expansion when intercellular distances were less than 6.4 μm [146]. The large surface area, added substrate dimension, and constrained migration paths of the electrospun fibers effectively increase intercellular distances, which would limit motility-induced aggregation and could explain the observed increase in differentiation of IPSCs and loss of residual proliferative cells on microfibrous substrates. This reduction in residual undifferentiated IPSCs could be used to supplement other methods for eliminating the risk of teratoma formation *in vivo* due to the presence of undifferentiated cells, however, additional studies are required to assess the tumorigenic potential of these cells once delivered *in vivo*.

After establishing a substrate geometry that accelerated iN maturation, the ability of these substrates to promote engraftment of human iN cells into the CNS was first probed in an *ex vivo* organotypic brain slice model. Delivery of iN cells on MEFS markedly improved both neurite outgrowth and electrical functionality after transplantation compared to the effects of injected isolated cell suspensions. This suggests that cell retention and survival are enhanced because transplantation of iN cells on MEFS preserves cell-cell contacts while avoiding the need for dissociation. Dissociation of cells prior to injection likely leads to increased anoikis [147, 148], contributing to diminished engraftment after transplantation. The improvement in electrical

activity after transplantation of iN cells in scaffolds is promising, and suggests that these benefits may translate *in vivo*.

Transplantation of iN cells in MEFS into the mouse striatum showed that the percentage of viable cells after 3 weeks was an order-of-magnitude greater than that relative to injection of isolated single cells. This increased survival is likely indicative of decreased anoikis or apoptosis that otherwise arises from enzymatic disruption of cell-cell and cell-matrix interactions [147, 148]. These results are promising particularly in light of recent studies investigating the effects of human iPSC-derived neurons on treating CNS disorders that have shown efficacy *in vivo* even with low levels of cell survival [43, 88], suggesting that increased cell survival could lead to amplified levels efficacy of these cell therapeutics. Additionally, host neuron postsynaptic marker was detected adjacent to pre-synaptic marker-expressing transplanted neurons, suggesting that single-factor reprogrammed neurons are capable of functionally integrating into host tissue. Interestingly, some authors have found that extensive lesions can actually enhance neuronal graft survival and integration, as denervated targets may provide a positive stimulatory effect to new neurons [149, 150], suggesting that even greater cell survival may be possible when applying this scaffold system in a neurodegenerative disease or injury context.

Additionally, the ability for 3D MEFS to support co-culture and concurrent transplantation of neuronal networks consisting of neurons of multiple subtypes was evaluated. Transplantation of intact networks of mixed subtype neuron populations could be an invaluable tool for treating complex brain disorders or injuries that affect multiple subtypes, or for priming transplanted neurons with pre-established synaptic inputs. For example, attempts for transplanting dopamine neurons derived from fetal brain tissue [151, 152] or derived from human IPSCs [43, 153] have been made and yield amelioration of Parkinson's Disease; with the paradigm we proposed one can envision a model to graft mini-neur0circuitry composed of excitatory-dopaminergic neurons into the host brain. We hypothesize that proper excitation from the mini-neurocircuitry could produce more profound amelioration of locomotive deficits in Parkinson's Disease.

Induced human neurons offer a rich cell source for a variety of *in vitro* and *in vivo* applications in modeling and treating CNS diseases and injuries. Our prototypes combining reprogramming technology and functionalized fibrous scaffolds epitomize a biomaterial device for subtype specific neuronal reprogramming and transplantation strategy that encourages transplant survival and engraftment. Similar prototypes could be engineered to apply human neuronal cells of varying subtypes for targeted treatment of a wide range of CNS disorders.

2.5 Supplementary Figures

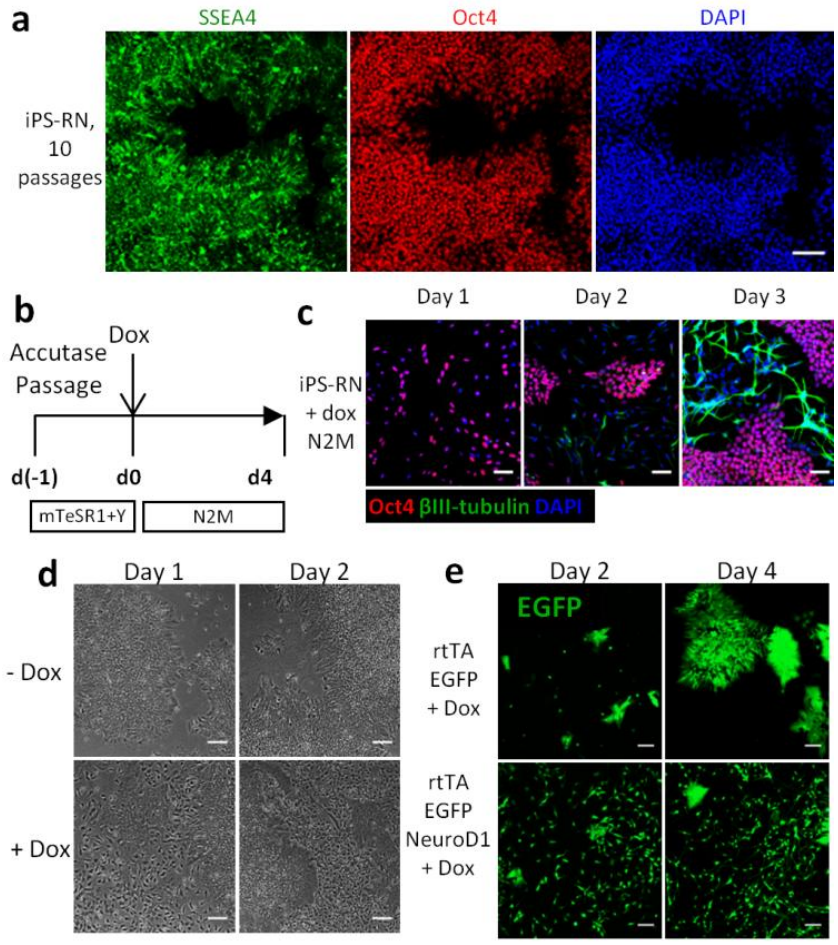

Supplementary Figure S2.1 - Derivation and characterization of RN-iPS cell lines.

(a) RN-iPS cells maintain expression of pluripotency markers OCT4 and SSEA4 after 10 passages in mTeSR-1 medium. (b) Schematic of plating and doxycycline (dox) addition for generation of iNs from RN-iPS cells. (c) Many RN-iPS cells lose Oct4 and gain βIII-tubulin expression 3 days after dox addition in N2M. (d) Bright field images after 1 or 2 days of dox treatment reveal that in the absence of dox, cells retain a characteristic undifferentiated iPS cell morphology, where in the presence of dox, cells around the periphery of colonies begin to take on an early neuronal cell morphology. (e) iPS cells infected with rtTA and EGFP show EGFP expression 2 and 4 days after dox addition, but maintain an undifferentiated morphology. iPS cells infected with rtTA, EGFP, and NeuroD1 also show EGFP expression 2 and 4 days after dox addition, but also show a distinct

conversion to progressively maturing neuronal morphologies. Scale bar = 100μm (a, d-e), 50 μm (c).

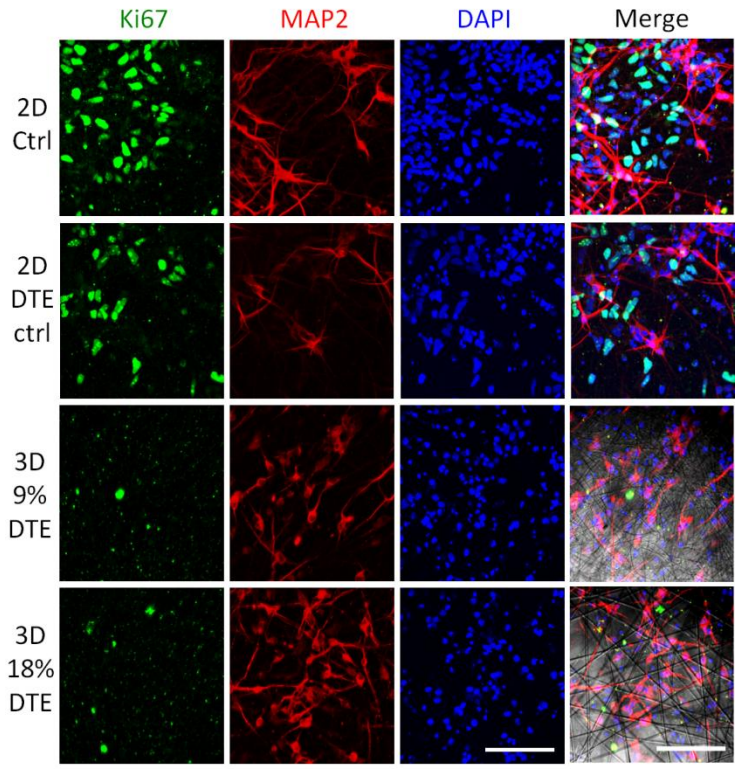

Supplementary Figure S2.2 - Comparison of neuronal selection and maturation in 2D and 3D substrates.

iN populations robustly express microtubule-associated protein 2 (MAP2) in 2D and 3D conditions, while populations of unconverted, proliferative Ki67-expressing iPS cells persist in iN populations plated in 2D conditions. Scale bar = 100 μm.

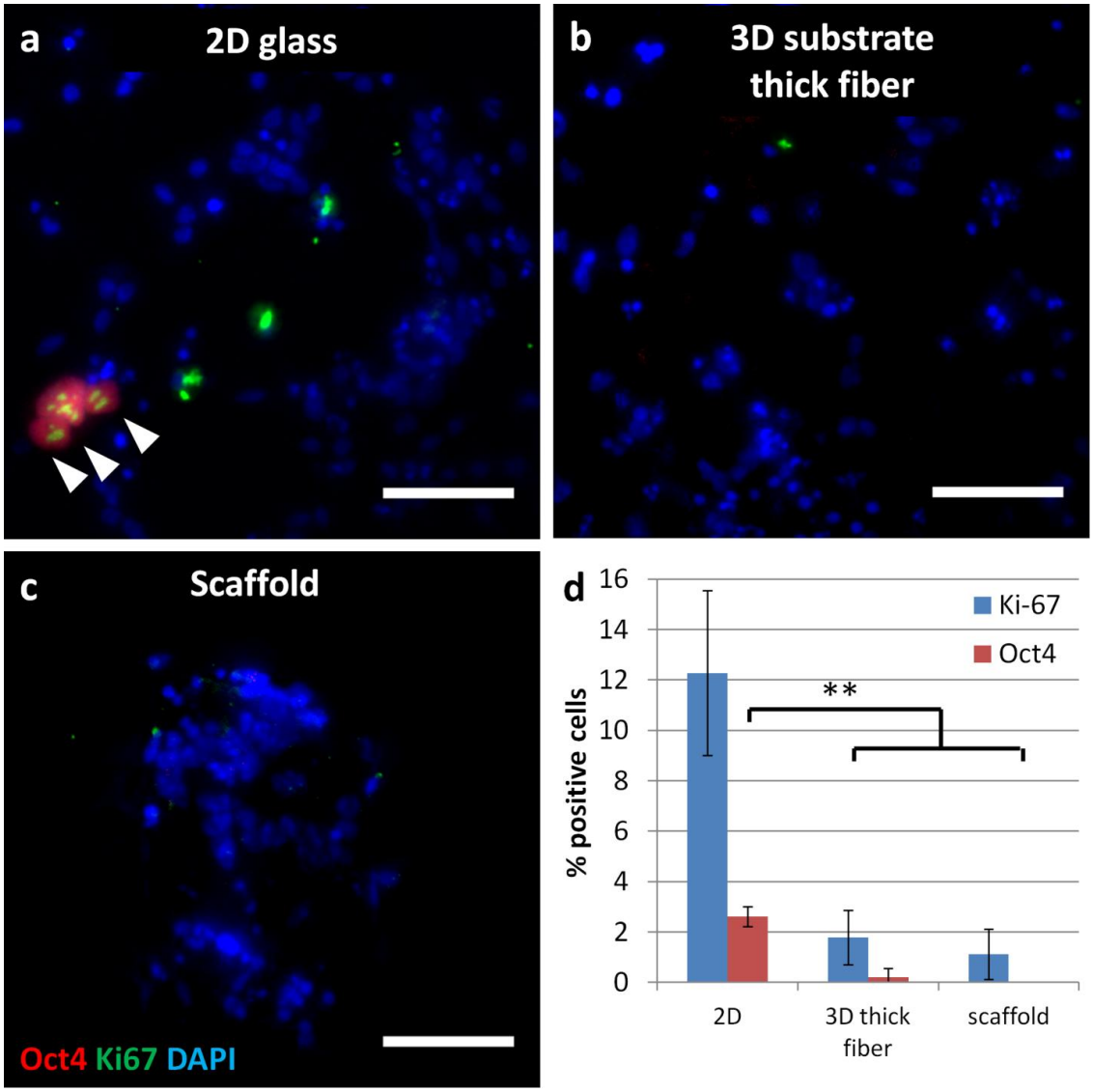

Supplementary Figure S2.3 - Characterization of unconverted induced neuronal cells.

(a) iNs replated onto 2D glass surfaces after initiating reprogramming contained populations of Ki67+ cells (green), a subpopulation of Ki-67+ cells were also Oct4+ (red). iNs replated onto thick fiber 3D substrates (b) or scaffolds (c) similarly had significantly fewer of both Ki-67+ and Oct4+ cells, **P<0.01 by 1-way ANOVA, , all error bars presented as mean ± 1 standard deviation.

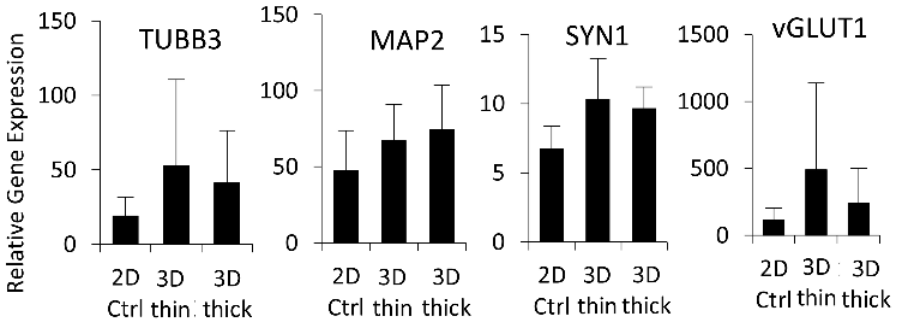

Supplementary Figure S2.4 - qRT-PCR analysis of induced neuron gene expression.

Analysis of gene expression profiles reveals similar gene expression profiles between the three substrates, all error bars presented as mean ± 1 standard deviation.

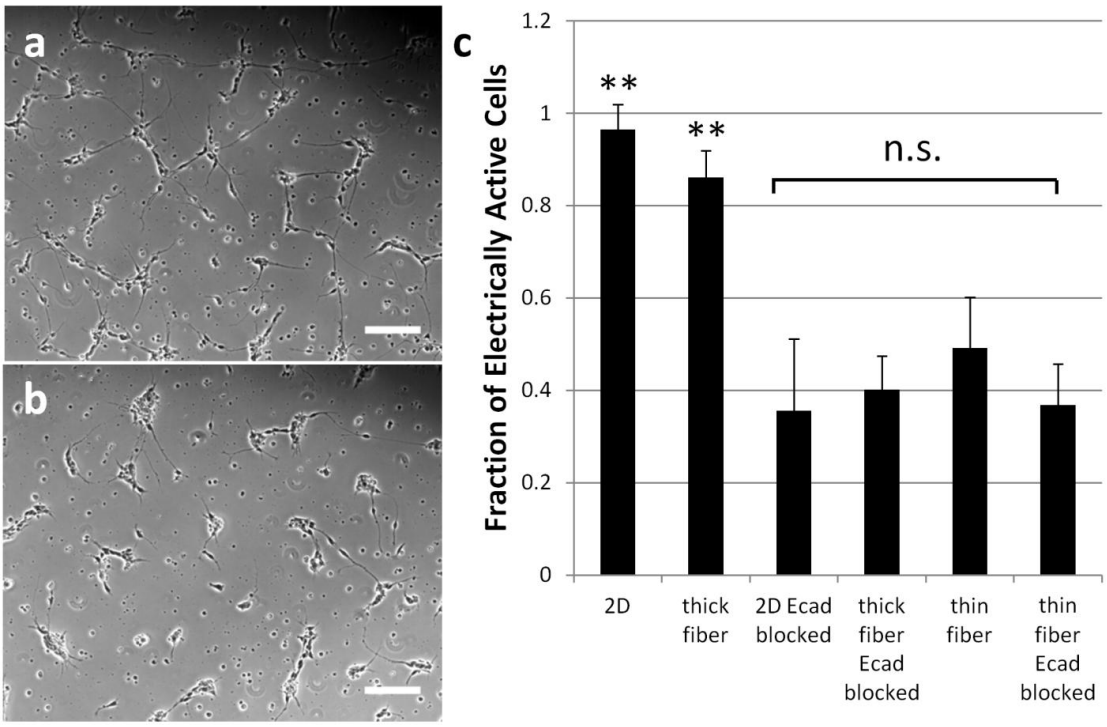

Supplementary Figure S2.5 - Fiber architecture controls neuronal development via cell-cell contact.

iN populations were incubated with 200 μg mL^{-1} E-cadherin antibody for 15 minutes prior to seeding onto substrates, either 2D or thick and thin fiber 3D substrates. Compared to uninhibited iN cells in 2D (a), iN cells with inhibited E-cadherin dependent cell-cell contact displayed reduced outgrowth in 2D (b). Inhibited cell-cell contact resulted in decreased activity measured by calcium imaging for iNs on 2-D and thick fiber substrates, but did not decrease activity in thin fiber substrates (c). **P<0.01 by 1-way ANOVA relative to respective Ecad blocked conditions. n.s. = not significant. Scale bar = 150 μm, all error bars presented as mean ± 1 standard deviation.

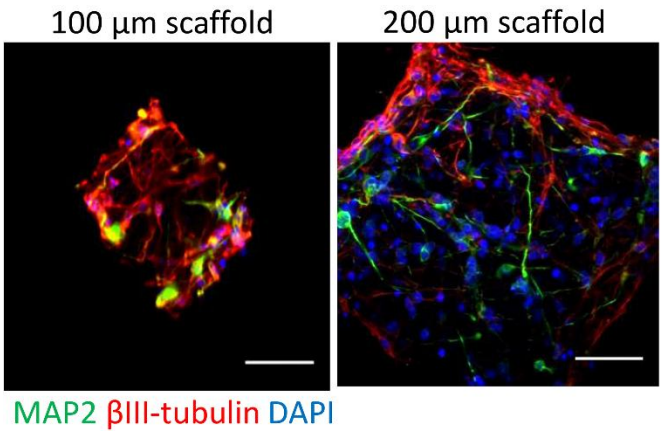

Supplementary Figure S2.6 - Characterization of neuronal maturation on microscale scaffolds.

Immunocytochemistry for pan-neuronal markers microtubule-associated protein 2 (MAP2) and βIII-tubulin in iNs after 4 days in 100 and 200 µm scaffold. Scale bar: 50 µm.

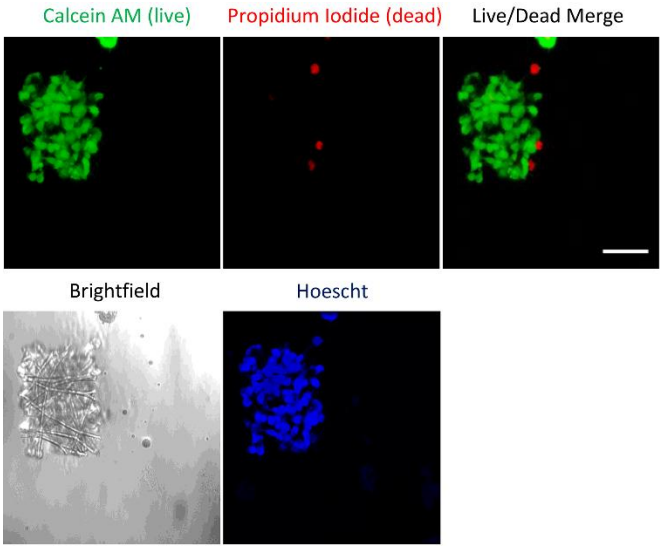

Supplementary Figure S2.7 - Live/dead imaging in a 100 µm scaffold.

On average, there were 82.6 ± 13.1 live cells per scaffold. Scale bar: 50 µm.

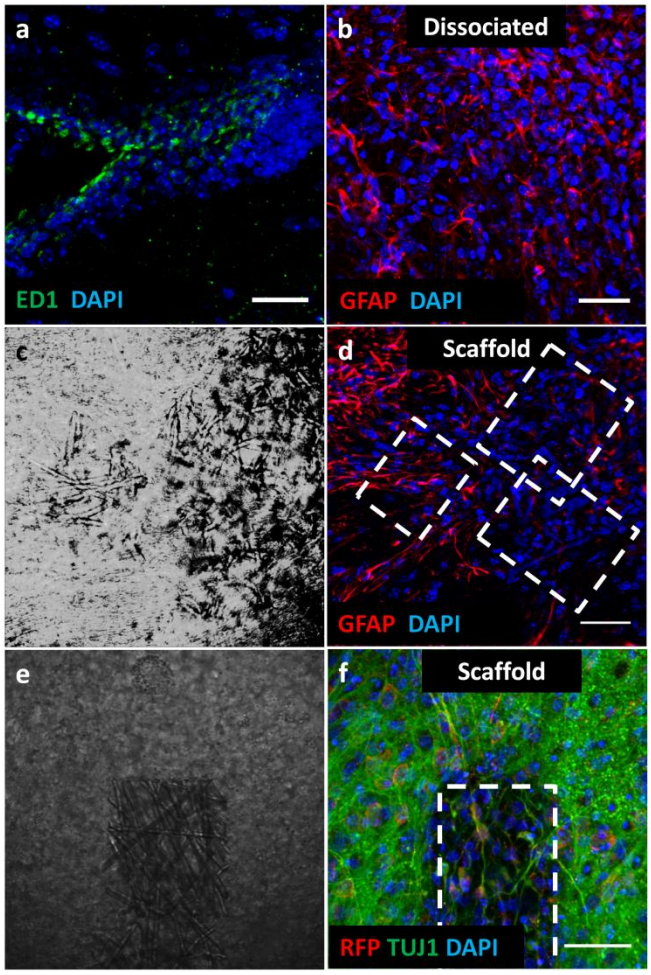

Supplementary Figure S2.8 - Host response to transplanted scaffolds.

(a) Activated microglia expressing ED1 or CD68 were seen in injection sites in mice receiving both dissociated and scaffold-supported iNs. Astrocytes, expressing glial fibrillary acidic protein (GFAP) were seen near the injection site in both mice receiving dissociated (b) and scaffold-supported iNs (c-d). Some degree of host tissue ingrowth was observed near transplanted scaffolds with no iNs nearby, visualized using brightfield (e) and immunostaining for βIII-tubulin and RFP, to detect fluorolabeled transplanted cells (f). Scale bars = 50 μm.

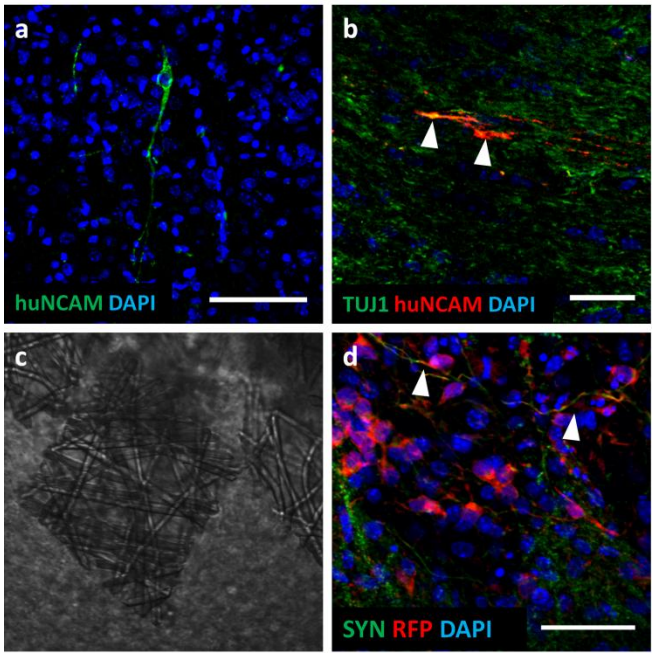

Supplementary Figure S2.9 - Characterization of transplanted iNs.

(a) 3 weeks post-transplantation into mouse striatum, iNs expressed neural cell adhesion molecule CD56, detected with a human specific antibody. Scale bar = 100 μm. (b) Cells that positively expressed human specific neural cell adhesion (red) molecule also expressed β-III tubulin (green), indicated by arrowheads pointing to yellow colored neurites. Scale bar = 50 μm. Scaffold supported RFP-labelled iNs (red), located near brightfield scaffolds (c) were found to express synaptophysin (green) (d), two such red-colored neurites with distinct green regions are indicated with arrowheads, scale bar = 50 μm.

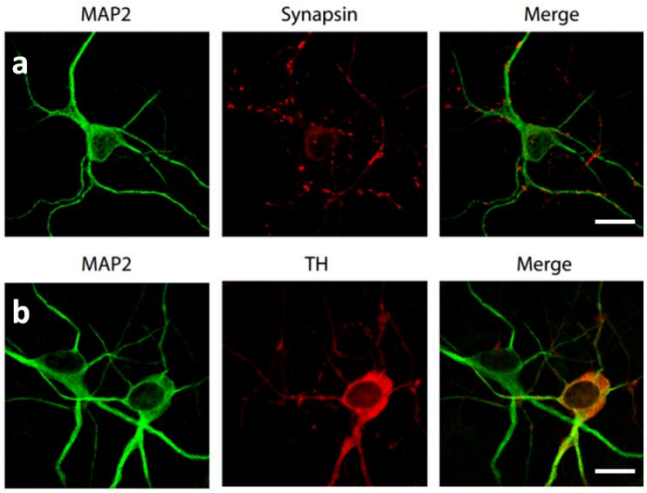

Supplementary Figure S2.10 - Induced DA neurons stain positively for mature neuronal markers and dopamine markers.

(a) iDA neurons express microtubule-associated protein 2 (MAP2) and Synapsin. (b) iDA neurons express MAP2 and tyrosine hydroxylase (TH). Scale bars = 20 μm.

.

Supplementary Table S2.1 - Antibodies used for immunocytochemistry.

Antibody	Species	Isotype	Dilution	Company	Product #
βIII-tubulin	mouse	IgG 2a	1:1000	Covance	MMS-435P
Map2	mouse	IgG 1	1:500	BD Biosciences	556320
Synaptophysin	rabbit	IgG	1:250	Millipore	04-1019
Oct4	mouse	IgG1	1:1000	Millipore	MAB4401
TH	mouse	IgG 2a	1:100-1:500	Millipore	MAB5280
GFP	chicken	IgY	1:1000	abcam	ab13970
RFP	rabbit	IgG	1:100	Abcam	ab62341
huNCAM	mouse	IgG1	1:100	Santa Cruz	sc-106
HuNu	mouse	IgG1	1:100	Millipore	MAB1281
ki67	rabbit	IgG	1:50-1:100	abcam	ab15580
E-cadherin	mouse	IgG1	1:10	Invitrogen	13-1700
vgat	mouse	IgG3	1:1000	synaptic systems	131 001
vglut	rabbit	IgG	1:1000	synaptic systems	135 302

Supplementary Table S2.2 - Taqman gene expression assays used for qRT-PCR.

Gene	Taqman Gene Expression Assay
GAPDH	Cat#: 4326317E
TUBB3	Hs00801390_s1
MAP2	Hs00258900_m1
SYN1	Hs00199577_m1
SLC17A7	Hs00220404_m1

CHAPTER 3 – INHIBITION OF SYNUCLEIN AGGREGATION WITH SYNTHETIC SCAVENGER RECEPTOR LIGANDS

The following chapter contains figures and major sections of text excerpted from the following manuscript submitted for publication:

Bennett N.K., Chmielowski R., Faig J.J., Francis N.A., Baum J., Pang Z.P., Uhrich K.E., Moghe P.V. Polymer Nanotherapeutics Ameliorate Microglial α-Synuclein Aggregation, Activation, and Neurotoxicity. *Submitted to Biomaterials, 8/16/16*.

Abstract

Neuroinflammation and synucleinopathy remain challenging aspects of PD requiring therapeutic intervention. The protein a-synuclein (ASYN), ubiquitously expressed inn the central nervous system and characteristically aggregated in Parkinson's disease, is a key therapeutic target relevant to these processes, yet its trafficking and aggregation by microglia has proven to be challenging. In these studies we demonstrate that ASYN internalization by microglia is mediated by scavenger receptors CD36 and SRA1, and followed quickly by the intracellular oligomerization of ASYN. Based on this observation, we designed a nanotherapeutic based on synthetic amphiphilic scavenger receptor ligands in order to regulate intracellular levels of ASYN within microglia. These molecules were complexed into serum-stable nanoparticles via flash nanoprecipitation around hydrophobic core molecules. Microglia treated with these nanotherapeutics had decreased monomeric ASYN internalization and decreased intracellular ASYN oligomerization. This therapeutic strategy may serve as a foundation towards future efforts in reducing the aggregation of ASYN in PD, and potentially slow the pathological spreading of toxic ASYN species.

3.1 Introduction

Aggregated and increased levels of extracellular α-synuclein (ASYN) are characteristic of Parkinson's disease (PD). As the primary cell type to rapidly internalize and degrade ASYN, microglia are a natural target for regulating ASYN trafficking and associated neuroinflammation [86]. While microglia play a role in the physiological clearing of ASYN, disruptions to the lysosomal clearance pathways caused by overabundance of ASYN [58] or by common mutations associated with idiopathic and familial PD [55-57] result in dramatic increases in extracellularly released ASYN [59]. Elevated levels of extracellular ASYN could in turn contribute to the interneuronal spreading of pathological ASYN species, particularly since neuron-to-glia transmitted ASYN has been observed to form pathogenic aggregates [76]. A considerable body of work also indicates that intercellularly transmitted ASYN from neuron-to-glia triggers microglial activation [70, 73-76]. The result of chronic and excessive ASYN exposure and microglial activation is the secretion of neurotoxic substances including reactive oxygen species [77]. Sustained microglial activation has a disproportionate influence on dopaminergic (DA) neuronal loss, given the relative abundance (4.5 fold microglia relative to neurons) [49] of microglia within the substantia nigra (SN), a prominent site of DA neuronal cell death, and is exacerbated by the inherently low antioxidant capacity of DA neurons. As DA neurons die, further ASYN monomers and aggregates are released into the extracellular space, propagating a cycle of microgliosis and neurotoxicity. Preventing initial ASYN-mediated microglial activation and ASYN aggregation during PD pathogenesis are two key precursor events that could halt the progressive loss of DA neurons.

A number of factors that are known to enhance the intracellular ASYN aggregation, including low local pH [78], high calcium concentrations [80], restricted space and high macromolecule concentrations [81, 82], are all characteristic of the vesicular space and account for why ASYN within intracellular vesicles has been observed to be especially prone to aggregation [154]. In order to reduce intracellular ASYN aggregation, it would then be desirable to identify and disrupt receptor-mediated internalization by microglia. Multiple membrane receptors, including toll-like receptors [155-158], scavenger receptors [74, 159, 160], and integrin

MAC1 [161, 162] have been implicated in microglial interactions with pathological proteins and activation in neurodegenerative disease. While TLR4 [163], TLR2 [156], and MAC1 [164] have been implicated as receptors that interact with ASYN, scavenger receptors have remained relatively unexplored. SRA1 and CD36 have been noted to mediate microglial interaction and activation by amyloid β [160, 165], which forms similar fibrillar structures as ASYN [166]. We hypothesized that scavenger receptors are a key target for regulating ASYN trafficking and reducing intracellular ASYN aggregation.

Research has been done previously to develop synthetic compounds that mimic the charge and hydrophobicity of scavenger receptor-binding ligands, including using sulfatide derivatives [167] and modified synthetic phospholipids [168]. Using amphiphilic macromolecules (AMs) as biomimetic synthetic ligands based on sugar-based backbone, aliphatic side chains, and a hydrophilic poly(ethylene glycol) (PEG) tail [169, 170], new structure-activity relations indicated that optimal hydrophobicity, stereochemistry, and charge promote binding affinity to scavenger receptors SRA1 and CD36 [171]. Due to their amphiphilic nature, these molecules can be complexed around hydrophobic core solutes via kinetic flash nanoprecipitation techniques, forming nanoparticles (NP) with the potential for drug encapsulation and demonstrated resistance to AM release in serum-rich environments [172]. In this study, we advance microglial scavenger receptor-mediated internalization of ASYN as a therapeutic target in the pathway of ASYN aggregate formation and propagation.

3.2 Materials and Methods

3.2.1. Microglia Isolation and Cell culture

Rat primary microglia were kindly provided by the lab of Dr. David Shreiber in the form of mixed glial populations. Microglia were isolated from mixed glial populations by mechanical dissociation, using a rotating shaker at 200 rpm for 30 minutes, followed by centrifugation of cell media. For all experiments, primary microglia were plated at a density of 50,000 cells per square centimeter and cultured in DMEM/F12 (Gibco) supplemented with 10% fetal bovine serum (Atlanta Biologicals). BV2 microglia were kindly provided by Drs. Bin Liu (University of Florida) and Jason Richardson (Northeast Ohio Medical University). BV2 microglia and SH-SY5Y (ATCC) were also both cultured in DMEM/F12 supplemented with 10% fetal bovine serum.

3.2.2. Pull-down assay

Histidine-tagged recombinant Human SRA1 protein (R&D) and CD36 (Sino Biological) were prepared to a final concentration of 20 μg/mL in PBS supplemented with 5 mM imidazole (Sigma). Nickel coated plates (Fisher Scientific) were washed three times with PBS, followed by addition of 50 μl (1 μg) of scavenger receptor protein solutions to each well and incubation for 1 hour at room temperature with 300 rpm agitation on a rotary plate shaker. In order to prevent non-specific binding of ASYN to the nickel plate [173], the plates were incubated with 5% bovine serum albumin (BSA) (Sigma) for 1 hour at room temperature with 300 rpm agitation. After three washes with PBS, ASYN (rPeptide) was added in PBS at seven concentrations from 3.33 μM to 0 μM into wells either coated or uncoated with scavenger receptor proteins and blocked with BSA, and incubated overnight at room temperature with 300 rpm agitation. The plate was washed three times with PBS, followed by incubation with a primary antibody against ASYN in PBS, and incubated for one hour at room temperature with 300 rpm agitation. After three washes with PBS, the plate was incubated with a fluorescent secondary antibody in PBS overnight at room temperature with 300 rpm agitation. After three washes with PBS, the fluorescence intensity in each well was measured using a Tecan Infinite M200 Pro microplate reader. Fluorescence in wells blocked with BSA and uncoated with scavenger receptors was subtracted from corresponding wells that were coated with scavenger receptors.

3.2.3. Amphiphilic molecule synthesis

Macromolecules 1cM and M12 were synthesized as previously detailed and characterized using established techniques including 1H NMR-spectroscopy, gel permeation chromatography, differential scanning calorimetry, and dynamic light scattering [174-176]. The critical micelle concentration, size, and charge data has been published in the literature [177].

3.2.4. Nanoparticle fabrication

NPs were prepared via flash nanoprecipitation, characterized by dynamic light scattering to determine particle size and polydispersity, and tested for serum stability as described previously [170, 172, 178]. In brief, a confined impinging jet mixer was utilized to mix 250 μL of an aqueous stream with 250 μL of 50/50 v/v% mixture of tetrahydrofuran (THF) (Sigma) and DMSO (Sigma) stream containing 40 mg/mL NP shell molecule, and 20 mg/mL hydrophobic core molecule. Upon mixing, the exit stream was immediately introduced into 4.5 mL of phosphate buffered saline (PBS) (PBS:THF of 9:1) and subsequently dialyzed against PBS to remove residual THF. Five percent of the mass of shell molecule was fluorescently labeled with Alexa Fluor 680 Succinimidyl Ester (Thermo Fischer) in order to facilitate detection *in vitro*.

3.2.5. ASYN internalization

Rat-derived primary microglia were pre-incubated with scavenger receptor-targeting treatments, including either 10 μg/mL SRA1 (R&D) and CD36 (Abcam) antibodies or NPs for 24 hours, followed by 24 hour co-incubation with 5 μM monomeric ASYN (rPeptide), [179] fluorescently labeled with DyLight 594 nm (Dy594) microscale antibody labeling kit (Thermo Fischer). For monomeric ASYN studies using live cells, extracellular non-internalized synuclein fluorescence quenched by adding 0.5 mg/mL trypan blue (VWR) for 30 minutes, followed by two washes with PBS [180]. Live cells were imaged on a Leica SP2 confocal microscope using a 40 x dry objective. Intracellular fluorescence quantification was performed using NIH-ImageJ software (http://rsb.info.nih.gov/ij/), by measuring mean grey value in cells segmented by applying the same fluorescence thresholds to all collected images. For untreated cell controls, fluorescence images were segmented based on cell boundaries visualized in brightfield images.

3.2.6. Cellular adhesion assay

A 96-well non-tissue culture treated plate was coated with nonadherent matrix, 50 μg/mL collagen IV (Sigma) in distilled water at 37 degrees Celsius for 1 hour, washed once, and air-dried, followed by addition of 1 μg monomeric ASYN (rPeptide) and air-drying [181]. 50,000 cells per well were plated in 100 μL media supplemented with 1 mg/mL BSA (Sigma) and placed in an incubator for 2 hours, either with or without the presence of scavenger receptor-binding competitors, including antibodies or NPs. The plate was then washed three times with PBS and the number of cells was determined using Alamar Blue assay (Life Technologies) and comparison to a standard curve of adherent cells detected using Alamar Blue.

3.2.7. Immunocytochemistry

Cells were fixed with 4% paraformaldehyde (Sigma) for 30 minutes at room temperature, or for studies using fibrillar ASYN, 4% paraformaldehyde, 4% sucrose (Sigma), and 1% Triton X-100 (Sigma) to solubilize monomeric ASYN. Cells were simultaneously blocked and permeabilized in blocking buffer containing PBS supplemented with 1% BSA, 5% normal goat serum (MP Biomedicals), and 0.1% Triton X-100 for 1 hour at room temperature. Primary antibodies were incubated in blocking buffer at 4 degrees Celsius overnight, followed by three 15 minute washes with PBS. Afterwards, cells were incubated with fluorophore-conjugated secondary antibodies (Alexa Fluor 488, 594, or 647 from Life Technologies) in blocking buffer for 1 hour at room temperature, followed by three 15 minute washes with PBS. Cells were counter-stained with either BOBO-1 (Thermo Fischer) or 4'6-Diamidino-2-phenylindole dihydrochloride (Sigma) to visualize cell nuclei. For studies where only extracellular or cell-surface species were imaged, Triton-X-100 was omitted from blocking buffer. Stained samples were imaged on a Leica SP2 laser scanning confocal microscope.

3.2.8. Western Blotting

Intracellular ASYN was collected by incubating cells with RIPA lysis buffer and protease and phosphatase inhibitor cocktails (Pierce). Samples were mixed with Bolt LDS Sample Buffer and Bolt Sample Reducing Agent (Thermo Fischer), and heated for 10min at 70 degrees Celsius, then loaded onto a Bolt 4-12% Bis-Tris Plus gel (Thermo Fischer) and run for approximately 60

minutes at 150 V. Samples were transferred onto methanol-activated polyvinyl difluoride (PVDF) membrane (Thermo Fischer) in methanol-free transfer buffer (Pierce) at 300 mA for 90 minutes at 4 degrees Celsius. The PVDF membrane was then blocked in PBS with 5% by weight milk (Santa Cruz Biotechnology) and 0.05% by volume Tween-20 (Sigma) for 1 hour with agitation. Primary antibodies were added in blocking buffer at 4 degrees Celcius overnight without agitation. PVDF membranes were then washed three times for 10 minutes in PBS with 0.05% by volume Tween-20, followed by incubation with secondary antibodies in blocking buffer for 1 hour at room temperature. PVDF membranes were then washed three times for 10 minutes in PBS with 0.05% by volume Tween-20, followed by developing using incubation with ECL blotting solution (Pierce) for 3 minutes. PVDF membranes were then developed using Kodak Biomax Carestream light film (Sigma).

3.2.9. Statistical analysis

All data are presented as mean±s.d. Statistical significance is evaluated by single-factor ANOVA, with $P<0.05$ considered statistically significant.

3.3 Results

3.3.1. Scavenger Receptors as Co-ordinated Binding Targets for α-Synuclein

We confirmed the binding ability of two of the key scavenger receptors in microglia, SRA1 and CD36, for monomeric ASYN using a ligand-receptor binding assay. Monomeric ASYN was observed to bind to both SRA1 and CD36, with dissociation constant values of 177 and 101 nM, respectively (**Figure 3.1A**), assuming a 1:1 binding stoichiometry. The fluorescence of the saturation plateau of monomeric ASYN binding to SRA1 was observed to be roughly twice that of CD36 (**Supplementary Figure S3.1**), which may suggest a binding stoichiometry of monomeric ASYN to SRA1 of greater than 1:1, however, this could be a result of differences in available ASYN antibody binding sites between the ASYN-SRA1 and ASYN-CD36 complexes. The ASYN-receptor interactions were also observed in a cellular context; when rat primary microglia were plated onto non-adhesive surfaces coated with monomeric ASYN, cellular attachment was significantly improved compared to nonadhesive surfaces alone, and attachment was significantly decreased in the presence of SRA1 or CD36 targeting antibodies (**Figure 3.1B**). Rat primary microglia populations isolated from rat pup cortices by mechanical agitation and used in these and later experiments were found to be highly pure, with few non-microglial cells present (**Supplementary Figure S3.2**).

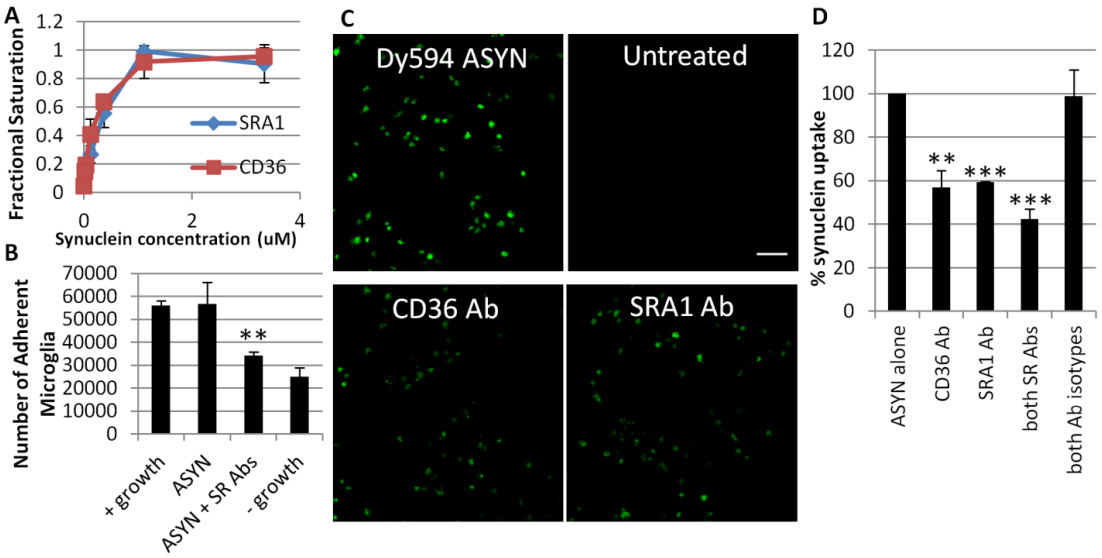

Figure 3.1 - Alpha-synuclein (ASYN) associates with scavenger receptors (SR).

A) Monomeric ASYN bound to histidine-tagged CD36 and SRA1 immobilized on a nickel-coated assay plate in a concentration dependent manner, with saturated binding at the two highest concentrations. B) Microglia seeded onto collagen IV and monomeric ASYN coated surfaces in the presence of SR-targeting antibodies had significantly reduced adherent cell numbers relative to microglia seeded onto collagen IV and monomeric ASYN coated surfaces without the addition of antibodies. **P<0.01 by 1-way ANOVA. C) Live-cell fluorescence imaging and D) quantification of intracellular fluorescence of microglia cultured for 24 hours with SR-targeting antibodies, followed by 24 hour co-treatment with fluorescently labeled monomeric ASYN and either CD36 or SRA1 antibodies. Each SR-targeting antibody separately and together significantly reduced intracellular fluorescence, relative to microglia treated with both antibody isotype controls. Scale bar = 50 μm. **P < 0.01, ***P<0.005 by 1-way ANOVA.

Next, we investigated whether scavenger receptors mediated ASYN internalization. Quantitative fluorescence intensity from internalized Dy594-labelled synuclein was significantly decreased following the antibody-based blocking of individual scavenger receptors (**Figure 3.1C,D**). Monomeric ASYN incubated with primary microglia, followed by Triton-X permeabilization, fixation, and staining for ASYN showed minimal observable fluorescence (**Supplementary Figure S3.3**), further suggesting that the fluorescence observed was primarily intracellular rather than cell-surface bound. Based on these results, we proposed a nanoparticle (NP) therapeutic with multiple scavenger-receptor binding capability as a design approach to regulate synuclein trafficking while enabling microglia-specific delivery of therapeutic molecules.

3.3.2 Amphiphilic Macromolecules (AMs) Lower α-Synuclein Uptake Competitively and Attenuate α-Synuclein Oligomerization in Microglia

Next, we investigated the molecules from the scavenger receptor-binding AM library, which most compete with ASYN uptake. Rat primary microglia were co-incubated with Dy594-labeled

synuclein and NPs comprised of different shell based AM molecules. Based on this selected screening, we observed that the molecule M12-P5 (abbreviated as 1cM) (**Figure 3.2A**) within the shell layer of NPs elicited the greatest reduction in the uptake of synuclein (**Figure 3.2B**). All NPs were used at the equivalent concentrations, with identical polystyrene cores (to present "biologically inactive cores"), and all had comparable shell molecule mass concentrations. As an additional validation, the NPs were evaluated as substrates for competitive inhibition of microglial binding to ASYN; here, 1cM shell NPs significantly decreased microglial adhesion to ASYN coated surfaces, similar to the effects of scavenger receptor antibodies (**Figure 3.2C**).

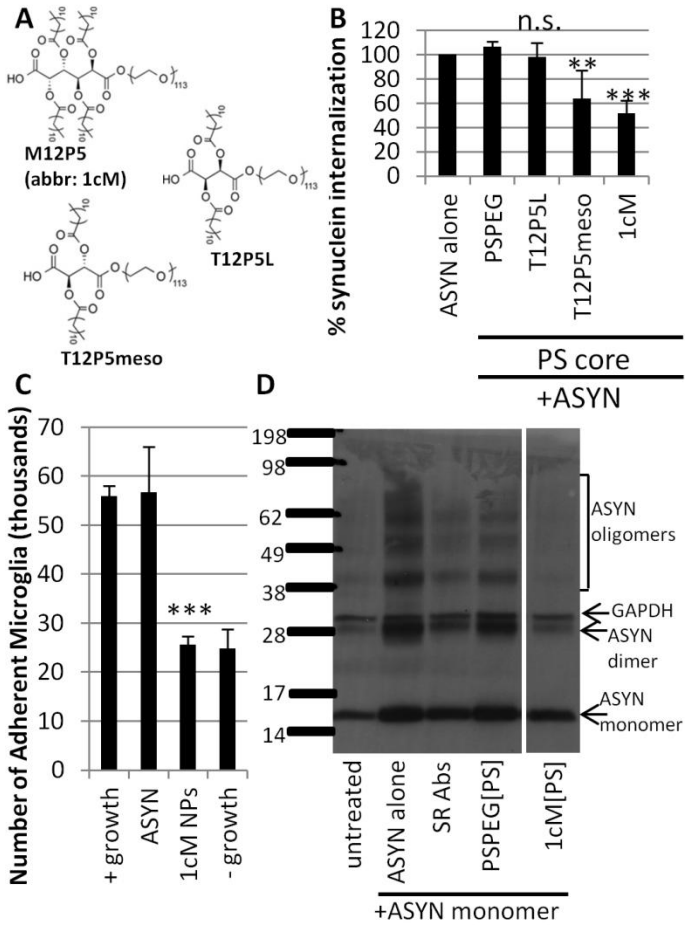

Figure 3.2 - Amphiphilic molecule (AM) library screening reveals candidate molecules for regulating ASYN trafficking.

A) The amphiphilic molecules tested in nanoparticle (NP) shell included polystyrene-PEG as well as M12P5 (abbreviated as 1cM), T12P5L and T12P5meso, who have similar sugar backbones with

aliphatic branches and hydrophilic PEG chains. B) Rat primary microglia were pre-incubated with NPs comprised of candidate AM molecules in the shell and polystyrene (PS) in the core, followed by co-incubation of microglia with NPs and fluorescently labelled monomeric ASYN. Intracellular fluorescence for each condition was normalized to background fluroescence of untreated microglia and to monomeric ASYN-only treated microglia. Microglial treatment with two AM shell NPs resulted in a significant decrease in intracellular fluorescent ASYN, with 1cM having a more significant effect relative to microglia treated with non SR-targeting polystyrene-polyethylene glycol (PSPEG) shell NPs. **P < 0.01, ***P<0.001, by 1-way ANOVA. C) Microglia seeded onto surfaces coated with collagen IV and monomeric ASYN in the presence of SR-targeting 1cM shell NPs had significantly reduced adherent cell numbers relative to microglia seeded onto surfaces coated with collagen IV and monomeric ASYN without the addition of NPs. Uncoated tissue culture plastic was used as a positive growth control, and collagen IV alone coated surfaces as a negative growth control. ***P<0.001 by 1-way ANOVA. D) Primary rat microglia treated with monomeric ASYN and SR-targeting NPs or antibodies were lysed after 24 hours in order to examine intracellular forms of ASYN. Oligomeric ASYN were detected within monomeric ASYN-treated microglia, and the presence of these species was decreased in SR antibody-treated microglia, and about absent in 1cM NP treated microglia. Monomeric ASYN is still internalized in the presence of SR-targeting antibodies.

Next, we explored the role of NPs to modulate the ASYN content of microglia. Treatment with scavenger receptor-targeting NPs was observed to lower the presence of intracellular ASYN aggregates, particularly oligomers, in monomeric ASYN treated primary microglia (**Figure 3.2D**, full gel in **Supplementary Figure S3.4A**). Oligomeric forms of ASYN were not detected in the extracellular media containing ASYN incubated for 24 hours at 37^{o}C (**Supplementary Figure S3.4B**), so the oligomers were cell-associated. Further, this data indicates that the formation of intracellular ASYN oligomers in microglia results from high internalization of monomeric ASYN, and that multi-receptor regulation of trafficking decreased intracellular ASYN aggregation. Preliminary studies are in progress to examine whether these microglial intracellular aggregates can be transmitted to neuronal cells.

3.4 Discussion

While a number of promising strategies are currently in use to ameliorate the motor deficits that occur in PD, there have been limited efforts to develop therapies addressing the progressive nature of the disease due to gradual loss of SN DA neurons. Despite improvements in symptoms, synucleinopathies, which involves in neuroinflammatory activation of microglial cells, may continue to propagate and causes cell toxicity. We hypothesized that microglia, a key cell in the trafficking of ASYN, would be a valuable cellular target in the brain in order to address nanotherapeutics to counteract persistent ASYN-mediated microglial activation and ASYN aggregation.

In this study, we demonstrated via several complementary experimental methods that monomeric ASYN associates with and is internalized by microglial scavenger receptors SRA1 and CD36. Others have examined the role of CD36 as a mediator of microglial activation via ASYN. Su et. al. have demonstrated that human ASYN overexpressing mice have increased levels of activated microglia [74]. Further, they have isolated microglia from CD36-deficient mice and found attenuated activation response to ASYN. Despite these efforts and the knowledge of other receptors such as Toll-like receptor [156] or macrophage antigen-1 [164] that mediate microglial activation by ASYN, there has been little validation on other scavenger receptors and few efforts developing therapeutics targeting multiple receptors responsible for microglial interaction with ASYN.

Our studies offer valuable insight into the nature of interactions between monomeric ASYN and scavenger receptors. M12-P5 (1cM), which has a mucic acid backbone and four aliphatic chains and relatively higher lipophilic character, more significantly reduced monomeric ASYN uptake by microglia, compared to AMs with a tartaric acid backbone and two aliphatic chains, molecules 16 and 17. Both T12P5meso and 1cM have acidic end groups, and both significantly reduced monomeric ASYN internalization by microglia, which may also suggest that cationic domains on scavenger receptors mediate interactions with ASYN. Since T12P5meso significantly reduced monomeric ASYN internalization while T12P5L did not, these findings suggest that stereochemistry significantly impacts the ability of AMs to competitively bind

scavenger receptors. Further study into the nature of interactions between ASYN and scavenger receptors, including stoichiometry and immediate downstream effects, may be valuable areas of investigation.

Our studies indicate that intracellular oligomerization of ASYN may be facilitated by internalized receptors. The observation that both scavenger receptor-targeting antibodies and AMs appeared to decrease the presence of intracellular ASYN oligomers suggests that scavenger receptors may play a role in the initiation of oligomerization. Our data reveals that while a multiple scavenger receptor-binding AM decreases internalized monomeric ASYN to similar levels as using multiple scavenger receptor-binding antibodies, NPs formed from these AMs have a more dramatic effect on decreasing the formation of intracellular ASYN oligomers. Key differences between these AMs and scavenger receptor antibodies include charge properties, lipophilicity, and binding sites on scavenger receptors. It is possible that AMs and antibodies may block binding sites for extracellular ASYN, but due to these differences, only the AMs appear to block epitopes on the internalized scavenger receptors that contributes to intracellular ASYN oligomerization. It has recently been discovered that amyloid-β stimulates activation of microglia through a heterotrimer of CD36, TLR4, and TLR6 [182]. Some similar receptor complex may play a role in the recognition and binding of ASYN, and even in intracellular oligomerization. The charge, lipophilic, or binding character of AMs may also likely prevent the formation of complexes of multiple ASYN-binding receptors to a greater degree than scavenger receptor-binding antibodies.

The observed inhibition of intracellular ASYN aggregation may be especially important if these oligomers contribute to the propagation of synucleinopathy, or directly contribute to neurotoxicity. Recent findings suggest that oligomeric species may be directly toxic to neurons, and indirectly neurotoxic by activating microglia [70, 183]. These intracellular oligomeric species may become released from microglia either on their own, or due to disruptions in lysosomal clearance pathways caused by overabundance of ASYN [58] or by common mutations associated with idiopathic and familial PD [55-57]. Once released by microglia, these oligomers could contribute to the progression of synucleinopathy by seeding the formation of oligomers in other

cells. Fibrillar ASYN sonicated into “pre-formed fibrils” have been observed to seed the growth of new fibrils and ASYN pathology *in vitro* [184] and *in vivo* [185]. Furthermore, ASYN pathology induced by genetic overexpression has been observed to spread within neuronal populations both *in vitro* and *in vivo* [186, 187]. However, whether the use of exogenously seeded aggregates or genetic overexpression reflect the physiological condition is unclear. If the intracellular aggregates observed in these studies could seed neuronal intracellular ASYN aggregates, these studies may be among the first identifying microglia as a key element in intiating ASYN aggregation from monomeric physiological ASYN in the process of synucleinopathy. We have further studies planned and in progress to identify if these intracellular oligomers can be released and transmitted to neuronal cells, and if they are capable of seeding further ASYN aggregation.

3.5 Supplementary Figures

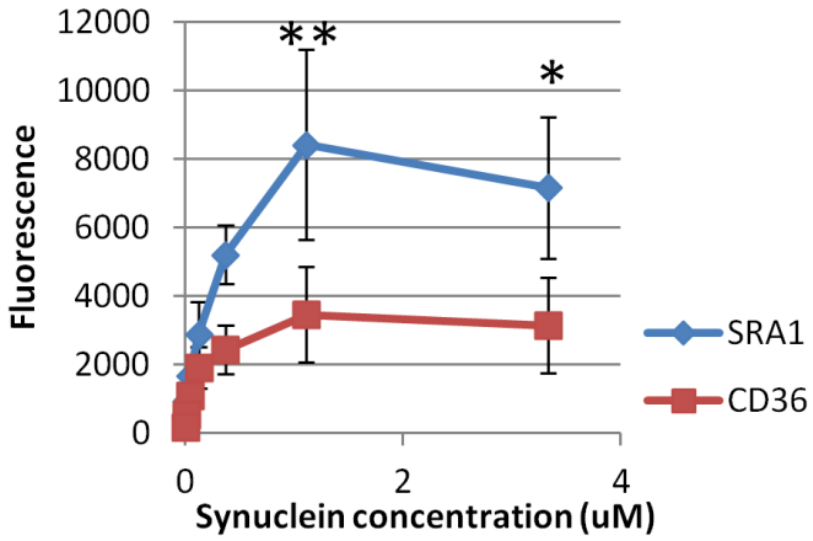

Supplementary Figure S3.1 - Fluorescence readings of antibody-detected ASYN associated with scavenger receptors coated on a Nickel-coated plate.

The significant difference in fluorescence intensity at saturation suggests that there may be a difference in stoichiometry of binding between synuclein and each scavenger receptor. **P<0.01, *P<0.05 by Student's t-test.

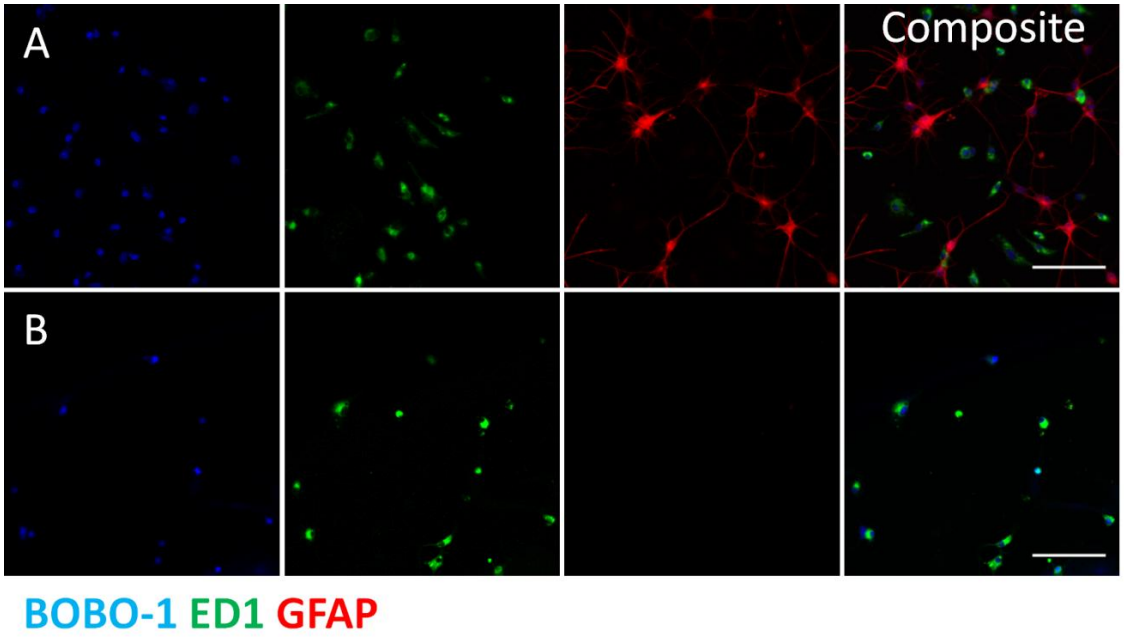

Supplementary Figure S3.2 – Primary microglia isolated from mixed glial populations

A) Mixed microglia, expressing ED1 (green) and astrocytes, expressing GFAP (red) isolated from rat cortex. B) With mechanical isolation, the resultant population is relatively pure with microglia. Scalebar = 100 μm.

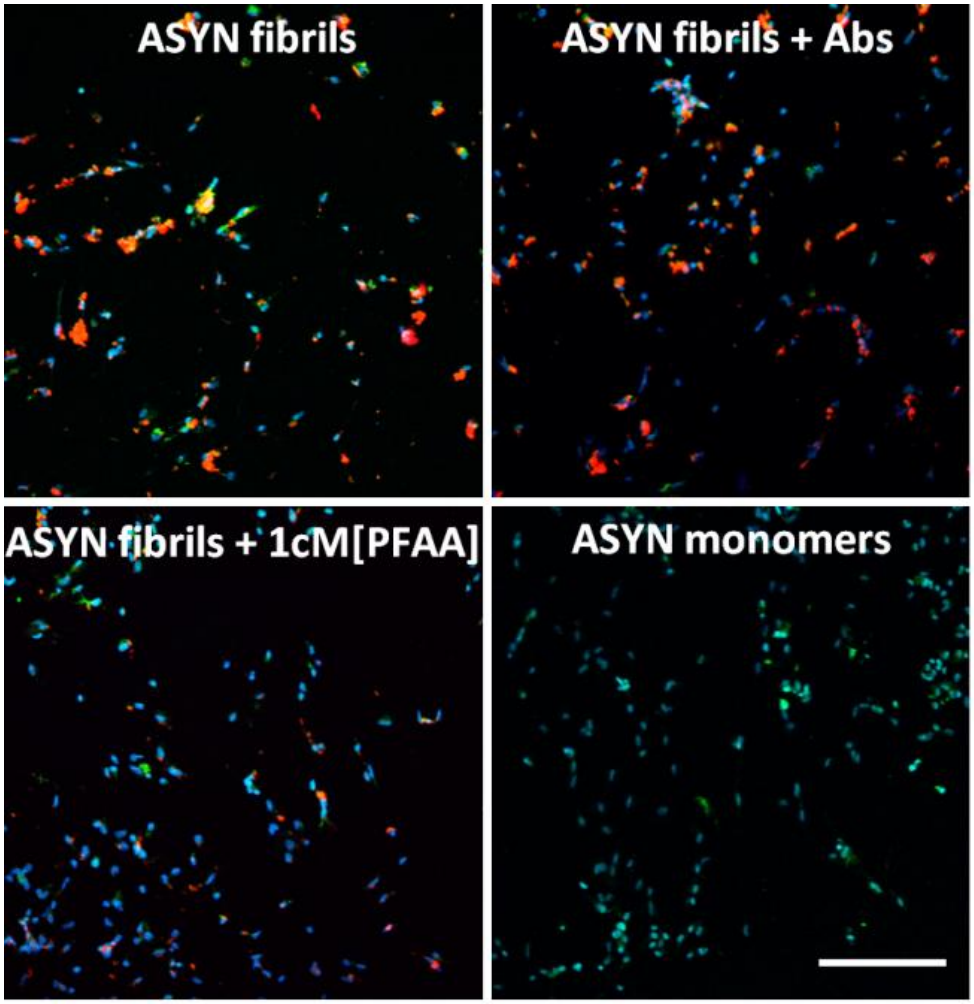

Supplementary Figure S3.3 – ASYN fibrils incubated with primary microglia and stained with permeabilization.

Primary rat microglia were incubated for 24 hours with either SR-targeting antibodies or SR-targeting NPs, followed by a 24 hour co-incubation with SR-targeting molecules and 5 uM ASYN monomer or the same mass of ASYN fibrils. Cells were fixed in 4% paraformaldehyde, 4% sucrose (Sigma), and 1% Triton X-100 (Sigma) to solubilize ASYN monomers. Microglial cell surface-bound ASYN was visualized by immunofluorescence staining for ASYN (red) and microglial cell marker ED1 (green) and nuclear stain BOBO-1 in the presence of permeabilization agents. Notably, the SR-targeting antibodies had little effect on reducing binding of synuclein fibrils, while NPs had a dramatic effect. Additionally, the stained ASYN was Triton-X insoluble, suggesting that it is indeed fibrillar. Scalebar = 200 μm.

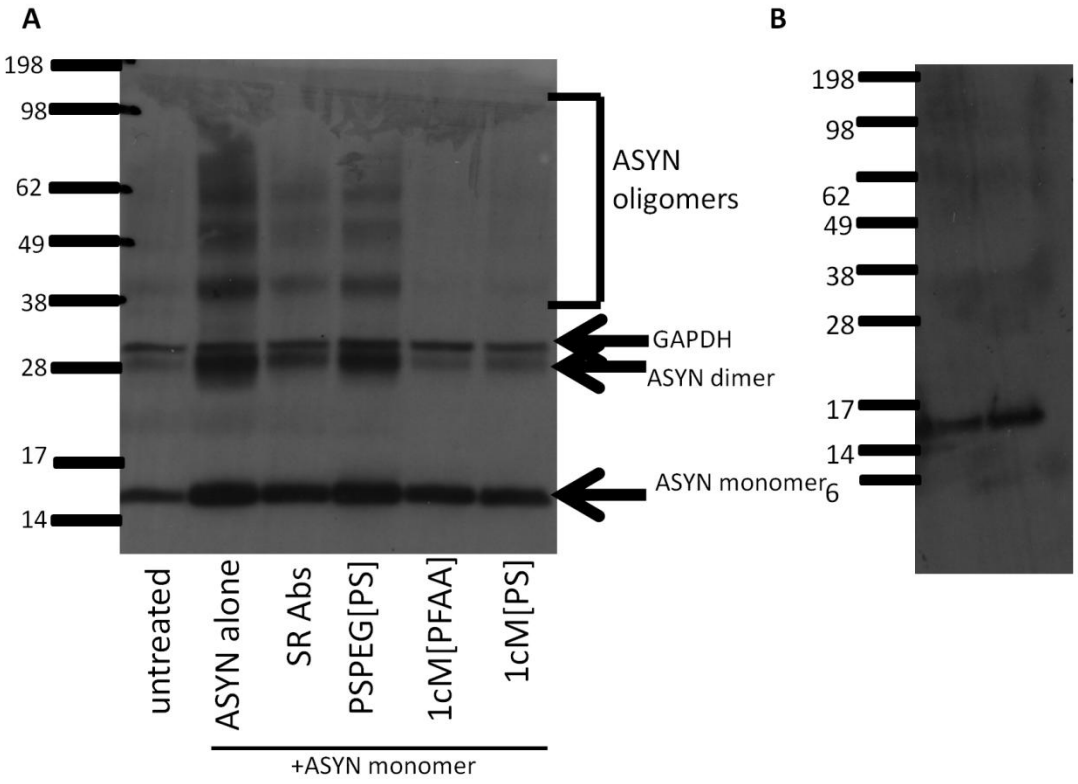

Supplementary Figure S3.4 – Full western blot of intra-microglial ASYN oligomerization.

A) Primary rat microglia treated with monomeric ASYN and SR-targeting NPs or antibodies were lysed after 24 hours in order to examine intracellular forms of ASYN. Cell lysates were analyzed by Western blot, with staining for ASYN and GAPDH. Oligomeric ASYN were detected within monomeric ASYN-treated microglia, and these were reduced in SR antibody-treated microglia, and about absent in 1cM NP treated microglia, irrespective of core composition. As observed previously, monomeric ASYN is still internalized in the presence of SR-targeting antibodies, confirming that microglia are still capable of clearing monomeric ASYN from the extracellular space. B) Extracellular media containing 5 μM monomeric ASYN does not form oligomers in 24 hours at 37 degrees Celsius.

CHAPTER 4 - MOLECULAR DISRUPTION OF ALPHA-SYNUCLEIN MEDIATED MICROGLIAL ACTIVATION

The following chapter contains figures and major sections of text excerpted from the following manuscript submitted for publication:

Bennett N.K., Chmielowski R., Faig J.J., Francis N.A., Baum J., Pang Z.P., Uhrich K.E., Moghe P.V. Polymer Nanotherapeutics Ameliorate Microglial α-Synuclein Aggregation, Activation, and Neurotoxicity. *Submitted to Biomaterials, 8/16/16*.

Abstract

The extracellular protein α-synuclein (ASYN), whose accumulation is characteristic of PD, is well documented to cause activation of microglia. However, the control of synuclein-mediated inflammatory responses has been challenging. In the previous chapter, we established that microglial internalization of monomeric ASYN was mediated by scavenger receptors (SR), CD36 and SRA1, and was rapidly accompanied by the formation of ASYN oligomers. Next, we designed a nanotechnology approach to regulate SR-mediated intracellular ASYN trafficking within microglia. In this chapter we describe engineering composite deactivating NPs with dual character, namely shell-based SR-binding amphiphiles, and core-based antioxidant poly (ferrulic acid), to investigate concerted inhibition of microglial oxidative activation. In ASYN-challenged microglia treated with NPs, we observed decreased ASYN-mediated acute microglial activation and diminished microglial neurotoxicity caused by exposure to aggregated ASYN. Composite NPs administered *in vivo* within the substantia nigra of fibrillar ASYN-challenged wild type mice attenuated microglial activation. Overall, SR-targeting AM nanotechnology represents a novel paradigm in alleviating microglial activation in the context of synucleinopathies like PD and other neurodegenerative diseases.

4.1 Introduction

In this and the previous chapter, the overall paradigm we investigated was the possible role of scavenger receptor-binding NPs in modulating the internalization of ASYN in microglia and subsequent cellular activation and intracellular accumulation of aggregated forms of ASYN (**Figure 4.1**). However, another key element of PD progression that we aimed to address was microglial activation, which can contribute to progressive neurodegeneration. In the process of microglial activation, intracellular reactive oxygen species (ROS) production is known to be a critical regulator [188, 189]. While ASYN phagocytosis alone has been shown to result in microglial production of intracellular ROS [70], internalized exogenous ASYN can result in ROS production through other means as well, including by disruptions in mitochondrial function [190, 191]. The prominent role of oxidative species both in the process of microglial activation and in neuronal dysfunction have led many to investigate the use of antioxidant therapies in the treatment PD [192-195].

One landmark study was a large, double-blinded and placebo-controlled clinical trial with 800 patients in early stages of PD, conducted to investigate the efficacy of α-tocopherol, a form of vitamin E, and selegiline on slowing the rate of PD progression [195]. Although some benefit was observed for selegiline, supplementation of α-tocopherol was found to not reduce the probability of requiring L-DOPA treatment. Despite these results, studies since then have continued to investigate the efficacy of α-tocopherol, including a more recent meta-analysis finding that dietary intake of α-tocopherol protected against PD. In addition, studies have since found that α-tocopherol succinate is more effective than its natural counterpart in inhibiting tumor cells and oxidation [196, 197], as well as in the *in vivo* protection against neurodegeneration in PD model rats [198]. Notably, α-tocopherol succinate is more water-soluble than α-tocopherol, and may more readily enter cells or react with oxidants in the cytosol or plasma rather than at cell membranes [199]. These results taken together suggest that the efficacy of antioxidants in treating PD may depend on a number of factors, including their ability to localize to relevant cells and regions of cells, as well as their ability to interact with relevant oxidative species and other antioxidants present within the cell [200]. We believe that a successful antioxidant therapy for

the treatment of PD must translate these considerations into design of appropriate antioxidant therapeutics with enhanced stability and intracellular delivery attributes.

Our research group has previously created polymeric and diacid forms of the antioxidant ferulic acid, which have demonstrated sustained antioxidant release with little bioactive decomposition [201]. We hypothesize that the scavenger receptor-based presentation of these stabilized antioxidants will concertedly ameliorate ASYN-induced microglial activation (**Figure 4.1**). Given the acute role of microglia in elevating oxidative damage to neurons, we also engineered composite deactivating NPs (**CODE NPs**) via a concerted approach to introduce antioxidant polymers via NPs. We demonstrate these phenomena using a series of NPs with graded SR-binding in cultured microglia and *in vivo* following intracranial injections of NPs after administration of ASYN. Such CODE NPs are the first generation therapeutic candidates to manage ASYN aggregation/transmission (long-term) and ameliorate oxidative stresses (short-term) within neurodegenerative pathophysiology.

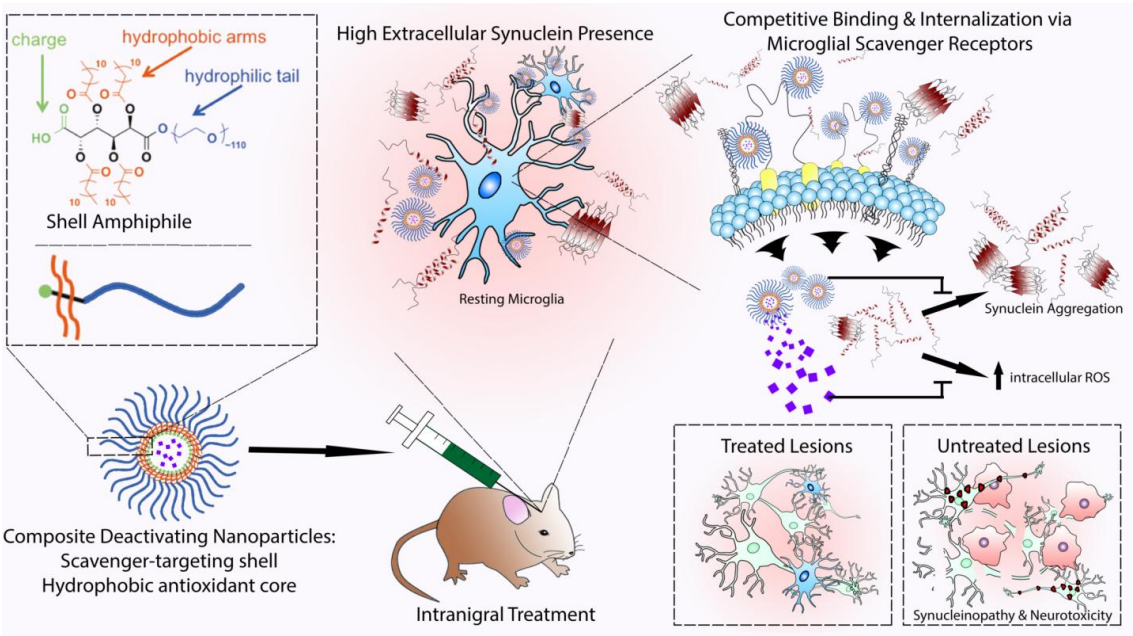

Figure 4.1 - Schematic of the new nanotechnology paradigm for scavenger receptor-mediated management of ASYN uptake and aggregation to counteract neurotoxicity in neurodegenerative diseases like PD.

We envision nanoparticles comprised of synthetic scavenger receptor-binding amphiphilic molecules to reduce both intracellular ASYN aggregation and microglial activation by regulating microglial interactions with monomeric and aggregated ASYN and delivering anti-inflammatory agents along these pathways, ultimately decreasing microglial-mediated neurotoxicity and synucleinopathy propagation.

4.2 Materials and Methods

4.2.1. Microglia Isolation and Cell culture

Rat primary microglia were kindly provided by the lab of Dr. David Shreiber in the form of mixed glial populations. Microglia were isolated from mixed glial populations by mechanical dissociation, using a rotating shaker at 200 rpm for 30 minutes, followed by centrifugation of cell media. For all experiments, primary microglia were plated at a density of 50,000 cells per square centimeter and cultured in DMEM/F12 (Gibco) supplemented with 10% fetal bovine serum (Atlanta Biologicals). BV2 microglia were kindly provided by Drs. Bin Liu (University of Florida) and Jason Richardson (Northeast Ohio Medical University). BV2 microglia and SH-SY5Y (ATCC) were also both cultured in DMEM/F12 supplemented with 10% fetal bovine serum.

4.2.2. Amphiphilic molecule synthesis

Macromolecules 1cM and M12 were synthesized as described in the previous chapter.

4.2.3. Antioxidant molecule synthesis

Ferulic acid-based derivatives (Acid FAA and FADG) were synthesized and characterized following previously developed methods [201]. Upon Acid FAA and FADG isolation, polymers were synthesized using a modified solution polymerization method [202]. In brief, ferulic acid-based derivative (1 equiv. Acid FAA or Acid FADG) was suspended in anhydrous dichloromethane (DCM) under argon. Triethylamine (4.4 equiv) was added, to acquire a pale yellow solution, and the reaction cooled to 0 ˚C. Triphosgene (1 equiv, dissolved in anhydrous DCM to acquire a 15 % w/v solution) was added drop-wise over 30 minutes. After stirring 4 h, the reaction was quenched with 1 N hydrochloric acid (50 mL) and allowed to stir for 15 minutes. The organic layer was then passed through a $MgSO_4$-packed gravity filter, collected in a round bottom flask, concentrated *in vacuo* to ~10 mL, and precipitated over 400 mL chilled diethyl ether. Pure polymer was isolated via vacuum filtration and dried under vacuum overnight. PFAA possessed a molecular weight of 44 kDa, a polydispersity index of 1.3, and a T_g of 84 ˚C. PFADG had a molecular weight of 26.2 kDa, a polydispersity index of 1.2, and a T_g of 102 ˚C. Further chemical analyses of these polymers is discussed by Ouimet *et al* [201].

4.2.4. Nanoparticle fabrication

NPs were prepared via flash nanoprecipitation and characterized as described in the previous chapter.

4.2.5. ASYN internalization

Rat-derived primary microglia were pre-incubated with scavenger receptor-targeting treatments, including either 10 μg/mL SRA1 (R&D) and CD36 (Abcam) antibodies or NPs for 24 hours, followed by 24 hour co-incubation with 5 μM monomeric ASYN (rPeptide), [179] fluorescently labeled with DyLight 594 nm (Dy594) microscale antibody labeling kit (Thermo Fischer) or 5 μM monomer-equivalent fibrillar ASYN. For fibrillar ASYN studies, cells were fixed prior to characterization by immunocytochemistry. For monomeric ASYN studies using live cells, extracellular non-internalized synuclein fluorescence quenched by adding 0.5 mg/mL trypan blue (VWR) for 30 minutes, followed by two washes with PBS [180]. Live cells were imaged on a Leica SP2 confocal microscope using a 40 x dry objective. Intracellular fluorescence quantification was performed using NIH-ImageJ software (http://rsb.info.nih.gov/ij/), by measuring mean grey value in cells segmented by applying the same fluorescence thresholds to all collected images. For untreated cell controls, fluorescence images were segmented based on cell boundaries visualized in brightfield images.

4.2.6. iROS detection

Rat-derived primary microglia were pre-incubated with scavenger receptor-targeting treatments or NPs for 24 hours, followed by co-incubation with monomeric ASYN (rPeptide). After 24 hours of co-incubation, iROS production was quantified using a 2',7' – dichlorofluorescin diacetate (DCFDA) detection assay kit (Abcam). In brief, cells were washed with 10% FBS supplemented assay buffer, and if applicable, incubated with 50 μM tert-butyl hydrogen peroxide for 2 hours as a positive iROS production control. Cells were then stained with a 40 μM DCFDA solution in supplemented assay buffer for 30 minutes [70], followed by 2 washes using supplemented assay buffer, followed by fluorescence measurement at 485 nm and 535 nm emission on a Tecan Infinite M200 Pro microplate reader. Fluorescence readings of supplemented assay buffer alone

were subtracted from all measurements, and DCFDA fluorescence was normalized to untreated cell controls.

4.2.7. Immunocytochemistry

Cells were fixed with 4% paraformaldehyde (Sigma) for 30 minutes at room temperature, or for studies using fibrillar ASYN, 4% paraformaldehyde, 4% sucrose (Sigma), and 1% Triton X-100 (Sigma) to solubilize monomeric ASYN. Cells were simultaneously blocked and permeabilized in blocking buffer containing PBS supplemented with 1% BSA, 5% normal goat serum (MP Biomedicals), and 0.1% Triton X-100 for 1 hour at room temperature. Primary antibodies were incubated in blocking buffer at 4 degrees Celsius overnight, followed by three 15 minute washes with PBS. Afterwards, cells were incubated with fluorophore-conjugated secondary antibodies (Alexa Fluor 488, 594, or 647 from Life Technologies) in blocking buffer for 1 hour at room temperature, followed by three 15 minute washes with PBS. Cells were counter-stained with either BOBO-1 (Thermo Fischer) or 4'6-Diamidino-2-phenylindole dihydrochloride (Sigma) to visualize cell nuclei. For studies where only extracellular or cell-surface species were imaged, Triton-X-100 was omitted from blocking buffer. Stained samples were imaged on a Leica SP2 laser scanning confocal microscope.

4.2.8. ASYN fibrillization

Fibrillization was carried out using 100 μL of 1 mg/mL monomeric ASYN (rPeptide) in a 96-well plate (BD Falcon), with a 5 mm glass bead (Sigma) for nucleation, and agitated at 300 rpm at 37 degrees Celsius for 50 hours minimum on a Southwest Science Multi-Therm plate shaker [203]. Plates were sealed using parafilm to minimize evaporation, and final volumes were corrected to initial volumes using sterile distilled water. Fibrillization was verified by sampling ASYN before and after fibrillization, by incubating 2 μM ASYN solution in PBS with 40 μM Thioflavin-T (Sigma) for 10 minutes at room temperature, followed by measuring fluorescence excitation and emission at 450 and 485 nm on a Tecan Infinite M200 Pro microplate reader.

4.2.9. Neurotoxicity Assay

BV2 immortalized microglia and SH-SY5Y neuroblastoma were used for neurotoxicity experiments. BV2 microglia were plated at 50,000 cells per square centimeter, and SH-SY5Y were plated separately at 100,000 cells per square centimeter. Microglia were treated with SR-targeting antibodies or antioxidant loaded nanoparticles, or non-SR targeting and no-antioxidant loaded NPs for 24 hours, followed by co-treatment with either 1μg/mL LPS (Sigma), 20 μM monomeric ASYN, which has been demonstrated to activate BV2 cells [204] or the same mass of fibrillar ASYN. SH-SY5Y cells were treated with media conditioned by the ASYN- or LPS-stimulated microglial cells for 24 hours. Cytotoxicity in response to stimulated microglia conditioned media was quantified in SH-SY5Y populations was quantified using a lactate dehydrogenase assay (Promega), normalized to a positive control of totally lysed SH-SY5Y cells, and to untreated BV2-conditioned SH-SY5Y cells.

4.2.10. Animal studies

All animal experiments were carried out according to the Rutgers University Policy on Animal Welfare and were approved by the Institutional Animal Care and Use Committee (IACUC) at Rutgers University Robert Wood Johnson Medical School. Wildtype C57BL/6 mice (Jackson Laboratory) were anesthetized with isoflurane (induction at 4% and maintained at 0.5-1% inhalation). ASYN fibrils were concentrated to 6 mg/mL using a 3 kDa MWCO Amicon centrifuge filter (Millipore). To maintain the same mass ratio between ASYN and NP shell molecule used in most previous experiments described, NP stock was concentrated to a final shell concentration of 5.6 mg/mL, using the same Amicon centrifuge filters. 1 μL total injection volume was injected into the substantia nigra pars compacta for each mouse, either fibrillar ASYN alone (0.5 μL 6 mg/mL fibrillar ASYN and 0.5 μL saline), fibrillar ASYN and 1cM shell and PFAA core NPs (0.5 μL 6 mg/mL fibrillar ASYN and 0.5 μL NP), or fibrillar ASYN and PSPEG shell and PS core NPs (0.5 μL 6 mg/mL fibrillar ASYN and 0.5 μL NP), with 1 μL saline injected on the opposite hemisphere using a 1 μl gastight Hamilton syringe. Bilateral injections were made at the following coordinates (in mm): AP, -2.9 (from bregma); ML, +/-1.3; DV, −4.5 (from dura). Mice were sacrificed and processed for immunohistochemistry 48 hours after injection. Quantification of

microglial recruitment and activation was performed by staining 50 μm sections of brain slices. Four representative brain slices were quantified per animal.

4.2.11. Statistical analysis

All data are presented as mean±s.d. Statistical significance is evaluated by single-factor ANOVA, with $P<0.05$ considered statistically significant.

4.3 Results

4.3.1. Composite-Deactivating (CODE) NPs with Synuclein-Regulating Shell and Antioxidative Core Ameliorate Activation and Neurotoxicity

The key shell chemistry of the AM with meso stereochemistry $M_{12}PEG$ (abbreviated as 1cM, to indicate the anionic carboxylic acid-functionalized mucic acid backbone) has been observed to bind scavenger receptors SRA1 and CD36 [205]. Thus, the scavenger receptor-targeting behavior of 1cM can confer preferential targeting to microglia, which highly express scavenger receptors [181]. To test this, NPs comprised of Alexa Fluor 680-conjugated 1cM shell and polystyrene core were incubated for 24 hours with mixed population of primary rat microglia and SH-SY5Y human neuroblastoma cells, labeled with CellTracker Green and Red, respectively. Microglia in culture were visualized to contain both CellTracker dyes, presumably due to phatocytosis of cell debris. Fluorescently labeled NPs were observed to localize primarily to microglia in mixed culture (**Supplementary Figure S4.1**). This SR-based targeting of microglia by NPs enables control of synuclein trafficking as well as delivery of additional pharmacologic factors that could further decrease microglial activation, as described next.

Microglia are known to increase production of ROS in early stages of activation [70], and antioxidant therapies have shown promise in PD [192-194]. Therefore, we first investigated effects on activation in primary rat microglia incubated with NPs made with different ferulic acid-derived core molecules. These molecules were selected from a limited screen of additional ferulic acid-derived molecules and other antioxidants (**Supplementary Figure S4.2**). We observed that antioxidant core selection affected microglial activation response. Antioxidant ferulic acid adipic polymer (PFAA) significantly decreased intracellular ROS production in microglia exposed to monomeric ASYN, while its non-polymeric form, ferulic acid (adipic) diacid (FAA acid) did not (**Figure 4.2**). These differences in detected intracellular ROS production are likely not due to changes in microglial viability (**Supplementary Figure S4.3A**) or microglial proliferation or aggregation (**Supplementary Figure S4.3B**). Notably, the addition of PFAA in the core of NPs did not lower the ability of the AMs to decrease the presence of intracellular ASYN oligomers

in monomeric ASYN treated microglia (**Supplementary Figure S3.4A**). Further, the addition of non-nanoparticle-based administration of PFAA in suspension did not affect monomeric ASYN-mediated ROS production, and did not reduce microglial neurotoxicity (data not shown), indicating the unique role of nanoparticle-based targeting and activity following cellular uptake.

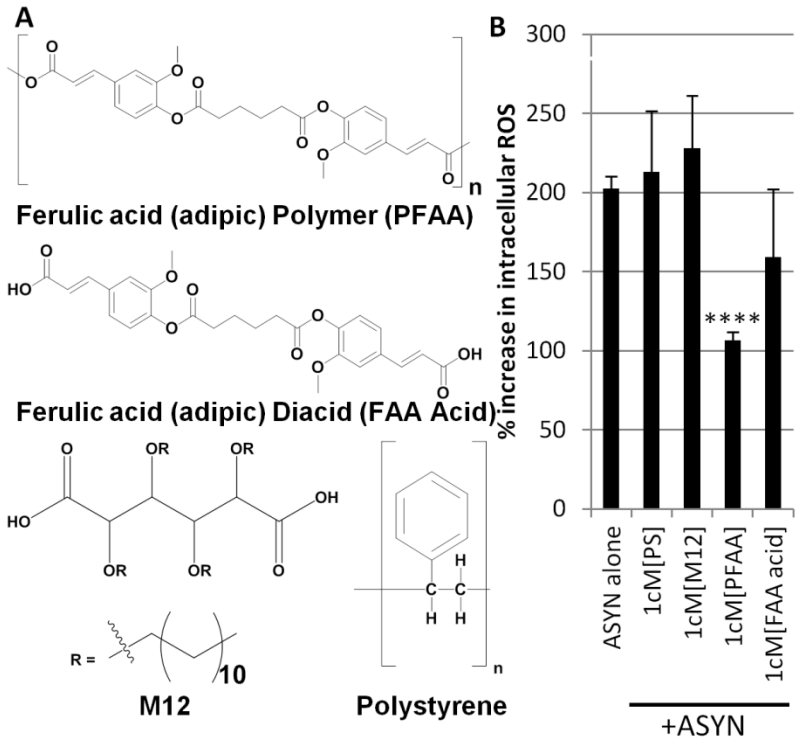

Figure 4.2 - Antioxidant delivery counters ASYN-mediated microglial activation.

A) Microglia were treated with NPs comprised of 1cM shell and different antioxidant cores, including ferulic-acid derived molecules, and non-antioxidant control cores, the mucid acid backbone of 1cM, and polystyrene. B) After 24 hour co-treatment with NPs and monomeric ASYN on microglia, intracellular reactive oxygen species (iROS) was detected using DCFDA dye. Only the polymeric form of ferulic acid was found to significantly reduce monomeric ASYN-mediated increases in iROS. PFAA was used in subsequent studies, and 1cM shell/PFAA core NPs have been identified as a NP formulation capable of reducing ASYN monomer uptake and ASYN-induced microglial activation. ****P<0.0001 by 1-way ANOVA.

It is well documented that aggregated forms of ASYN, particularly oligomers, cause increased microglial activation [156], neuronal damage [75, 206-208] and neurotoxicity [183,

209]. Fibrillar ASYN and Lewy bodies are reported to be generally more structurally stable and have decreased toxicity [210, 211] compared to oligomers, while fibrillization-impaired, oligomer-producing mutant mice displayed significantly more neurotoxicity [209]. Therefore, it has been proposed that stabilization of the fibrillization pathway, encouraging Lewy body or fibrillar sequestration of oligomers could be of therapeutic interest [212]. For this reason, we examined the ability of scavenger-targeting NPs to moderate the trafficking of higher order forms of ASYN. Primary microglia co-treated with NPs and 71 μg/mL ASYN fibrils appeared to have a dramatic effect on reducing fibrillar ASYN binding or internalization, compared to untreated or scavenger receptor antibody-treated controls (**Figure 4.3A**). Extracellular staining of microglia incubated with the same mass concentration of ASYN monomers (71 μg/mL or approximately 5 μM) is depicted as well for comparison. ASYN fibrillization was monitored using Thioflavin-T fluorescence, and bound or internalized ASYN was confirmed to be in the form of Triton-X insoluble fibrils (**Supplementary Figure S3.3**). Antioxidant-loaded NPs were observed to similarly decrease fibrillar ASYN-mediated microglial activation, quantified by intracellular ROS production (**Figure 4.3B**). In these experiments, it should be noted that the antioxidant-loaded NPs had a more significant reduction in fibrillar ASYN-mediated intracellular ROS production compared to monomeric ASYN-mediated intracellular ROS production.

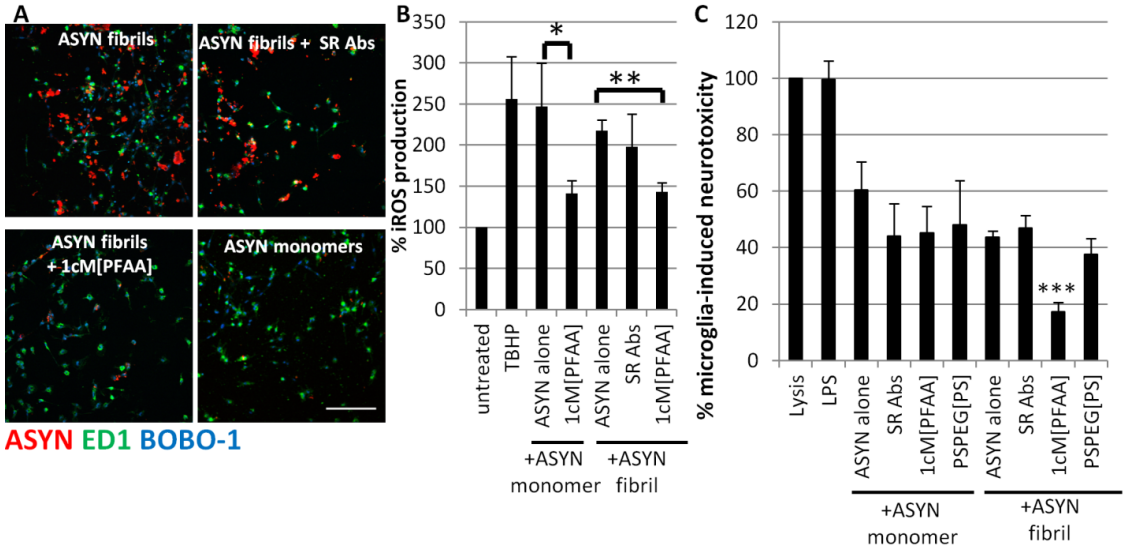

Figure 4.3 - CODE NPs reduce ASYN-induced microglial neurotoxicity and activation by fibrillar ASYN.

A) Primary rat microglia were incubated with either SR-targeting antibodies or SR-targeting NPs, followed by co-incubation with SR-targeting molecules and monomeric ASYN or the same mass of fibrillar ASYN. Microglial cell surface-bound ASYN was visualized by immunofluorescence staining for ASYN (red) and microglial cell marker ED1 (green) and nuclear stain BOBO-1 in the absence of permeabilization agents. Scalebar = 200 μm. B) Primary rat microglia were incubated with either SR-targeting Abs or NPs prior to co-incubation with monomeric ASYN or the same mass of fibrillar ASYN. Microglial activation in response to ASYN was quantified by measuring iROS relative to untreated microglia. ASYN monomers, fibrils, and tert-butyl hydroperoxide (TBHP) all caused high degrees of microglial activation. SR-targeting antioxidant containing NPs were found to reduce fibrillar ASYN-mediated microglial activation, while SR-targeting antibody treatments did not, relative to microglia treated with fibrillar ASYN alone. *P<0.05, **P<0.01 by 1-way ANOVA. C) BV2 microglia were treated with SR-targeting antibodies or antioxidant loaded nanoparticles, or non-SR targeting and no-antioxidant loaded NPs for 24 hours, followed by co-treatment with either 20 μM monomeric ASYN or the same mass of fibrillar ASYN. SH-SY5Y cells were treated with media conditioned by the ASYN- or LPS-stimulated microglial cells. Cytotoxicity in response to stimulated microglia conditioned media was quantified in SH-SY5Y populations. Thus, the SR-targeted, antioxidant loaded CODE particles significantly reduce neurotoxicity from fibrillar ASYN but not monomer-mediated microglial activation. ***P<0.001 by 1-way ANOVA.

An organotypic coculture system based on BV2 immortalized microglia and SH-SY5Y neuroblastoma was used to recapitulate an advanced PD state. BV2 microglia have been observed to behave similarly to activated microglia [213], while SH-SY5Y cells have been commonly used as dopaminergic model cells in neurotoxicity studies [214-216]. BV2 microglia were treated with SR-targeting antibodies or antioxidant loaded nanoparticles, or non-SR targeting and non-antioxidant loaded NPs for 24 hours, followed by co-treatment with either 20 μM monomeric ASYN [204] or the same mass of fibrillar ASYN. SH-SY5Y cells were treated with media conditioned by the ASYN- or LPS-stimulated microglial cells for 24 hours. The SR-targeted,

antioxidant loaded particles significantly reduced neurotoxicity from fibrillar ASYN but not monomer-mediated microglial activation (**Figure 4.3C**). Treatment of BV2 microglia with non-NP based administration of PFAA did not appear to counteract activation caused by monomeric or fibrillar ASYN (**Supplementary Figure S4.4A**). Further, 24 hour treatment with residual fibrillar ASYN in conditioned media was not a significant contributor to toxicity in SH-SY5Y cells (**Supplementary Figure S4.4B**).

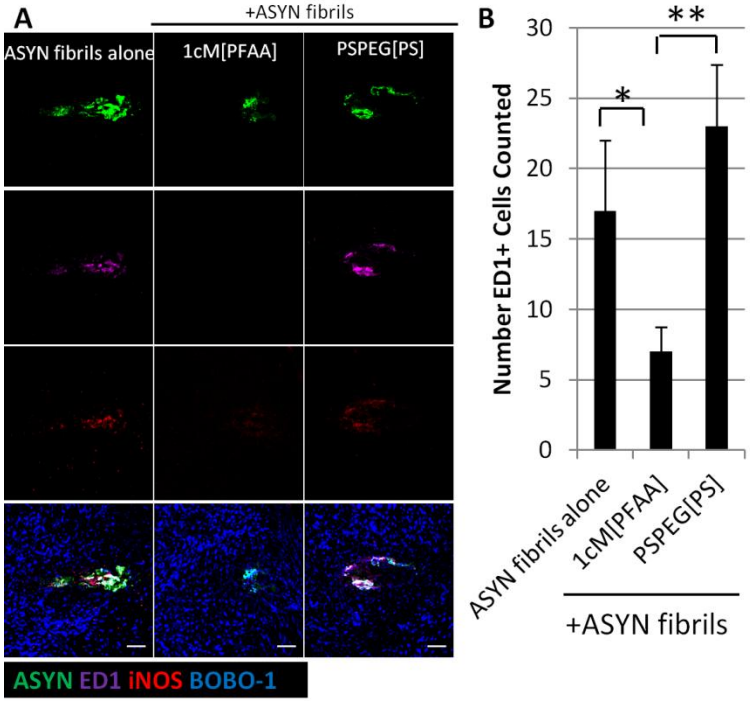

Figure 4.4 - 1cM NPs reduce microglial recruitment and activation in response to fibrillar ASYN in vivo.

A) Wildtype mice were injected in the substantia nigra pars compacta (SNpc) one hemisphere with 1 µL saline and 1 µL total injection volume of either 3 µg fibrillar ASYN and saline, fibrillar ASYN with 1cM shell PFAA core NPs, or fibrillar ASYN with PSPEG shell PS core NPs. After two days, animals were perfused and brains were collected, sliced, and stained for ASYN (green), activated microglia marker ED1 (magenta), iNOS (red), and given nuclear stain BOBO-1 (blue). Three representative slices are depicted. Scale bar = 100 µm. B) Four representative 50 µm-thick brain slices were quantified per animal, and the number of ED1+ cells in the vicinity of ASYN

staining were counted. There was a significant decrease in the number of ED1+ cells located in the vicinity of ASYN fibrils injected into the SNpc. *P<0.05, **P<0.01 by 1-way ANOVA.

Finally, we investigated whether SR-targeting, antioxidant-delivering CODE NPs could reduce microglial activation in response to aggregated ASYN species *in vivo*. 1cM shell PFAA core NPs were co-injected with ASYN fibrils into mouse substantia nigra pars compacta (SNpc), and resulting activated microglia were quantified, compared to mice with co-injected PSPEG shell PS core NPs (non-SR-targeting, non-antioxidant core NPs) and ASYN fibrils, and ASYN fibrils alone. 1cM shell PFAA core NPs appeared to significantly decrease the presence of activated microglia, visualized by staining for ED1, in the vicinity of co-injected fibrillar ASYN, relative to mice that received either PSPEG shell PS core NPs or no NP treatment (**Figure 4.4A-B**). No fibrillar ASYN or activated microglial recruitment was observed in sham-injected mouse hemispheres (**Supplementary Figure S4.5**).

4.4 Discussion

While pharmacological and surgical interventions are currently in use to address the debilitating motor symptoms of PD, there has been limited success in addressing the progressive nature of the disease due to continued loss of SN DA neurons, presenting a key therapeutic challenge. A growing body of evidence suggests that a major contributing factor to PD progression is the activation of microglia by aggregated forms of ASYN, and the subsequent cycle of neurotoxicity and continued ASYN relese and aggregation. We hypothesized that composite deactivating nanoparticles, capable of both reducing microglial interactions with aggregated ASYN and targeting delivery of stabilized antioxidants would reduce microglial activation and neurotoxicity.

Previous attempts to regulate inflammation in models of PD through pharmacological inhibition of microglia using myeloperoxidase inhibitors, minocycline, or nonsteroidal anti-inflammatory agents have shown inconsistent results [77, 217-221]. However, it may be that activation pathways specific to PD or ASYN must be targeted for enhanced therapeutic effect. Likewise, large-scale clinical studies of the effects of antioxidants on slowing the progression of PD have had mixed results [195], however, more recent findings suggest that the efficacy of some antioxidants can be improved by chemical modification affecting their availability within cells [198]. We observed that different antioxidant molecules derived from the same base molecule, ferulic acid, had differential efficacy at reducing monomeric ASYN-mediated microglial activation. Some of the differences in efficacy may be attributable to antioxidant stability, as we have observed that the chemical structure of PFAA allows for an extremely slow release of ferulic acid over months of storage at 2-8 degrees Celsius (data not shown), which may translate to more prolonged intracellular or intravesicular release of antioxidants. The ferulic acid diacid core NPs were observed to be much larger in size (~600 nm) compared to the antioxidant polymer NPs (~200 nm), which could result in different interactions with microglial scavenger receptors, different uptake, and different stability between formulations.

A key advantage of the NP formulation was the ability to target delivery of screened hydrophobic core antioxidant molecules to microglia. Notably, α-tocopherol was effective at

reducing microglial activation in response to ASYN monomers. This stands in contrast to its results in the clinical trials mentioned previously, but is similar to what was observed with *in vivo* studies using chemically modified α-tocopherol of increased hydrophilicity. We also observed that NP-delivered PFAA was able to reduce microglial neurotoxicity, but PFAA was not effective when not paired with a SR-targeting shell. Additionally, we demonstrated that the targeted delivery of this lead ferulic acid-derived antioxidant molecule was able to decrease the presence of activated microglia in the vicinity of fibrillar ASYN *in vivo*. Taken together, these data suggest that targeted delivery of antioxidants to microglia is a critical factor in the efficacy of antioxidant therapies for PD. Further studies may be warranted to further decouple the importance of antioxidant stability and intracellular delivery towards overall efficacy. Additional valuable studies may also investigate the efficacy *in vivo* of this NP formulation in more closely disease-relevant conditions, including the ability to decrease microglial activation in response to other pathogenic forms of ASYN like oligomers, or the ability to decrease longer term, more chronic microglial activation in response to ASYN.

Aggregated forms of ASYN are characteristic of advanced stages of PD, and have been observed to be cause an activation and neurotoxic response in microglia, particularly in oligomeric forms [70]. For this reason, we investigated the effects of multipronged scavenger receptor-targeting NPs on aggregated ASYN trafficking, focusing first on fibrillar ASYN. In future studies, we hope to investigate the impact of these NPs on oligomeric ASYN species as well. NPs were observed to have more of an effect than antibody treatments in reducing extracellular bound or internalized ASYN fibrils. Others have claimed that fibrils are a less toxic form of ASYN compared to oligomers [210, 211], and that a possible therapeutic strategy may be to encourage sequestration of ASYN in higher order fibrillar forms to decrease the presence of oligomeric species [212]. By reducing the binding of fibrillar ASYN to the surface of microglia, these NP treatments may encourage the increased fibrillization of ASYN in the extracellular space. A possible mechanism for 1cM NPs achieving these effects may be due to the multimeric or charged nature of the NPs, such that they are able to influence a larger region of the cell surface, including other cell surface receptors, besides the individual scavenger receptor to which a single 1cM

molecule may bind. As mentioned previously, the NPs may also be able to prevent the formation of multi-receptor complexes, which may play a role in the binding of ASYN fibrils. Further investigation may be warranted to elucidate the nature of interactions between multimeric NPs, cell surface receptors, and multimeric receptor substrates.

In summary of the data from Chapters 3 and 4, scavenger receptor targeted nanoparticles can be designed to concertedly regulate two critical phenomena underlying synucleinopathies, the intracellular conversion of a-synuclein to oligomers upon microglial clearance, which may be a key route to export and transmission of synuclein aggregates, leading to chronic neurotoxicity; and the acute management of hyperoxidative damage caused by microglia to neurons.

4.5 Supplementary Figures

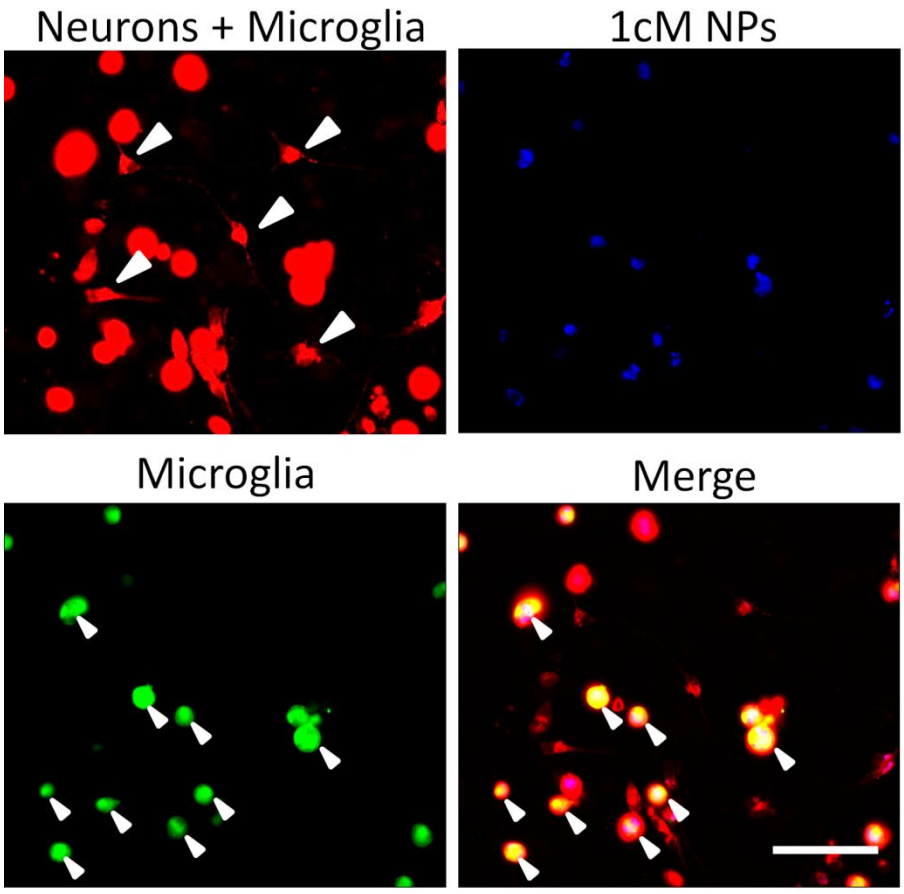

Supplementary Figure S4.1 - Rat primary microglia and SH-SY5Y human neuroblastoma were used to model a mixed cell-type brain environment.

Microglia were labelled with red and green celltracker dye, and neuroblastoma were labelled with red celltracker dyes prior to co-plating. Celltracker red-labelled neuroblastoma cells are fairly easy to distinguish based on their neuronal/bipolar morphology, indicated with downward pointing arrows, and are visible in red, but not green. Celltracker green-labelled microglia are indicated with the upward pointing arrows. These mixed cell populations were incubated with fluorescently labelled 1cM shell NPs (blue). The merged image has no instances of neuronal morphology cells with a magenta color, indicating that the neuroblastoma did not readily internalize the NPs, while a number of white cells are indicated with upward facing arrows, indicating that microglia in the mixed population readily internalized the NPs. Scale bar = 50 um.

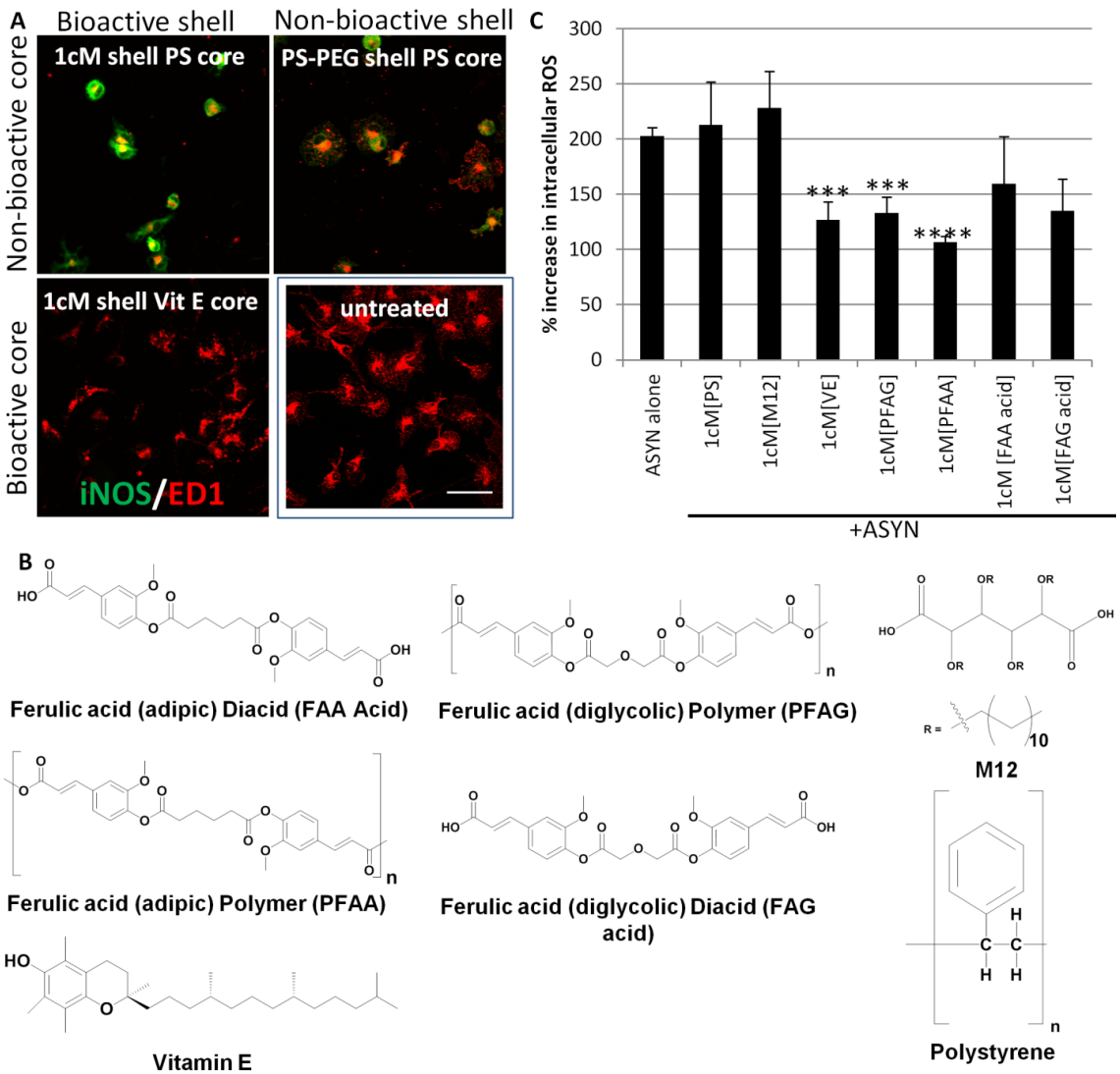

Supplementary Figure S4.2 - Antioxidant delivery counters ASYN-mediated microglial activation.

A) Microglia were treated with NPs made with different combinations of bioactive or non-bioactive shell and core. Non-bioactive cores paired with either type of shell produced activated microglia, visualized by increased expression of inducible nitric oxide synthase (iNOS, green), with microglia visualized using ED1 (red). By adding an antioxidant vitamin E core, microglia were not activated, relative to untreated microglia. Scale bar = 50 μm. B) Microglia were treated with NPs comprised of 1cM shell and 7 different cores, 6 antioxidants, including four ferulic-acid derived molecules, and polystyrene. C) After 24 hour co-treatment with NPs and monomeric ASYN on microglia, intracellular reactive oxygen species (iROS) was detected using DCFDA dye.

Three molecules were found to significantly reduce monomeric ASYN-mediated increases in iROS. PFAA was used in subsequent studies, and 1cM shell/PFAA core NPs have been identified as a NP formulation capable of reducing ASYN monomer uptake and ASYN-induced microglial activation. ***P<0.001, ****P<0.0001 by 1-way ANOVA.

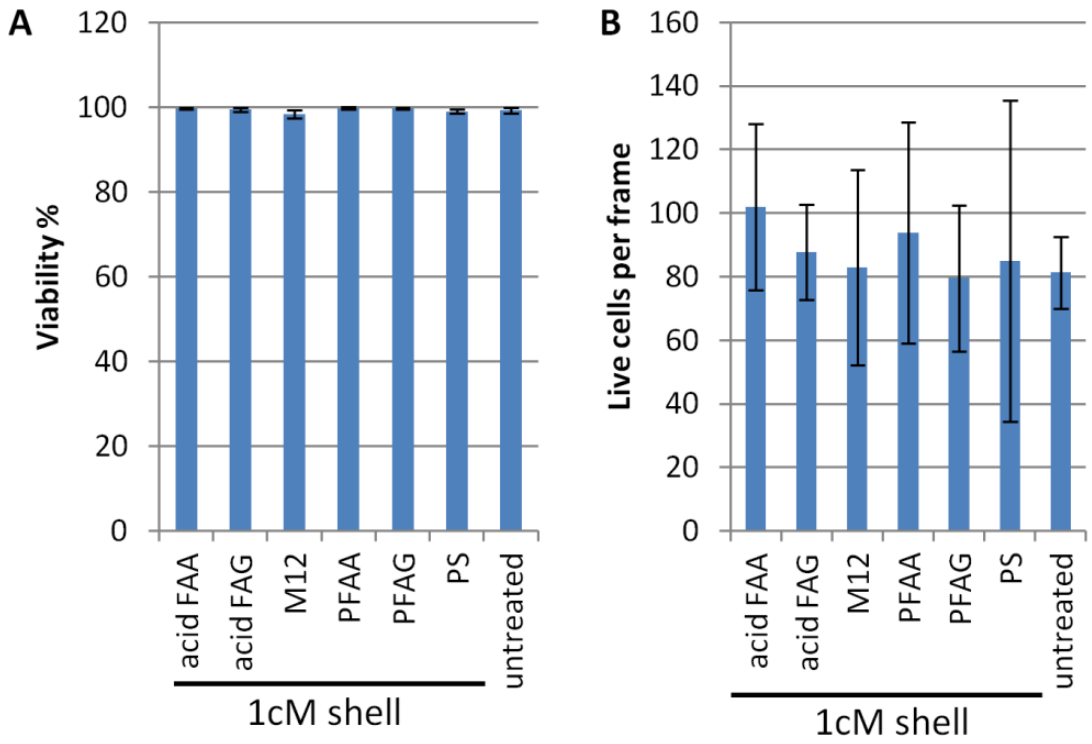

Supplementary Figure S4.3 – NP formulations do not affect microglial viability or proliferation.

A) Rat primary microglia were treated with 1cM shell NPs with varying cores for 48 hours, prior to quantification of viability using Calcein AM and propidium iodide. Microglia did not display diminished viability in response to any NP treatment. B) Microglia did not appear to have different numbers of live cells per frame, suggesting no difference in proliferation or aggregation in response to NP treatment.

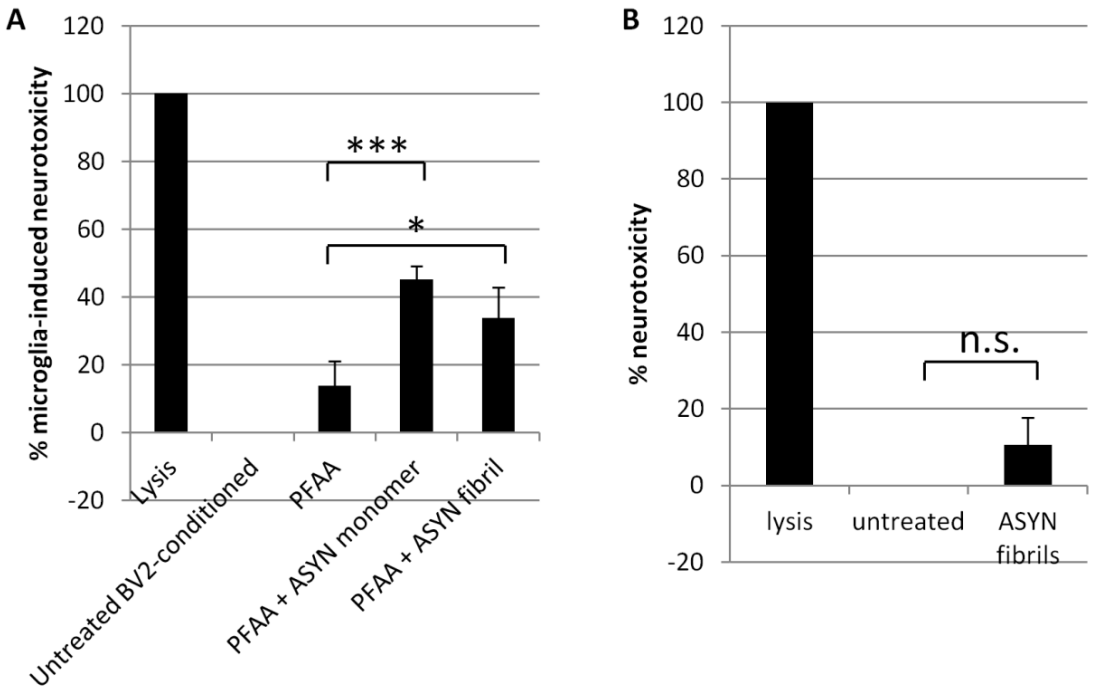

Supplementary Figure S4.4 – Unencapsulated PFAA does not reduce fibrillar ASYN-mediated neurotoxicity

A) BV2 Microglia were treated with PFAA for 24 hours, followed by co-treatment with either 20 μM monomeric ASYN or the same mass of fibrillar ASYN. SH-SY5Y neuroblastoma cells were treated with media conditioned by the ASYN-stimulated microglial cells for 24 hours. Cytotoxicity in response to stimulated microglia conditioned media was quantified in SH-SY5Y populations was quantified using a lactate dehydrogenase assay, normalized to a positive control of totally lysed SH-SY5Y cells, and to untreated BV2-conditioned SH-SY5Y cells. Treatment of BV2 microglia with either ASYN species together with PFAA resulted in significant increases in neurotoxicity of conditioned media, compared to treatment of BV2 with the PFAA molecule alone. *$P<0.05$, ***$P<0.001$ by 1-way ANOVA. B) Neuroblastoma cells were treated with media containing fibrillar ASYN for 24 hours. Cytotoxicity in response to ASYN-containing media was quantified in SH-SY5Y populations was quantified using a lactate dehydrogenase assay, normalized to a positive control of totally lysed SH-SY5Y cells, and to untreated SH-SY5Y cells. The fibrillar ASYN did not cause significant neurotoxicity in the neuroblastoma population. N.S. by 1-way ANOVA.

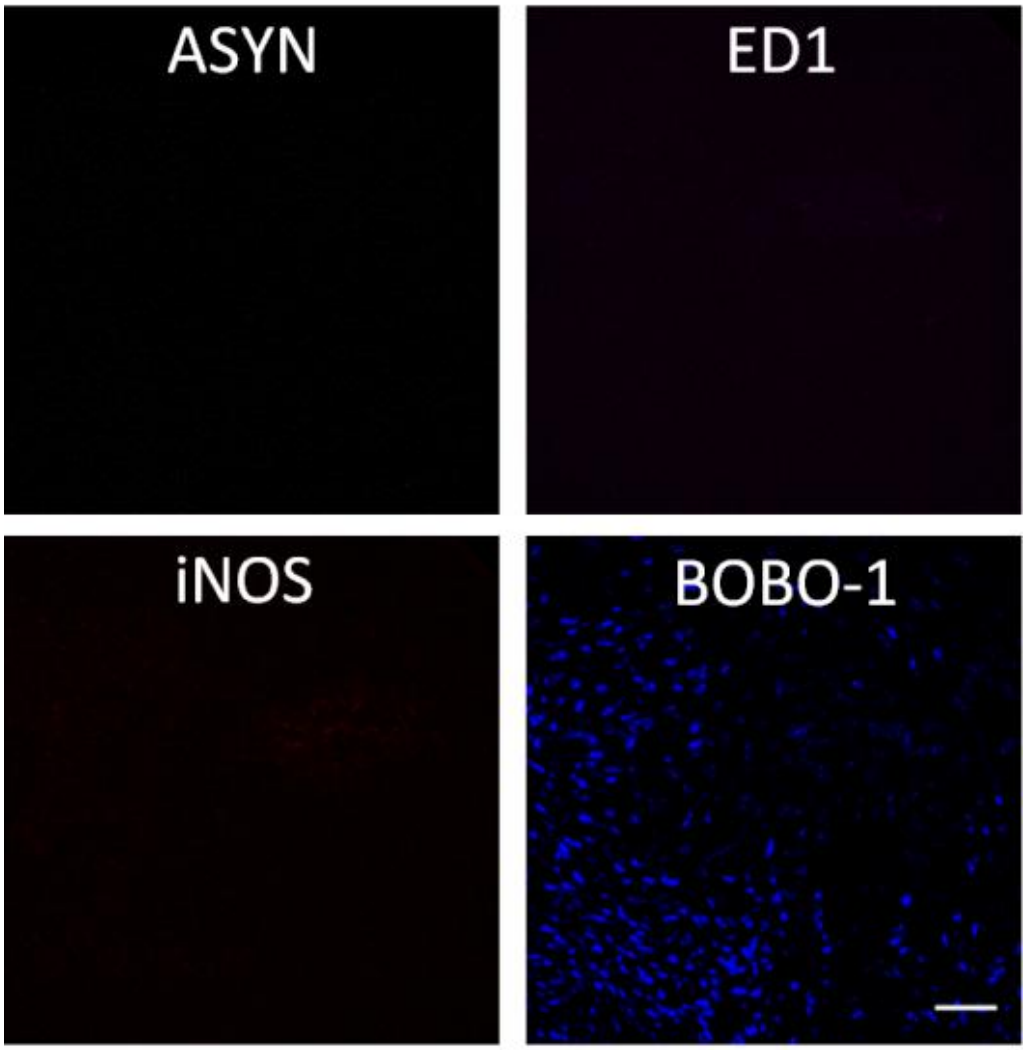

Supplementary Figure S4.5 - Representative images from a mouse brain hemisphere receiving a sham procedure with injection of saline.

No staining was observed for ASYN (green), ED1 (magenta), iNOS (red), with BOBO-1 nuclear staining seen in blue. Scalebar = 100 μm.

CHAPTER 5 - DISSERTATION SUMMARY AND FUTURE DIRECTIONS

5.1 Dissertation Summary

A number of neurodegenerative diseases are characterized by similar disease elements, including progressive neuronal loss, the presence of pathological protein aggregates, and occasionally activated microglia. Parkinson's disease is one such devastating neurodegenerative disease that presents these critical therapeutic challenges. Neurons in the CNS are challenged through the propagation of synucleinopathy and by activated microglia, with DA neuronal deficits leading to severe motor symptoms. In this work, we have presented two novel paradigms for addressing these challenges, via 1) cell replacement therapy with reprogrammed human neuronal populations supported by 3D fibrous scaffolds, and 2) molecular interventions regulating microglial interactions with ASYN.

In the first part of this work, we investigated the potential for fibrous synthetic substrates ability to support and transplant populations of human reprogrammed neurons using polymeric microfibrous electrospun scaffolds. We discovered that fibrous substrate geometries could be tuned to shift reprogrammed cell populations more towards neuronal differentiation or maintenance of pluripotency. We next generated injectable microscale scaffolds out of these fibrous substrates, and found that these constructs improved survival of transplanted neuronal populations by at least an order of magnitude over dissociated cell transplantation. Overall, these results can serve to guide the design of future transplantable scaffolds, by demonstrating ways that geometric and functionalization properties affect the culture, maturation, and transplantation of mature neuronal populations.

Next, we first identified scavenger receptors as a receptor for ASYN and designed a nanotherapeutic targeting this interaction using synthetic amphiphilic scavenger receptor ligands. We found that these amphiphilic molecules could reduce ASYN internalization and intracellular aggregation by microglia. We used nanoparticle constructs made from these synthetic scavenger receptor ligands to target delivery of antioxidants to microglia, ultimately decreasing microglial activation in response to aggregated ASYN *in vitro* and *in vivo*, and decreasing microglial

neurotoxicity. Overall, the studies described in this dissertation provide a valuable foundation for therapeutic strategies against fundamental aspects of PD and could serve to halt disease progression and address symptoms emerging in late stages of the disease.

5.2 Future Directions

5.2.1 Transplantation of reprogrammed neuronal populations in self-assembling peptide nanofibrous scaffolds

As Parkinson's disease and other neurodegenerative diseases are noted to involve overly-activated microglia and neurotoxicity, it is important that transplantation scaffolds be designed to be minimally immunogenic. For that reason, we have investigated the ability of a self-assembling peptide nanofiber scaffold (SAPNS) to support the culture and transplantation of reprogrammed neuronal populations, alongside our work with synthetic polymer electrospun microfibrous scaffolds. This material is formed from a peptide with alternating sequences of the amino acids arginine, alanine, and aspartic acid, known as RADA16-I or commercially known as Puramatrix. Since RADA16-I is made from natural amino acids, its products from breaking down elicit no immune response or inflammation *in vivo*. These peptides can undergo spontaneous assembly into nanofiber scaffolds when exposed to culture media or physiological salt concentrations [222-224] (**Figure 5.1**). These SAPNS resemble a hydrogel with a water composition of over than 99%, have fibers approximately 10 nm in diameter and pores between 5-200 nm, surrounding cells in a similar manner to native nanofibrous extracellular matrix [222-224]. The peptide RADA16-I has been shown to support attachment and growth of a wide variety of mammalian cells, particularly neural stem/progenitor cells [225-229]. Since these peptides are synthetic, they can be modified by incorporating various functional motifs within the peptide sequence to modulate cell behaviors such as cell adhesion or differentiation [230]. We hypothesize that the RADA16-I SAPNS will support in vitro 3D cultures of reprogrammed neurons.

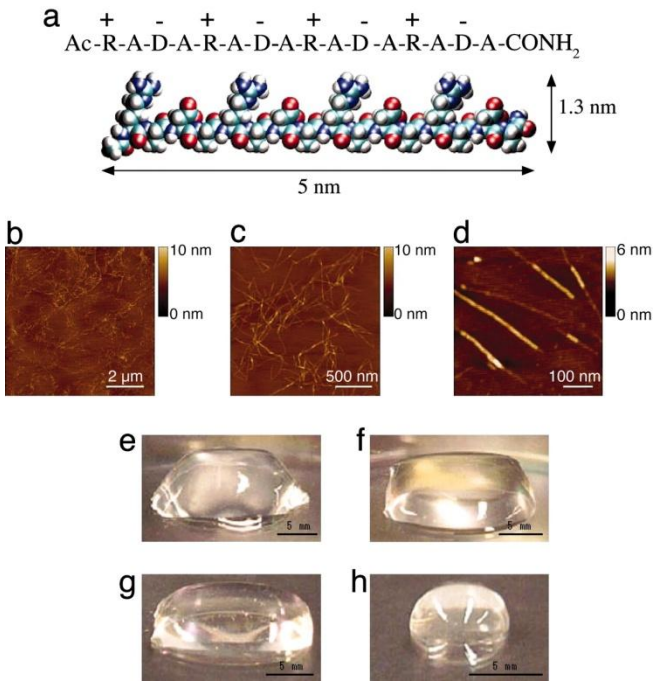

Figure 5.1 – Depiction of the RADA16-I peptide molecule and self-assembled gels. (a) The amino acid sequence and dimensions of the RADA16-I peptide molecule are shown. (b–d) Atomic force microscopy reveals nanofibrous geometry of self-assembled peptide hydrogels. (e–h) The qualities of the self-assembled hydrogel are affected by a number of parameters including the concentration of peptide used and whether the peptide suspension is sonicated prior to gelation. Figure reproduced with permission from [231], Copyright (2005) National Academy of Sciences, U.S.A.

Our key findings using this material scaffolds were that the timing of encapsulation of reprogrammed IPSCs in the hydrogels dictated whether reprogrammed neuronal populations could survive. Since the base peptide has no functional adhesion sites and only charge-based properties, we found that it was critical for IPSCs to be encapsulated prior to intiating neuronal conversion. Similar to previous findings from our lab, the pluripotent stem cells were capable of remodeling their fibrous environment with secreted extracellular matrix proteins [102]. Ultimately, the reprogrammed neuronal populations were able to survive and mature within the remodeled nanofibrous substrates and their transplantation into immunocompromised mouse

striatum while supported within SAPNS was improved significantly over the transplantation as dissociated cells (**Figure 5.2**).

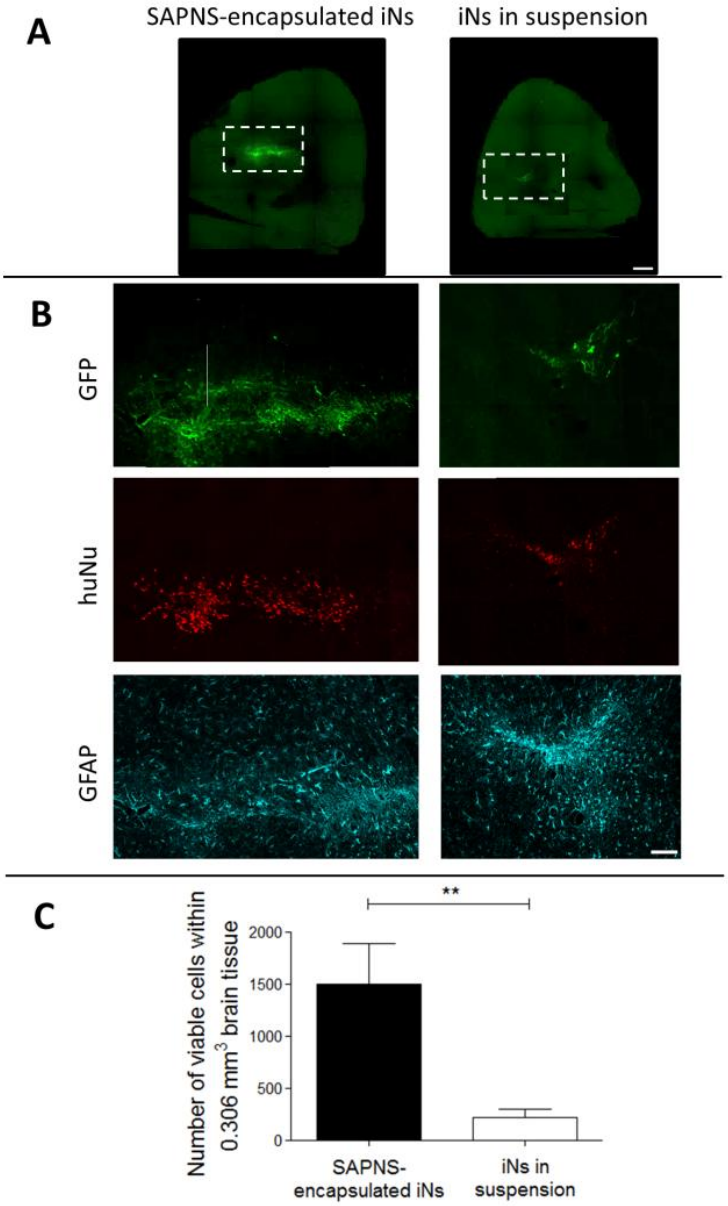

Figure 5.2 - RADA16-I SAPNS supported the transplantation of GFP-labelled iNs *in vivo*.

A) GFP-labeled iNs visualized within the mouse brain, transplanted either encapsulated in SAPNS or dissociated. Scale bar: 500 μm. B) Inset from A are depicted, indicating either GFP, human-specific nuclei, and astrocyte presence via GFAP expression. Scale bar: 100 μm. C) Quantification

of the viable cells within a fixed volume of brain tissue indicate a significant improvement in transplanted iN survival. Error bars: standard deviation. ** indicates $p<0.01$. Figure reprinted with permission from [232].

5.2.2 Transplantation of Mature DA neuronal populations

Sourcing DA neurons from fetal midbrain cells or human embryonic stem cells is fraught with ethical considerations and immune rejection. Furthermore, transplanting neuronal population sources with low subtype and regional purity have been observed to have diminished functional recovery in PD models [43, 233]. New breakthroughs in making patient-specific DA neurons from sources like fibroblasts [234] and IPSCs or embryonic stem cells [43, 235] could have significant potential to revolutionize human cell therapy in patients (**Figure 5.3**). For such strategies to be realized, however, technologies that can enrich for selected subtypes of midbrain DA neurons or control postmitotic DA neuron maturation are also sorely needed [236]. Thus, the development of robust approaches to *source* enriched human DA neurons, enhance their survival, and guide specification post-transplantation is critical to the success of this approach to manage PD.

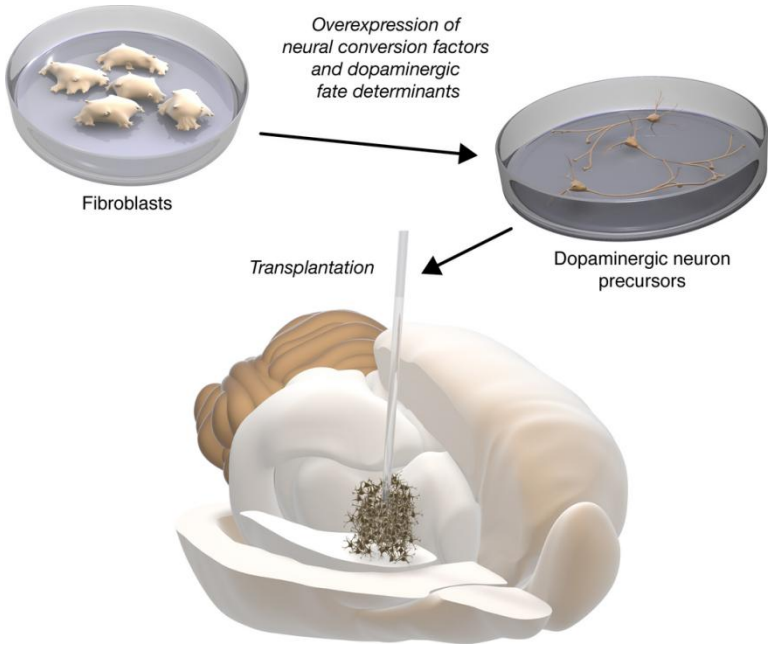

Figure 5.3 - Schematic depicting the possibility of generating transplantable mature DA neurons via reprogramming.

One technique for generating mature DA neurons from patient-derived cells would be through induced overexpression of dopaminergic-specific neuronal transcription factors. Figure reproduced with permission from [23].

Our early successes with high viability transplantation of reprogrammed neuronal populations *in vivo* have encouraged us to begin examining the ability of these same types of scaffolds to support and transplant appropriate subtypes of neurons for neurodegenerative, or in the case of PD, midbrain DA neurons. We have begun investigating multiple methods of deriving midbrain DA neurons, including the method developed by Kriks et. al., using soluble factors and morphogens to differentiate pluripotent stem cells via dual-SMAD inhibition and floor plate patterning (**Figure 5.4**).

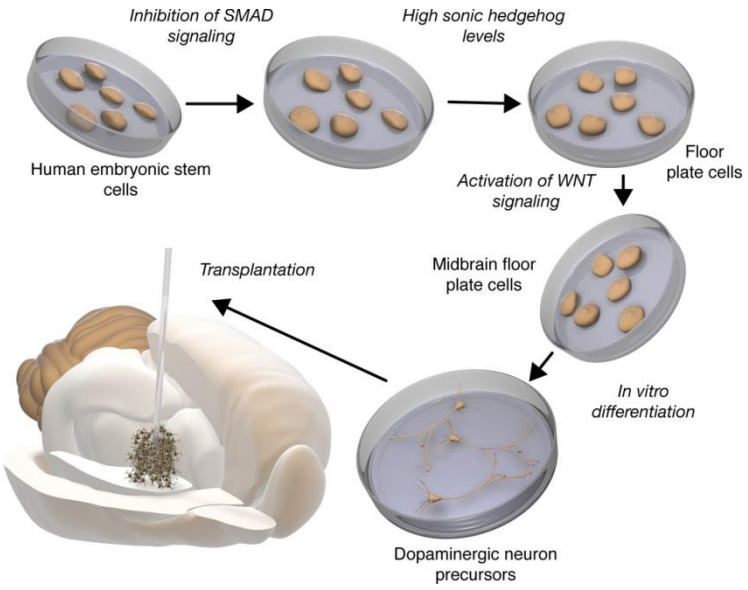

Figure 5.4 - Schematic depicting the possibility of generating transplantable mature DA neurons via soluble factor differentiation.

One technique for generating mature DA neurons from pluripotent cells would be through patterning of cells using a combination of SMAD inhibition, sonic hedgehog, and WNT signaling. Figure reproduced with permission from [23].

While some of the methods we have investigated have yielded inconsistent results, others have demonstrated the ability to generate phenotypically mature neurons that release DA detectable via high performance liquid chromatograpy (**Figure 5.5**). In order to provide subtype-specific support to these mature neurons during transplantation, we intend to investigate modifications of RADA16-I peptide with recently discovered peptides such as DA Neuron Stimulating Peptide-11 (DNSP-11) and Cerebral DA Neurotrophic Factor (CDNF), which have been observed to specifically protect DA neurons and improve DA production, [237-240].

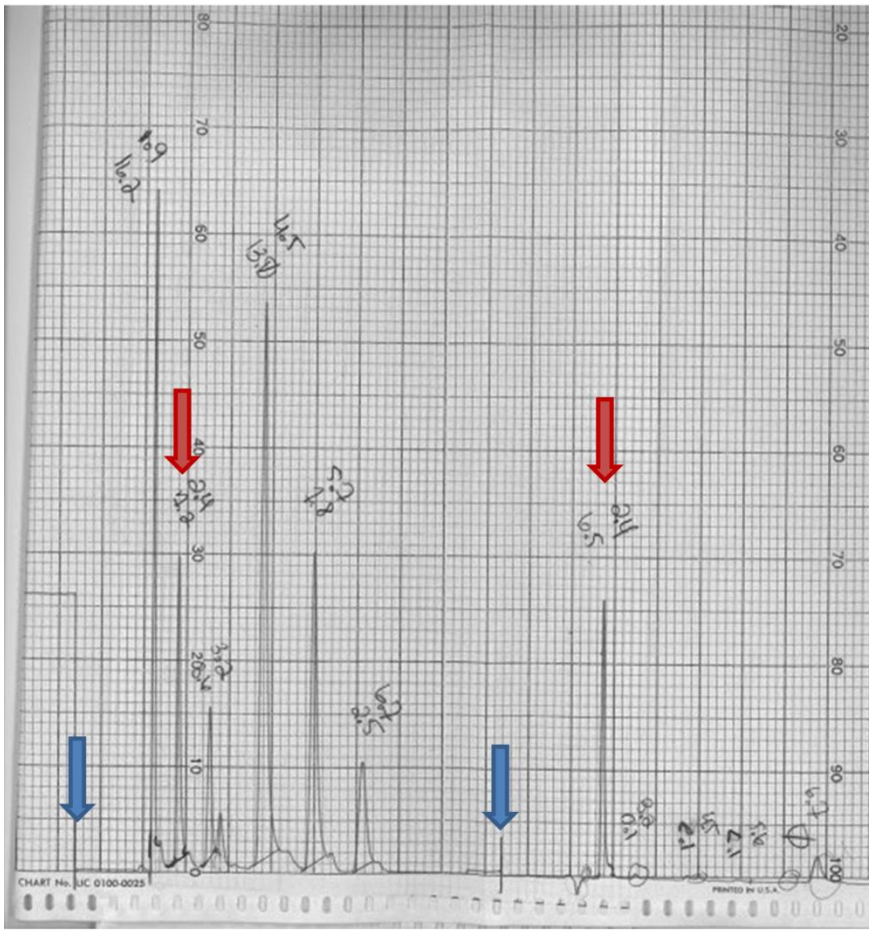

Figure 5.5 – High performance liquid chromatograpy detection of DA released by DA neurons derived from IPSCs.

In the depicted trace, the first two arrows correspond to an injection of neurotransmitter standards, with the blue arrow corresponding to the beginning of the standard injection and the red arrow corresponding to a known detection peak for DA. The second set of arrows correspond to an injection of media conditioned by differentiated pluripotent stem cells for 15 minutes, with the blue arrow again indicating the beginning of the sample injection. The peak indicated by the second red arrow was eluted and detected at the same time as the known DA peak, indicating that the differentiated cells are spontaneously producing DA. Source: Ongoing collaborative study with Dr. Nicola Francis.

5.2.3 Blood-brain barrier crossing modifications to amphiphilic molecules

While the nanoparticle formulations investigated show promise in decreasing microglial activation in response to ASYN challenge *in vivo* and in decreasing intracellular aggregation of ASYN in microglia, a key remaining challenge is making these particles readily available in the brain space. It is possible that a nanotherapeutic targeting the microglial pathways described would need to be administered regularly, so repeated surgical administration may not be desirable. One possible solution would be to modify the scavenger receptor-targeting amphiphilic molecules of the nanoparticle shells to be able to cross the blood-brain barrier (BBB).

Conferring cationic properties onto nanoparticles has generally been considered to be an effective means of increasing their permeability across the BBB [241, 242]. However, introducing cationic charge onto primary amines is typically associated with h a high degree of toxicity. This toxicity is not observed if primary amines are conferred with a quaternary ammonium [241, 243]. For these reasons, we investigated conferring a quaternary ammonium cationic charge onto our scavenger receptor-targeting amphiphilic molecules. In order to investigate the BBB-crossing potential of these quaternary ammonium-modified 1cM (quat), micelles of quats were incubated on the apical side of an *in vitro* model of the BBB, using human brain endothelial cells grown on a transwell membrane (**Figure 5.6A**). Due to the permanent cationic charge, the addition of these molecules on one side of the endothelial monolayer results in a quantifiable change in electrical potential across the membrane. As quaternary ammonium-modified molecules have been observed to be transported across the BBB via choline transporter [244, 245], hemicholinium-3, a

choline transporter inhibitor, was added in order to see if the decrease in membrane potential would be inhibited. We observed that the choline transporter inhibitor did have significantly more positive membrane potential over time, indicating that the quaternary ammonium-labelled 1cM appeared to be crossing the BBB model via choline transporters (**Figure 5.6B**). These studies would need to be followed up with further confirmation of the molecules crossing the endothelial cell monolayer, as well as verification that the quaternary ammonium charge does not impact the molecules' ability to target scavenger receptors. Future studies may also investigate ideal nanoparticle shell compositions, in terms of proportion of quats and unmodified 1cM.

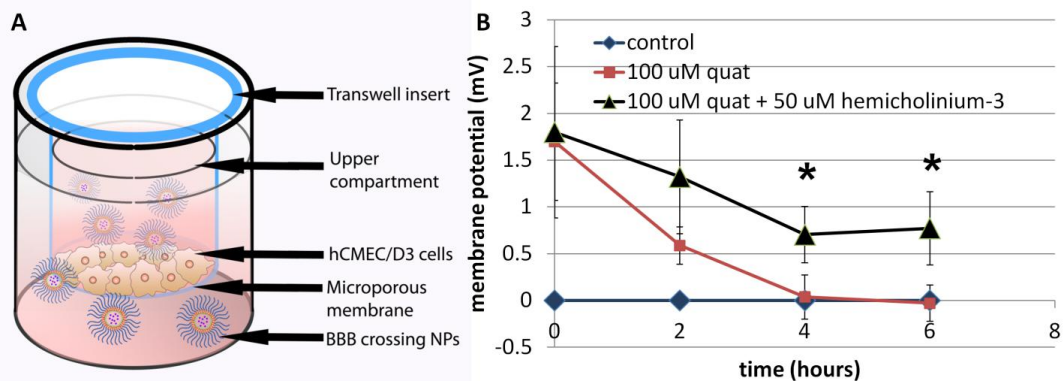

Figure 5.6 – Investigation of quaternary ammonium-modified 1cM ability to cross an *in vitro* BBB model.

A) A cartoon depicting the experimental setup, with a human brain endothelial cell monolayer on transwell microporous membranes mimicking the BBB. Scavenger receptor-targeting micelles or nanoparticles could be added to the upper compartment, and detected if they cross into the lower compartment. B) A choline transporter inhibitor slowed the crossing of quaternary ammonium-modified 1cM (quat), quantified via changes in membrane potential across the endothelial cell monolayer. $P<0.05$ via Student's t-test at each respective timepoint.

5.2.4 Further investigation into synthetic scavenger receptor ligand-mediated inhibition of ASYN oligomerization

One of the key findings of chapter 4 was that nanoparticles comprised of synthetic scavenger receptor ligand molecules were able to reduce the presence of intracellular ASYN

oligomers. In the discussion section, we offer some possible explanations for how this may be possible, namely, through reduction of intracellular monomeric ASYN levels, or through possible disruptions to receptor complexes that may interact with ASYN in unknown ways. Future studies may pursue the mechanism by which multiple receptors observed to interact with monomeric ASYN can contribute to intracellular oligomerization. We hope to investigate if pharmacological agents known to inhibit the formation of the CD36, TLR4, TLR6 heterotrimer have any or no additional effect at inhibiting ASYN oligomerization in the presence of synthetic scavenger receptor-targeting molecules. We also hope to screen our library of amphiphilic molecules to investigate if there are other chemistries better suited for inhibiting ASYN intracellular aggregation within microglia. The result of these studies may offer more mechanistic insight into how ASYN may interact with these receptor complexes, and if synthetic scavenger receptor ligands can target these interactions.

Recently, we have observed that mouse immortalized BV2 microglia appear to have key differences in intracellular ASYN oligomerization processes. Western blot of cell lysates from BV2 cells treated with ASYN monomer revealed the presence of only a single pentameric ASYN oligomer (**Figure 5.7**). Notably, pentameric forms of ASYN have been observed to form pore-like structures that deeply embed into cell membranes, and could be responsible for cellular dysfunction [246].

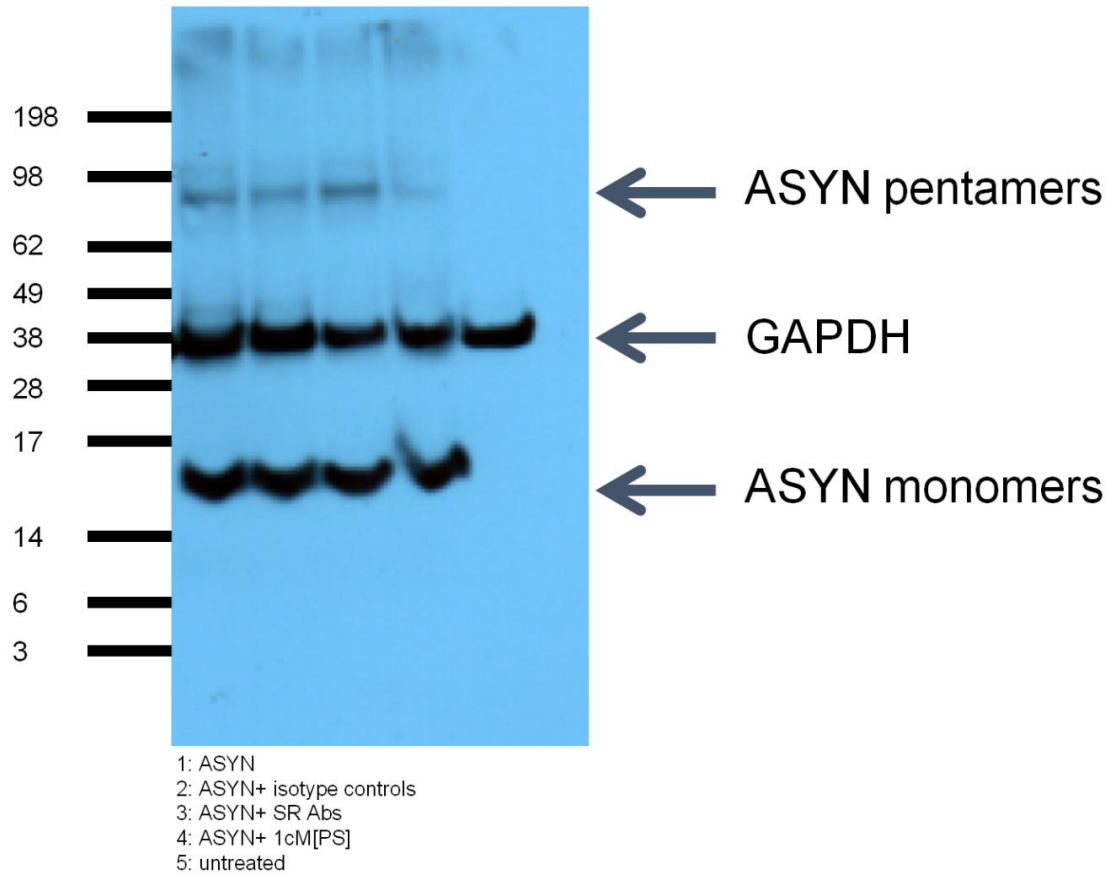

Figure 5.7 – Activated microglia preferentially form pentameric ASYN oligomers.

BV2 microglia were treated for 24 hours with either 10 μg/mL SR-targeting antibodies, 10 μg/mL of the respective antibody isotypes, or with 1cM shell polystyrene core NPs, followed by a 24 hour co-incubation with the same treatments and 5 μM monomeric ASYN. A pentameric ASYN band is visible in all lanes except in microglia not treated with ASYN, and in microglia that received the NP treatment.

Again, we observed that 1cM nanoparticles reduced the presence of these oligomers. In future studies we may attempt to isolate the oligomeric forms that are inhibited by synthetic scavenger receptor ligands and characterize the specific detrimental effects they may have on microglia or neurons. As stated previously, BV2 microglia are known to behave like activated microglia, therefore, the observed differences in intracellular ASYN oligomerization processes may be related to the microglial activation state. This possibility may prompt us to expand our investigation of antioxidant and anti-inflammatory core molecules within 1cM nanoparticles, to

investigate how core molecules of different concentration or stability may impact the nanoparticles' ability to inhibit the formation of pathological ASYN oligomeric species.

CHAPTER 6 - REFERENCES

1. Jankovic, J., *Parkinson's disease: clinical features and diagnosis.* J Neurol Neurosurg Psychiatry, 2008. **79**(4): p. 368-76.
2. Obeso, J.A., et al., *Missing pieces in the Parkinson's disease puzzle.* Nat Med, 2010. **16**(6): p. 653-61.
3. Kowal, S.L., et al., *The current and projected economic burden of Parkinson's disease in the United States.* Mov Disord, 2013. **28**(3): p. 311-8.
4. Bergman, H. and G. Deuschl, *Pathophysiology of Parkinson's disease: from clinical neurology to basic neuroscience and back.* Mov Disord, 2002. **17 Suppl 3**: p. S28-40.
5. Häggström, M., *Basal ganglia circuits*, in *Inkscape*, Basal_ganglia_circuits.svg, Editor 2010. p. based on images by Andrew Gillies/User:Anaru and Patrick J. Lynch, Sources for circuits:Introduction to Parkinson's Disease By Zaneta Navratilova. Modified from Nestler et. al, 2001, p. 306 and Ottley et. al, 1999.eMedicine > Parkinson Disease: Multimedia Author: Robert A Hauser. Coauthor(s): Rajesh Pahwa, Kelly E Lyons, Theresa McClain. Creative Commons Attribution-Share Alike 3.0 Unported license: https://creativecommons.org/licenses/by-sa/3.0/deed.en.
6. Albin, R.L., A.B. Young, and J.B. Penney, *The functional anatomy of basal ganglia disorders.* Trends Neurosci, 1989. **12**(10): p. 366-75.
7. Ehringer, H. and O. Hornykiewicz, *[Distribution of noradrenaline and dopamine (3-hydroxytyramine) in the human brain and their behavior in diseases of the extrapyramidal system].* Klin Wochenschr, 1960. **38**: p. 1236-9.
8. Häggström, M., *Basal ganglia circuits in Parkinson's disease*, in *Inkscape*, Basal_ganglia_in_Parkinson's_disease.png, Editor 2010. p. Derivative of Basal ganglia circuits.png, based on images by Andrew Gillies/User:Anaru, Creative Commons Attribution-Share Alike 3.0 Unported license: https://creativecommons.org/licenses/by-sa/3.0/deed.en.
9. Smeets, W.J. and A. Gonzalez, *Catecholamine systems in the brain of vertebrates: new perspectives through a comparative approach.* Brain Res Brain Res Rev, 2000. **33**(2-3): p. 308-79.
10. Braak, H., et al., *Staging of brain pathology related to sporadic Parkinson's disease.* Neurobiol Aging, 2003. **24**(2): p. 197-211.
11. Brooks, D.J., *Optimizing levodopa therapy for Parkinson's disease with levodopa/carbidopa/entacapone: implications from a clinical and patient perspective.* Neuropsychiatr Dis Treat, 2008. **4**(1): p. 39-47.
12. Fabbrini, G., et al., *Levodopa-induced dyskinesias.* Mov Disord, 2007. **22**(10): p. 1379-89; quiz 1523.
13. Gerlach, M., P. Riederer, and D. Scheller, *Mechanisms underlying and medical management of L-Dopa-associated motor complications.* J Neural Transm, 2011. **118**(12): p. 1659-60.
14. Goldenberg, M.M., *Medical management of Parkinson's disease.* P T, 2008. **33**(10): p. 590-606.
15. Merims, D. and N. Giladi, *Dopamine dysregulation syndrome, addiction and behavioral changes in Parkinson's disease.* Parkinsonism Relat Disord, 2008. **14**(4): p. 273-80.
16. Benabid, A.L., et al., *[Treatment of Parkinson tremor by chronic stimulation of the ventral intermediate nucleus of the thalamus].* Rev Neurol (Paris), 1989. **145**(4): p. 320-3.

17. Xu, F., et al., *Deep brain stimulation of pallidal versus subthalamic for patients with Parkinson's disease: a meta-analysis of controlled clinical trials.* Neuropsychiatr Dis Treat, 2016. **12**: p. 1435-44.
18. Hickey, P. and M. Stacy, *Deep Brain Stimulation: A Paradigm Shifting Approach to Treat Parkinson's Disease.* Front Neurosci, 2016. **10**: p. 173.
19. Benabid, A.L., et al., *Long-term suppression of tremor by chronic stimulation of the ventral intermediate thalamic nucleus.* Lancet, 1991. **337**(8738): p. 403-6.
20. Novakova, L., et al., *Increase in body weight is a non-motor side effect of deep brain stimulation of the subthalamic nucleus in Parkinson's disease.* Neuro Endocrinol Lett, 2007. **28**(1): p. 21-5.
21. Hack, N., et al., *Impulsive and compulsive behaviors in Parkinson Study Group (PSG) centers performing deep brain stimulation surgery.* J Parkinsons Dis, 2014. **4**(4): p. 591-8.
22. Doshi, P.K., *Long-term surgical and hardware-related complications of deep brain stimulation.* Stereotact Funct Neurosurg, 2011. **89**(2): p. 89-95.
23. Lindvall, O., *Clinical translation of stem cell transplantation in Parkinson's disease.* J Intern Med, 2016. **279**(1): p. 30-40.
24. Perlow, M.J., et al., *Brain grafts reduce motor abnormalities produced by destruction of nigrostriatal dopamine system.* Science, 1979. **204**(4393): p. 643-7.
25. Bjorklund, A. and U. Stenevi, *Reconstruction of the nigrostriatal dopamine pathway by intracerebral nigral transplants.* Brain Res, 1979. **177**(3): p. 555-60.
26. Backlund, E.O., et al., *Transplantation of adrenal medullary tissue to striatum in parkinsonism. First clinical trials.* J Neurosurg, 1985. **62**(2): p. 169-73.
27. Lindvall, O., et al., *Transplantation in Parkinson's disease: two cases of adrenal medullary grafts to the putamen.* Ann Neurol, 1987. **22**(4): p. 457-68.
28. Brundin, P., et al., *Human fetal dopamine neurons grafted in a rat model of Parkinson's disease: immunological aspects, spontaneous and drug-induced behaviour, and dopamine release.* Exp Brain Res, 1988. **70**(1): p. 192-208.
29. Freed, C.R., et al., *Transplantation of embryonic dopamine neurons for severe Parkinson's disease.* N Engl J Med, 2001. **344**(10): p. 710-9.
30. Politis, M., *Dyskinesias after neural transplantation in Parkinson's disease: what do we know and what is next?* BMC Med, 2010. **8**: p. 80.
31. Politis, M., et al., *Serotonergic neurons mediate dyskinesia side effects in Parkinson's patients with neural transplants.* Sci Transl Med, 2010. **2**(38): p. 38ra46.
32. Ganz, J., et al., *Cell replacement therapy for Parkinson's disease: how close are we to the clinic?* Expert Rev Neurother, 2011. **11**(9): p. 1325-39.
33. Ormerod, B.K., T.D. Palmer, and M.A. Caldwell, *Neurodegeneration and cell replacement.* Philosophical Transactions of the Royal Society B: Biological Sciences, 2008. **363**(1489): p. 153-170.
34. Lindvall, O. and Z. Kokaia, *Stem cells in human neurodegenerative disorders — time for clinical translation?* The Journal of Clinical Investigation, 2010. **120**(1): p. 29-40.
35. Marchetto, M.C.N., B. Winner, and F.H. Gage, *Pluripotent stem cells in neurodegenerative and neurodevelopmental diseases.* Human Molecular Genetics, 2010. **19**(R1): p. R71-R76.
36. Inoue, H., *Neurodegenerative disease-specific induced pluripotent stem cell research.* Experimental Cell Research, 2010. **316**(16): p. 2560-2564.
37. Naegele, J.R., et al., *Recent advancements in stem cell and gene therapies for neurological disorders and intractable epilepsy.* Neuropharmacology, 2010. **58**(6): p. 855-864.

38. Shihabuddin, L.S. and I. Aubert, *Stem cell transplantation for neurometabolic and neurodegenerative diseases.* Neuropharmacology, 2010. **58**(6): p. 845-854.
39. Kim, S.U. and J. de Vellis, *Stem cell-based cell therapy in neurological diseases: A review.* Journal of Neuroscience Research, 2009. **87**(10): p. 2183-2200.
40. Schwarz, S.C. and J. Schwarz, *Translation of stem cell therapy for neurological diseases.* Translational Research, 2010. **156**(3): p. 155-160.
41. Vierbuchen, T., et al., *Direct conversion of fibroblasts to functional neurons by defined factors.* Nature, 2010. **463**(7284): p. 1035-1041.
42. Pang, Z.P., et al., *Induction of human neuronal cells by defined transcription factors.* Nature, 2011. **476**(7359): p. 220-3.
43. Kriks, S., et al., *Dopamine neurons derived from human ES cells efficiently engraft in animal models of Parkinson's disease.* Nature, 2011. **480**(7378): p. 547-51.
44. Zeng, H., et al., *Specification of region-specific neurons including forebrain glutamatergic neurons from human induced pluripotent stem cells.* PLoS One, 2010. **5**(7): p. e11853.
45. Delli Carri, A., et al., *Developmentally coordinated extrinsic signals drive human pluripotent stem cell differentiation toward authentic DARPP-32+ medium-sized spiny neurons.* Development, 2013. **140**(2): p. 301-12.
46. Hirsch, E.C., S. Vyas, and S. Hunot, *Neuroinflammation in Parkinson's disease.* Parkinsonism Relat Disord, 2012. **18 Suppl 1**: p. S210-2.
47. Maries, E., et al., *The role of alpha-synuclein in Parkinson's disease: insights from animal models.* Nat Rev Neurosci, 2003. **4**(9): p. 727-38.
48. Hirsch, E.C., et al., *Animal models of Parkinson's disease in rodents induced by toxins: an update.* J Neural Transm Suppl, 2003(65): p. 89-100.
49. Block, M.L. and J.S. Hong, *Microglia and inflammation-mediated neurodegeneration: multiple triggers with a common mechanism.* Prog Neurobiol, 2005. **76**(2): p. 77-98.
50. Loeffler, D.A., et al., *Levodopa administration to normal rats: influence on striatal oxidized glutathione concentration.* Ann N Y Acad Sci, 1994. **738**: p. 421-6.
51. Loeffler, D.A., et al., *Effects of enhanced striatal dopamine turnover in vivo on glutathione oxidation.* Clin Neuropharmacol, 1994. **17**(4): p. 370-9.
52. Kim, W.G., et al., *Regional difference in susceptibility to lipopolysaccharide-induced neurotoxicity in the rat brain: role of microglia.* J Neurosci, 2000. **20**(16): p. 6309-16.
53. Sidhu, A., C. Wersinger, and P. Vernier, *Does alpha-synuclein modulate dopaminergic synaptic content and tone at the synapse?* FASEB J, 2004. **18**(6): p. 637-47.
54. Giasson, B.I. and V.M. Lee, *Are ubiquitination pathways central to Parkinson's disease?* Cell, 2003. **114**(1): p. 1-8.
55. Healy, D.G., et al., *Phenotype, genotype, and worldwide genetic penetrance of LRRK2-associated Parkinson's disease: a case-control study.* Lancet Neurol, 2008. **7**(7): p. 583-90.
56. Kumari, U. and E.K. Tan, *LRRK2 in Parkinson's disease: genetic and clinical studies from patients.* FEBS J, 2009. **276**(22): p. 6455-63.
57. Fraser, K.B., et al., *LRRK2 secretion in exosomes is regulated by 14-3-3.* Hum Mol Genet, 2013. **22**(24): p. 4988-5000.
58. Winslow, A.R., et al., *alpha-Synuclein impairs macroautophagy: implications for Parkinson's disease.* J Cell Biol, 2010. **190**(6): p. 1023-37.
59. Alvarez-Erviti, L., et al., *Lysosomal dysfunction increases exosome-mediated alpha-synuclein release and transmission.* Neurobiol Dis, 2011. **42**(3): p. 360-7.
60. Lee, H.J., E.J. Bae, and S.J. Lee, *Extracellular alpha--synuclein-a novel and crucial factor in Lewy body diseases.* Nat Rev Neurol, 2014. **10**(2): p. 92-8.

61. Bernardo, A., et al., *Nuclear receptor peroxisome proliferator-activated receptor-gamma is activated in rat microglial cells by the anti-inflammatory drug HCT1026, a derivative of flurbiprofen.* J Neurochem, 2005. **92**(4): p. 895-903.
62. Bernardo, A., et al., *Dynamic regulation of microglial functions by the non-steroidal anti-inflammatory drug NCX 2216: implications for chronic treatments of neurodegenerative diseases.* Neurobiol Dis, 2006. **22**(1): p. 25-32.
63. Sairam, K., et al., *Non-steroidal anti-inflammatory drug sodium salicylate, but not diclofenac or celecoxib, protects against 1-methyl-4-phenyl pyridinium-induced dopaminergic neurotoxicity in rats.* Brain Res, 2003. **966**(2): p. 245-52.
64. Carta, A.R. and A. Pisanu, *Modulating microglia activity with PPAR-gamma agonists: a promising therapy for Parkinson's disease?* Neurotox Res, 2013. **23**(2): p. 112-23.
65. Sastre, M. and S.M. Gentleman, *NSAIDs: How they Work and their Prospects as Therapeutics in Alzheimer's Disease.* Front Aging Neurosci, 2010. **2**: p. 20.
66. Juurlink, D.N., *Rosiglitazone and the case for safety over certainty.* JAMA, 2010. **304**(4): p. 469-71.
67. Kaul, S., et al., *Thiazolidinedione drugs and cardiovascular risks: a science advisory from the American Heart Association and American College Of Cardiology Foundation.* J Am Coll Cardiol, 2010. **55**(17): p. 1885-94.
68. Nissen, S.E. and K. Wolski, *Effect of rosiglitazone on the risk of myocardial infarction and death from cardiovascular causes.* N Engl J Med, 2007. **356**(24): p. 2457-71.
69. Araki, E., et al., *Cyclooxygenase-2 inhibitor ns-398 protects neuronal cultures from lipopolysaccharide-induced neurotoxicity.* Stroke, 2001. **32**(10): p. 2370-5.
70. Zhang, W., et al., *Aggregated alpha-synuclein activates microglia: a process leading to disease progression in Parkinson's disease.* FASEB J, 2005. **19**(6): p. 533-42.
71. Bronstein, D.M., et al., *Glia-dependent neurotoxicity and neuroprotection in mesencephalic cultures.* Brain Res, 1995. **704**(1): p. 112-6.
72. Liu, B., et al., *Role of nitric oxide in inflammation-mediated neurodegeneration.* Ann N Y Acad Sci, 2002. **962**: p. 318-31.
73. Theodore, S., et al., *Targeted overexpression of human alpha-synuclein triggers microglial activation and an adaptive immune response in a mouse model of Parkinson disease.* J Neuropathol Exp Neurol, 2008. **67**(12): p. 1149-58.
74. Su, X., et al., *Synuclein activates microglia in a model of Parkinson's disease.* Neurobiol Aging, 2008. **29**(11): p. 1690-701.
75. Hsu, L.J., et al., *alpha-synuclein promotes mitochondrial deficit and oxidative stress.* Am J Pathol, 2000. **157**(2): p. 401-10.
76. Lee, H.J., et al., *Direct transfer of alpha-synuclein from neuron to astroglia causes inflammatory responses in synucleinopathies.* J Biol Chem, 2010. **285**(12): p. 9262-72.
77. Sanchez-Guajardo, V., et al., *Neuroimmunological processes in Parkinson's disease and their relation to alpha-synuclein: microglia as the referee between neuronal processes and peripheral immunity.* ASN Neuro, 2013. **5**(2): p. 113-39.
78. Hoyer, W., et al., *Impact of the acidic C-terminal region comprising amino acids 109-140 on alpha-synuclein aggregation in vitro.* Biochemistry, 2004. **43**(51): p. 16233-16242.
79. Kabaria, S., et al., *Inhibition of miR-34b and miR-34c enhances alpha-synuclein expression in Parkinson's disease.* Febs Letters, 2015. **589**(3): p. 319-25.
80. Lowe, R., et al., *Calcium(II) selectively induces alpha-synuclein annular oligomers via interaction with the C-terminal domain.* Protein Science, 2004. **13**(12): p. 3245-3252.
81. Uversky, V.N., et al., *Accelerated alpha-synuclein fibrillation in crowded milieu.* Febs Letters, 2002. **515**(1-3): p. 99-103.

82. Shtilerman, M.D., T.T. Ding, and P.T. Lansbury, *Molecular crowding accelerates fibrillization of alpha-synuclein: Could an increase in the cytoplasmic protein concentration induce Parkinson's disease?* Biochemistry, 2002. **41**(12): p. 3855-3860.
83. Fujiwara, H., et al., *alpha-Synuclein is phosphorylated in synucleinopathy lesions.* Nat Cell Biol, 2002. **4**(2): p. 160-4.
84. Roberts, H.L. and D.R. Brown, *Seeking a mechanism for the toxicity of oligomeric alpha-synuclein.* Biomolecules, 2015. **5**(2): p. 282-305.
85. Lee, K.W., et al., *Enhanced phosphatase activity attenuates alpha-synucleinopathy in a mouse model.* J Neurosci, 2011. **31**(19): p. 6963-71.
86. Lee, H.J., et al., *Clearance and deposition of extracellular alpha-synuclein aggregates in microglia.* Biochem Biophys Res Commun, 2008. **372**(3): p. 423-8.
87. Takahashi, K. and S. Yamanaka, *Induction of pluripotent stem cells from mouse embryonic and adult fibroblast cultures by defined factors.* Cell, 2006. **126**(4): p. 663-76.
88. Zhang, Y., et al., *Rapid single-step induction of functional neurons from human pluripotent stem cells.* Neuron, 2013. **78**(5): p. 785-98.
89. Evans, M.J. and M.H. Kaufman, *Establishment in culture of pluripotential cells from mouse embryos.* Nature, 1981. **292**(5819): p. 154-6.
90. Thomson, J.A., et al., *Embryonic stem cell lines derived from human blastocysts.* Science, 1998. **282**(5391): p. 1145-7.
91. Watanabe, K., et al., *A ROCK inhibitor permits survival of dissociated human embryonic stem cells.* Nat Biotechnol, 2007. **25**(6): p. 681-6.
92. Harb, N., T.K. Archer, and N. Sato, *The Rho-Rock-Myosin signaling axis determines cell-cell integrity of self-renewing pluripotent stem cells.* PLoS One, 2008. **3**(8): p. e3001.
93. Ohgushi, M., et al., *Molecular pathway and cell state responsible for dissociation-induced apoptosis in human pluripotent stem cells.* Cell Stem Cell, 2010. **7**(2): p. 225-39.
94. Haque, A., et al., *Characterization and neural differentiation of mouse embryonic and induced pluripotent stem cells on cadherin-based substrata.* Biomaterials, 2012. **33**(20): p. 5094-106.
95. Takeichi, M., *The cadherin superfamily in neuronal connections and interactions.* Nat Rev Neurosci, 2007. **8**(1): p. 11-20.
96. Shi, P., K. Shen, and L.C. Kam, *Local presentation of L1 and N-cadherin in multicomponent, microscale patterns differentially direct neuron function in vitro.* Dev Neurobiol, 2007. **67**(13): p. 1765-76.
97. Xu, C., et al., *Feeder-free growth of undifferentiated human embryonic stem cells.* Nat Biotechnol, 2001. **19**(10): p. 971-4.
98. Martin, M.J., et al., *Human embryonic stem cells express an immunogenic nonhuman sialic acid.* Nat Med, 2005. **11**(2): p. 228-32.
99. Braam, S.R., et al., *Recombinant vitronectin is a functionally defined substrate that supports human embryonic stem cell self-renewal via alpha V beta 5 integrin.* Stem Cells, 2008. **26**(9): p. 2257-2265.
100. Miyazaki, T., et al., *Recombinant human laminin isoforms can support the undifferentiated growth of human embryonic stem cells.* Biochemical and Biophysical Research Communications, 2008. **375**(1): p. 27-32.
101. Meng, Y., et al., *Characterization of integrin engagement during defined human embryonic stem cell culture.* FASEB J, 2010. **24**(4): p. 1056-65.
102. Carlson, A.L., et al., *Microfibrous substrate geometry as a critical trigger for organization, self-renewal, and differentiation of human embryonic stem cells within synthetic 3-dimensional microenvironments.* FASEB J, 2012. **26**(8): p. 3240-51.

103. Cherry, J.F., et al., *Oriented, multimeric biointerfaces of the L1 cell adhesion molecule: an approach to enhance neuronal and neural stem cell functions on 2-D and 3-D polymer substrates.* Biointerphases, 2012. **7**(1-4): p. 22.
104. Prang, P., et al., *The promotion of oriented axonal regrowth in the injured spinal cord by alginate-based anisotropic capillary hydrogels.* Biomaterials, 2006. **27**(19): p. 3560-9.
105. Stokols, S. and M.H. Tuszynski, *Freeze-dried agarose scaffolds with uniaxial channels stimulate and guide linear axonal growth following spinal cord injury.* Biomaterials, 2006. **27**(3): p. 443-51.
106. Johnson, P.J., S.R. Parker, and S.E. Sakiyama-Elbert, *Controlled release of neurotrophin-3 from fibrin-based tissue engineering scaffolds enhances neural fiber sprouting following subacute spinal cord injury.* Biotechnol Bioeng, 2009. **104**(6): p. 1207-14.
107. Tajdaran, K., et al., *An engineered biocompatible drug delivery system enhances nerve regeneration after delayed repair.* J Biomed Mater Res A, 2016. **104**(2): p. 367-76.
108. Horn, E.M., et al., *Influence of cross-linked hyaluronic acid hydrogels on neurite outgrowth and recovery from spinal cord injury.* J Neurosurg Spine, 2007. **6**(2): p. 133-40.
109. Liu, S., G. Said, and M. Tadie, *Regrowth of the rostral spinal axons into the caudal ventral roots through a collagen tube implanted into hemisected adult rat spinal cord.* Neurosurgery, 2001. **49**(1): p. 143-50; discussion 150-1.
110. Kehoe, S., X.F. Zhang, and D. Boyd, *FDA approved guidance conduits and wraps for peripheral nerve injury: a review of materials and efficacy.* Injury, 2012. **43**(5): p. 553-72.
111. Lohmeyer, J.A., et al., *The Clinical Use of Artificial Nerve Conduits for Digital Nerve Repair: A Prospective Cohort Study and Literature Review.* Journal of Reconstructive Microsurgery, 2009. **25**(1): p. 55-61.
112. Teng, Y.D., et al., *Functional recovery following traumatic spinal cord injury mediated by a unique polymer scaffold seeded with neural stem cells.* Proc Natl Acad Sci U S A, 2002. **99**(5): p. 3024-9.
113. Kutikov, A.B. and J. Song, *Biodegradable PEG-Based Amphiphilic Block Copolymers for Tissue Engineering Applications.* ACS Biomater Sci Eng, 2015. **1**(7): p. 463-480.
114. Diban, N., et al., *Poly(epsilon-caprolactone) films with favourable properties for neural cell growth.* Curr Top Med Chem, 2014. **14**(23): p. 2743-9.
115. Ertel, S.I. and J. Kohn, *Evaluation of a series of tyrosine-derived polycarbonates as degradable biomaterials.* J Biomed Mater Res, 1994. **28**(8): p. 919-30.
116. Yu, C. and J. Kohn, *Tyrosine-PEG-derived poly(ether carbonate)s as new biomaterials. Part I: synthesis and evaluation.* Biomaterials, 1999. **20**(3): p. 253-64.
117. Tziampazis, E., J. Kohn, and P.V. Moghe, *PEG-variant biomaterials as selectively adhesive protein templates: model surfaces for controlled cell adhesion and migration.* Biomaterials, 2000. **21**(5): p. 511-20.
118. Hoven, V.P., A. Poopattanapong, and J. Kohn, *Acid-containing tyrosine-derived polycarbonates: Wettability and surface reactivity.* Macromolecular Symposia, 2004. **216**: p. 87-97.
119. Eriksson, C., A. Bjorklund, and K. Wictorin, *Neuronal differentiation following transplantation of expanded mouse neurosphere cultures derived from different embryonic forebrain regions.* Exp Neurol, 2003. **184**(2): p. 615-35.
120. Salewski, R.P., et al., *Transplantation of neural stem cells clonally derived from embryonic stem cells promotes recovery after murine spinal cord injury.* Stem Cells Dev, 2015. **24**(1): p. 36-50.

121. Meissner, K.K., D.L. Kirkham, and L.C. Doering, *Transplants of neurosphere cell suspensions from aged mice are functional in the mouse model of Parkinson's.* Brain Res, 2005. **1057**(1-2): p. 105-12.
122. Bez, A., et al., *Neurosphere and neurosphere-forming cells: morphological and ultrastructural characterization.* Brain Res, 2003. **993**(1-2): p. 18-29.
123. Aguado, B.A., et al., *Improving viability of stem cells during syringe needle flow through the design of hydrogel cell carriers.* Tissue Eng Part A, 2012. **18**(7-8): p. 806-15.
124. Guvendiren, M., H.D. Lu, and J.A. Burdick, *Shear-thinning hydrogels for biomedical applications.* Soft Matter, 2012. **8**(2): p. 260-272.
125. Lam, J., et al., *Delivery of iPS-NPCs to the Stroke Cavity within a Hyaluronic Acid Matrix Promotes the Differentiation of Transplanted Cells.* Adv Funct Mater, 2014. **24**(44): p. 7053-7062.
126. Arulmoli, J., et al., *Combination scaffolds of salmon fibrin, hyaluronic acid, and laminin for human neural stem cell and vascular tissue engineering.* Acta Biomater, 2016.
127. Nakaji-Hirabayashi, T., K. Kato, and H. Iwata, *Hyaluronic acid hydrogel loaded with genetically-engineered brain-derived neurotrophic factor as a neural cell carrier.* Biomaterials, 2009. **30**(27): p. 4581-9.
128. Wang, T.Y., et al., *Functionalized composite scaffolds improve the engraftment of transplanted dopaminergic progenitors in a mouse model of Parkinson's disease.* Biomaterials, 2016. **74**: p. 89-98.
129. Terpstra, B.T., et al., *Increased cell suspension concentration augments the survival rate of grafted tyrosine hydroxylase immunoreactive neurons.* J Neurosci Methods, 2007. **166**(1): p. 13-9.
130. Takahashi, K., et al., *Induction of Pluripotent Stem Cells from Adult Human Fibroblasts by Defined Factors.* Cell, 2007. **131**(5): p. 861-872.
131. Watanabe, K., et al., *A ROCK inhibitor permits survival of dissociated human embryonic stem cells.* Nat Biotech, 2007. **25**(6): p. 681-686.
132. Treiser, M.D., et al., *Cytoskeleton-based forecasting of stem cell lineage fates.* Proc Natl Acad Sci U S A, 2009. **107**(2): p. 610-615.
133. Citri, A., et al., *Calcium binding to PICK1 is essential for the intracellular retention of AMPA receptors underlying long-term depression.* J Neurosci, 2010. **30**(49): p. 16437-52.
134. Skaper, S.D., C. Argentini, and M. Barbierato, *Culture of neonatal rodent microglia, astrocytes, and oligodendrocytes from cortex and spinal cord.* Methods Mol Biol, 2012. **846**: p. 67-77.
135. Bourke, S.L. and J. Kohn, *Polymers derived from the amino acid -tyrosine: polycarbonates, polyarylates and copolymers with poly(ethylene glycol).* Advanced Drug Delivery Reviews, 2003. **55**(4): p. 447-466.
136. Hooper, K.A., N.D. Macon, and J. Kohn, *Comparative histological evaluation of new tyrosine-derived polymers and poly (L-lactic acid) as a function of polymer degradation.* J Biomed Mater Res, 1998. **41**(3): p. 443-54.
137. Christopherson, G.T., H. Song, and H.-Q. Mao, *The influence of fiber diameter of electrospun substrates on neural stem cell differentiation and proliferation.* Biomaterials, 2009. **30**(4): p. 556-564.
138. Espuny-Camacho, I., et al., *Pyramidal neurons derived from human pluripotent stem cells integrate efficiently into mouse brain circuits in vivo.* Neuron, 2013. **77**(3): p. 440-56.
139. Gertz, C.C., et al., *Accelerated neuritogenesis and maturation of primary spinal motor neurons in response to nanofibers.* Dev Neurobiol, 2010. **70**(8): p. 589-603.

140. Cherry, J.F., et al., *Engineered N-cadherin and L1 biomimetic substrates concertedly promote neuronal differentiation, neurite extension and neuroprotection of human neural stem cells.* Acta Biomater, 2014. **10**(10): p. 4113-26.
141. Landers, J., et al., *Carbon nanotube composites as multifunctional substrates for in situ actuation of differentiation of human neural stem cells.* Adv Healthc Mater, 2014. **3**(11): p. 1745-52.
142. Bruses, J.L., *N-cadherin signaling in synapse formation and neuronal physiology.* Mol Neurobiol, 2006. **33**(3): p. 237-52.
143. Tan, Z.J., et al., *N-cadherin-dependent neuron-neuron interaction is required for the maintenance of activity-induced dendrite growth.* Proc Natl Acad Sci U S A, 2010. **107**(21): p. 9873-8.
144. Piccoli, G., U. Rutishauser, and J.L. Bruses, *N-cadherin juxtamembrane domain modulates voltage-gated Ca2+ current via RhoA GTPase and Rho-associated kinase.* J Neurosci, 2004. **24**(48): p. 10918-23.
145. Xu, Y., et al., *Revealing a core signaling regulatory mechanism for pluripotent stem cell survival and self-renewal by small molecules.* Proc Natl Acad Sci U S A, 2010. **107**(18): p. 8129-34.
146. Li, L., et al., *Individual cell movement, asymmetric colony expansion, rho-associated kinase, and E-cadherin impact the clonogenicity of human embryonic stem cells.* Biophys J, 2010. **98**(11): p. 2442-51.
147. Marchionini, D.M., et al., *Interference with anoikis-induced cell death of dopamine neurons: implications for augmenting embryonic graft survival in a rat model of Parkinson's disease.* J Comp Neurol, 2003. **464**(2): p. 172-9.
148. Frisch, S.M. and R.A. Screaton, *Anoikis mechanisms.* Curr Opin Cell Biol, 2001. **13**(5): p. 555-62.
149. Kirik, D., C. Winkler, and A. Bjorklund, *Growth and functional efficacy of intrastriatal nigral transplants depend on the extent of nigrostriatal degeneration.* J Neurosci, 2001. **21**(8): p. 2889-96.
150. Nikkhah, G., et al., *Microtransplantation of dopaminergic cell suspensions: further characterization and optimization of grafting parameters.* Cell Transplant, 2009. **18**(2): p. 119-33.
151. Studer, L., et al., *Enhanced proliferation, survival, and dopaminergic differentiation of CNS precursors in lowered oxygen.* J Neurosci, 2000. **20**(19): p. 7377-83.
152. Studer, L., V. Tabar, and R.D. McKay, *Transplantation of expanded mesencephalic precursors leads to recovery in parkinsonian rats.* Nat Neurosci, 1998. **1**(4): p. 290-5.
153. Wernig, M., et al., *Neurons derived from reprogrammed fibroblasts functionally integrate into the fetal brain and improve symptoms of rats with Parkinson's disease.* Proc Natl Acad Sci U S A, 2008. **105**(15): p. 5856-61.
154. Lee, H.J., S. Patel, and S.J. Lee, *Intravesicular localization and exocytosis of alpha-synuclein and its aggregates.* Journal of Neuroscience, 2005. **25**(25): p. 6016-6024.
155. De Paola, M., et al., *Synthetic and natural small molecule TLR4 antagonists inhibit motoneuron death in cultures from ALS mouse model.* Pharmacological Research, 2016. **103**: p. 180-187.
156. Kim, C., et al., *Neuron-released oligomeric alpha-synuclein is an endogenous agonist of TLR2 for paracrine activation of microglia.* Nat Commun, 2013. **4**: p. 1562.
157. Lee, J.Y., et al., *Absence of toll-like receptor 4 (TLR4) extends survival in the hSOD1(G93A) mouse model of amyotrophic lateral sclerosis.* Journal of Neuroinflammation, 2015. **12**.

158. Liu, S.R., et al., *TLR2 Is a Primary Receptor for Alzheimer's Amyloid beta Peptide To Trigger Neuroinflammatory Activation.* Journal of Immunology, 2012. **188**(3): p. 1098-1107.
159. Coraci, I.S., et al., *CD36, a class B scavenger receptor, is expressed on microglia in Alzheimer's disease brains and can mediate production of reactive oxygen species in response to beta-amyloid fibrils.* American Journal of Pathology, 2002. **160**(1): p. 101-112.
160. El Khoury, J.B., et al., *CD36 mediates the innate host response to beta-amyloid.* J Exp Med, 2003. **197**(12): p. 1657-66.
161. Gao, H.M., et al., *HMGB1 Acts on Microglia Mac1 to Mediate Chronic Neuroinflammation That Drives Progressive Neurodegeneration.* Journal of Neuroscience, 2011. **31**(3): p. 1081-1092.
162. Hu, X.M., et al., *Macrophage Antigen Complex-1 Mediates Reactive Microgliosis and Progressive Dopaminergic Neurodegeneration in the MPTP Model of Parkinson's Disease.* Journal of Immunology, 2008. **181**(10): p. 7194-7204.
163. Stefanova, N., et al., *Toll-like receptor 4 promotes alpha-synuclein clearance and survival of nigral dopaminergic neurons.* Am J Pathol, 2011. **179**(2): p. 954-63.
164. Zhang, W., et al., *Microglial PHOX and Mac-1 are essential to the enhanced dopaminergic neurodegeneration elicited by A30P and A53T mutant alpha-synuclein.* Glia, 2007. **55**(11): p. 1178-88.
165. El Khoury, J., et al., *Scavenger receptor-mediated adhesion of microglia to beta-amyloid fibrils.* Nature, 1996. **382**(6593): p. 716-9.
166. Serpell, L.C., et al., *Fiber diffraction of synthetic alpha-synuclein filaments shows amyloid-like cross-beta conformation.* Proc Natl Acad Sci U S A, 2000. **97**(9): p. 4897-902.
167. Yoshiizumi, K., et al., *Studies on scavenger receptor inhibitors. Part 1: Synthesis and structure-activity relationships of novel derivatives of sulfatides.* Bioorganic & Medicinal Chemistry, 2002. **10**(8): p. 2445-2460.
168. Boullier, A., et al., *Phosphocholine as a pattern recognition ligand for CD36.* Journal of Lipid Research, 2005. **46**(5): p. 969-976.
169. Gu, L., et al., *Sugar-based amphiphilic polymers for biomedical applications: from nanocarriers to therapeutics.* Acc Chem Res, 2014. **47**(10): p. 2867-77.
170. Lewis, D.R., et al., *Sugar-based amphiphilic nanoparticles arrest atherosclerosis in vivo.* Proc Natl Acad Sci U S A, 2015. **112**(9): p. 2693-8.
171. Chnari, E., et al., *Nanoscale anionic macromolecules can inhibit cellular uptake of differentially oxidized LDL.* Biomacromolecules, 2006. **7**(2): p. 597-603.
172. York, A.W., et al., *Kinetically assembled nanoparticles of bioactive macromolecules exhibit enhanced stability and cell-targeted biological efficacy.* Adv Mater, 2012. **24**(6): p. 733-9.
173. Brown, D.R., *Metal binding to alpha-synuclein peptides and its contribution to toxicity.* Biochem Biophys Res Commun, 2009. **380**(2): p. 377-81.
174. Djordjevic, J., et al., *Amphiphilic Scorpion-like Macromolecules as Micellar Nanocarriers.* Journal of Bioactive and Compatible Polymers, 2008. **23**(6): p. 532-551.
175. Iverson, N.M., et al., *Controllable inhibition of cellular uptake of oxidized low-density lipoprotein: structure-function relationships for nanoscale amphiphilic polymers.* Acta Biomater, 2010. **6**(8): p. 3081-91.
176. Tian, L., et al., *Amphiphilic scorpion-like macromolecules: Design, synthesis, and characterization.* Macromolecules, 2004. **37**(2): p. 538-543.

177. Wang, J., et al., *Nanoscale amphiphilic macromolecules as lipoprotein inhibitors: the role of charge and architecture.* International Journal of Nanomedicine, 2007. **2**(4): p. 697-705.
178. Chnari, E., et al., *Engineered polymeric nanoparticles for receptor-targeted blockage of oxidized low density lipoprotein uptake and atherogenesis in macrophages.* Biomacromolecules, 2006. **7**(6): p. 1796-805.
179. Lee, E.J., et al., *Alpha-synuclein activates microglia by inducing the expressions of matrix metalloproteinases and the subsequent activation of protease-activated receptor-1.* J Immunol, 2010. **185**(1): p. 615-23.
180. Holm, T., et al., *Studying the uptake of cell-penetrating peptides.* Nat Protoc, 2006. **1**(2): p. 1001-5.
181. Alarcon, R., et al., *Expression of scavenger receptors in glial cells. Comparing the adhesion of astrocytes and microglia from neonatal rats to surface-bound beta-amyloid.* J Biol Chem, 2005. **280**(34): p. 30406-15.
182. Stewart, C.R., et al., *CD36 ligands promote sterile inflammation through assembly of a Toll-like receptor 4 and 6 heterodimer.* Nature Immunology, 2010. **11**(2): p. 155-U75.
183. Karpinar, D.P., et al., *Pre-fibrillar alpha-synuclein variants with impaired beta-structure increase neurotoxicity in Parkinson's disease models.* EMBO J, 2009. **28**(20): p. 3256-68.
184. Volpicelli-Daley, L.A., K.C. Luk, and V.M. Lee, *Addition of exogenous alpha-synuclein preformed fibrils to primary neuronal cultures to seed recruitment of endogenous alpha-synuclein to Lewy body and Lewy neurite-like aggregates.* Nat Protoc, 2014. **9**(9): p. 2135-46.
185. Paumier, K.L., et al., *Intrastriatal injection of pre-formed mouse alpha-synuclein fibrils into rats triggers alpha-synuclein pathology and bilateral nigrostriatal degeneration.* Neurobiol Dis, 2015. **82**: p. 185-99.
186. Desplats, P., et al., *Inclusion formation and neuronal cell death through neuron-to-neuron transmission of alpha-synuclein.* Proc Natl Acad Sci U S A, 2009. **106**(31): p. 13010-5.
187. Hansen, C., et al., *alpha-Synuclein propagates from mouse brain to grafted dopaminergic neurons and seeds aggregation in cultured human cells.* J Clin Invest, 2011. **121**(2): p. 715-25.
188. Pawate, S., et al., *Redox regulation of glial inflammatory response to lipopolysaccharide and interferon gamma.* Journal of Neuroscience Research, 2004. **77**(4): p. 540-551.
189. Qin, L.Y., et al., *NADPH oxidase mediates lipopolysaccharide-induced neurotoxicity and proinflammatory gene expression in activated microglia.* Journal of Biological Chemistry, 2004. **279**(2): p. 1415-1421.
190. Parihar, M.S., et al., *Alpha-synuclein overexpression and aggregation exacerbates impairment of mitochondrial functions by augmenting oxidative stress in human neuroblastoma cells.* International Journal of Biochemistry & Cell Biology, 2009. **41**(10): p. 2015-2024.
191. Junn, E. and M.M. Mouradian, *Human alpha-synuclein over-expression increases intracellular reactive oxygen species levels and susceptibility to dopamine.* Neuroscience Letters, 2002. **320**(3): p. 146-150.
192. Angeles, D.C., et al., *Antioxidants inhibit neuronal toxicity in Parkinson's disease-linked LRRK2.* Ann Clin Transl Neurol, 2016. **3**(4): p. 288-94.
193. Etminan, M., S.S. Gill, and A. Samii, *Intake of vitamin E, vitamin C, and carotenoids and the risk of Parkinson's disease: a meta-analysis.* Lancet Neurol, 2005. **4**(6): p. 362-5.

194. Miyake, Y., et al., *Dietary intake of antioxidant vitamins and risk of Parkinson's disease: a case-control study in Japan.* Eur J Neurol, 2011. **18**(1): p. 106-13.
195. *Effects of tocopherol and deprenyl on the progression of disability in early Parkinson's disease.* N Engl J Med, 1993. **328**(3): p. 176-83.
196. Prasad, K.N. and J. Edwards-Prasad, *Vitamin E and cancer prevention: recent advances and future potentials.* J Am Coll Nutr, 1992. **11**(5): p. 487-500.
197. Prasad, K.N. and J. Edwardsprasad, *Effects of Tocopherol (Vitamin-E) Acid Succinate on Morphological Alterations and Growth-Inhibition in Melanoma-Cells in Culture.* Cancer Research, 1982. **42**(2): p. 550-555.
198. Roghani, M. and G. Behzadi, *Neuroprotective effect of vitamin E on the early model of Parkinson's disease in rat: behavioral and histochemical evidence.* Brain Res, 2001. **892**(1): p. 211-7.
199. Sies, H., *Oxidative stress: oxidants and antioxidants.* Exp Physiol, 1997. **82**(2): p. 291-5.
200. Vertuani, S., A. Angusti, and S. Manfredini, *The antioxidants and pro-antioxidants network: an overview.* Curr Pharm Des, 2004. **10**(14): p. 1677-94.
201. Ouimet, M.A., et al., *Ferulic Acid-Based Polymers with Glycol Functionality as a Versatile Platform for Topical Applications.* Biomacromolecules, 2015. **16**: p. 2911-2919.
202. Faig, J.J., et al., *Attenuating Oxidative Stress Via Oxalate Ester-Containing Ferulic Acid-Based Poly(anhydride-esters) that Scavenge Hydrogen Peroxide.* Macromolecular Chemistry and Physics, 2016. **217**(1): p. 108-114.
203. Giehm, L. and D.E. Otzen, *Strategies to increase the reproducibility of protein fibrillization in plate reader assays.* Anal Biochem, 2010. **400**(2): p. 270-81.
204. Boza-Serrano, A., et al., *The role of Galectin-3 in alpha-synuclein-induced microglial activation.* Acta Neuropathol Commun, 2014. **2**: p. 156.
205. Plourde, N.M., et al., *Structure-activity relations of nanolipoblockers with the atherogenic domain of human macrophage scavenger receptor A.* Biomacromolecules, 2009. **10**(6): p. 1381-91.
206. Danzer, K.M., et al., *Different species of alpha-synuclein oligomers induce calcium influx and seeding.* J Neurosci, 2007. **27**(34): p. 9220-32.
207. Volles, M.J., et al., *Vesicle permeabilization by protofibrillar alpha-synuclein: implications for the pathogenesis and treatment of Parkinson's disease.* Biochemistry, 2001. **40**(26): p. 7812-9.
208. Cremades, N., et al., *Direct observation of the interconversion of normal and toxic forms of alpha-synuclein.* Cell, 2012. **149**(5): p. 1048-59.
209. Winner, B., et al., *In vivo demonstration that alpha-synuclein oligomers are toxic.* Proc Natl Acad Sci U S A, 2011. **108**(10): p. 4194-9.
210. Spillantini, M.G., et al., *Alpha-synuclein in Lewy bodies.* Nature, 1997. **388**(6645): p. 839-40.
211. Tanaka, M., et al., *Aggresomes formed by alpha-synuclein and synphilin-1 are cytoprotective.* J Biol Chem, 2004. **279**(6): p. 4625-31.
212. Dehay, B., et al., *Targeting alpha-synuclein for treatment of Parkinson's disease: mechanistic and therapeutic considerations.* Lancet Neurol, 2015. **14**(8): p. 855-66.
213. Bocchini, V., et al., *An immortalized cell line expresses properties of activated microglial cells.* J Neurosci Res, 1992. **31**(4): p. 616-21.
214. Balasooriya, I.S. and K. Wimalasena, *Are SH-SY5Y and MN9D cell lines truly dopaminergic?* Faseb Journal, 2007. **21**(6): p. A1274-A1274.

215. Guo, Z., et al., *Protection against 1-methyl-4-phenyl pyridinium-induced neurotoxicity in human neuroblastoma SH-SY5Y cells by Soyasaponin I by the activation of the phosphoinositide 3-kinase/AKT/GSK3beta pathway.* Neuroreport, 2016. **27**(10): p. 730-6.
216. Kim, B.W., et al., *Pathogenic Upregulation of Glial Lipocalin-2 in the Parkinsonian Dopaminergic System.* J Neurosci, 2016. **36**(20): p. 5608-22.
217. Peterson, L.J. and P.M. Flood, *Oxidative stress and microglial cells in Parkinson's disease.* Mediators Inflamm, 2012. **2012**: p. 401264.
218. Kaindlstorfer, C., et al., *Failure of Neuroprotection Despite Microglial Suppression by Delayed-Start Myeloperoxidase Inhibition in a Model of Advanced Multiple System Atrophy: Clinical Implications.* Neurotox Res, 2015.
219. Yang, L., et al., *Minocycline enhances MPTP toxicity to dopaminergic neurons.* J Neurosci Res, 2003. **74**(2): p. 278-85.
220. Bornebroek, M., et al., *Nonsteroidal anti-inflammatory drugs and the risk of Parkinson disease.* Neuroepidemiology, 2007. **28**(4): p. 193-6.
221. Etminan, M., B.C. Carleton, and A. Samii, *Non-steroidal anti-inflammatory drug use and the risk of Parkinson disease: a retrospective cohort study.* J Clin Neurosci, 2008. **15**(5): p. 576-7.
222. Zhang, S., et al., *Spontaneous assembly of a self-complementary oligopeptide to form a stable macroscopic membrane.* Proc Natl Acad Sci U S A, 1993. **90**(8): p. 3334-8.
223. Zhang, S., et al., *Self-complementary oligopeptide matrices support mammalian cell attachment.* Biomaterials, 1995. **16**(18): p. 1385-93.
224. Zhang, S., et al., *Unusually stable beta-sheet formation in an ionic self-complementary oligopeptide.* Biopolymers, 1994. **34**(5): p. 663-72.
225. Holmes, T.C., et al., *Extensive neurite outgrowth and active synapse formation on self-assembling peptide scaffolds.* Proc Natl Acad Sci U S A, 2000. **97**(12): p. 6728-33.
226. Cheng, T.Y., et al., *Neural stem cells encapsulated in a functionalized self-assembling peptide hydrogel for brain tissue engineering.* Biomaterials, 2013. **34**(8): p. 2005-16.
227. Yla-Outinen, L., et al., *Three-dimensional growth matrix for human embryonic stem cell-derived neuronal cells.* J Tissue Eng Regen Med, 2014. **8**(3): p. 186-94.
228. Thonhoff, J.R., et al., *Compatibility of human fetal neural stem cells with hydrogel biomaterials in vitro.* Brain Res, 2008. **1187**: p. 42-51.
229. Zhang, Z.X., et al., *Compatibility of Neural Stem Cells with Functionalized Self-assembling Peptide Scaffold In vitro.* Biotechnology and Bioprocess Engineering, 2010. **15**(4): p. 545-551.
230. Gelain, F., et al., *Designer self-assembling peptide nanofiber scaffolds for adult mouse neural stem cell 3-dimensional cultures.* PLoS One, 2006. **1**: p. e119.
231. Yokoi, H., T. Kinoshita, and S. Zhang, *Dynamic reassembly of peptide RADA16 nanofiber scaffold.* Proc Natl Acad Sci U S A, 2005. **102**(24): p. 8414-9.
232. Francis, N.L., et al., *Self-Assembling Peptide Nanofiber Scaffolds for 3-D Reprogramming and Transplantation of Human Pluripotent Stem Cell-Derived Neurons.* Acs Biomaterials Science & Engineering, 2016. **2**(6): p. 1030-1038.
233. Kuan, W.L., et al., *The importance of A9 dopaminergic neurons in mediating the functional benefits of fetal ventral mesencephalon transplants and levodopa-induced dyskinesias.* Neurobiol Dis, 2007. **25**(3): p. 594-608.
234. Caiazzo, M., et al., *Direct generation of functional dopaminergic neurons from mouse and human fibroblasts.* Nature, 2011. **476**(7359): p. 224-7.

235. Grealish, S., et al., *Human ESC-derived dopamine neurons show similar preclinical efficacy and potency to fetal neurons when grafted in a rat model of Parkinson's disease.* Cell Stem Cell, 2014. **15**(5): p. 653-65.
236. Studer, L., *Derivation of dopaminergic neurons from pluripotent stem cells.* Prog. Brain Res., 2012. **200**: p. 243-63.
237. Bradley, L.H., et al., *Dopamine neuron stimulating actions of a GDNF propeptide.* PLoS One, 2010. **5**(3): p. e9752.
238. Kelps, K.A., et al., *Evaluation of the physical and in vitro protective activity of three synthetic peptides derived from the pro- and mature GDNF sequence.* Neuropeptides, 2011. **45**(3): p. 213-8.
239. Airavaara, M., et al., *CDNF protects the nigrostriatal dopamine system and promotes recovery after MPTP treatment in mice.* Cell Transplant, 2012. **21**(6): p. 1213-23.
240. Lindholm, P. and M. Saarma, *Novel CDNF/MANF family of neurotrophic factors.* Dev Neurobiol, 2010. **70**(5): p. 360-71.
241. Gil, E.S., et al., *Quaternary ammonium beta-cyclodextrin nanoparticles for enhancing doxorubicin permeability across the in vitro blood-brain barrier.* Biomacromolecules, 2009. **10**(3): p. 505-16.
242. Vinogradov, S.V., E.V. Batrakova, and A.V. Kabanov, *Nanogels for oligonucleotide delivery to the brain.* Bioconjug Chem, 2004. **15**(1): p. 50-60.
243. Brownlie, A., I.F. Uchegbu, and A.G. Schatzlein, *PEI-based vesicle-polymer hybrid gene delivery system with improved biocompatibility.* Int J Pharm, 2004. **274**(1-2): p. 41-52.
244. Allen, D.D. and P.R. Lockman, *The blood-brain barrier choline transporter as a brain drug delivery vector.* Life Sci, 2003. **73**(13): p. 1609-15.
245. Geldenhuys, W.J., et al., *3D-QSAR study of bis-azaaromatic quaternary ammonium analogs at the blood-brain barrier choline transporter.* Bioorg Med Chem, 2005. **13**(13): p. 4253-61.
246. Tsigelny, I.F., et al., *Dynamics of alpha-synuclein aggregation and inhibition of pore-like oligomer development by beta-synuclein.* FEBS J, 2007. **274**(7): p. 1862-77.